Thermodynamic and Crystallographic Properties

of Tin Base Alloys

by

Michael B. Walls

Submitted in Partial Fulfillment of the Requirements

for the Degree of

Master of Science in Engineering

in the

Materials Science Engineering

Program

Adviser ______________________ Date

Dean of Graduate School ______________________ Date

YOUNGSTOWN STATE UNIVERSITY.

August, 1978

ABSTRACT

THERMODYNAMIC AND CRYSTALLOGRAPHIC PROPERTIES

OF TIN BASE ALLOYS

Michael B. Walls

MASTER OF SCIENCE IN ENGINEERING

Youngstown State University, 1976

This thesis was performed in order to study the nature of the phase transformation in tin, and the possible application of crystallographic and thermodynamic properties to it. X-Ray diffraction and calorimetric experimentation was performed on a large number of alloys that varied in solute additions and compositions. Considerable work was performed on calculation techniques and tabulation of data in the hopes of further experimentation.

The phase transformation was determined to be a nucleation and growth type reaction through general observations. A large dependence of the transformation was deduced to be due to the electronic structure differences between the tin solvent and the various solute additions. Regression analysis showed that more experimental work is needed to justify equations for the crystallographic data due to the large amounts of scatter inherent to diffraction patterns. Thermodynamic calculations revealed the need for a heat gain correction for the experimental temperature range.

ACKNOWLEDGEMENTS

I would like to express my gratitude for
contributions by Thomas Benton,
Paul Perrotta, and Richard Eversley
in this investigation, and also
to Dr. Richard W. Jones and
Dr. Shaffia Ahmed for advice and counsel.

Michael Bailey Walls

TABLE OF CONTENTS

PAGE

ABSTRACT ii

ACKNOWLEDGEMENTS iii

TABLE OF CONTENTS iv

LIST OF SYMBOLS vi

TABLE OF FIGURES vii

LIST OF TABLES viii

CHAPTER

I. INTRODUCTION 1

Related Studies on Tin 1

Purpose of Investigation 7

II. MATERIALS AND EQUIPTMENT 8

General Sample Preparation 8

X-Ray Sample Preparation 10

Description of X-Ray Apparatus 11

Calorimetric Sample Preparation 13

Description of Calorimeter Apparatus 14

III. EXPERIMENTAL METHODS 16

X-Ray Methods 16

X-Ray Calculations 18

Calorimetric Methods 19

Calorimetric Calculations 20

IV. EXPERIMENTAL RESULTS 22

Crystallographic Results 22

Thermodynamic Results 34

Miscellaneous Observations 37

PAGE

V. DISCUSSION 40

VI. CONCLUSIONS.. 45

APPENDIX A. Calculation of X-Ray Results........................ 48

APPENDIX B. Figures of X-Ray Results............................ 56

APPENDIX C. Figures of Calorimetric Results..................... 90

APPENDIX D. Calculation of Theoretical Habit Plane.............. 129

BIBLIOGRAPHY.. 131

LIST OF FIGURES

FIGURE		PAGE
1.	Constant Temperature X-Ray Diffraction Laboratory Apparatus	12
2.	Photograph of Laboratory Equipment	13
3.	Calorimetric Samples	15
4.	Modified Olsen Calorimeter	16
5.	Half Section Diagram of Specimen Stage	17
6.	Photograph of Constant Temperature - Atmosphere Camera Attachment	18

LIST OF TABLES

TABLE		PAGE
1.	Alloying effects on the growth rate of alpha tin.......	5
2.	Impurity concentrations of as recieved Tin.............	8
3.	Specimen compositions of Tin Base Alloys...............	8
4.	Experimental X-Ray results.............................	23
5.	Eoefficients of thermal expansion......................	26
6.	Regression formulae of experimental alloy systems......	27
7.	Multiple regression analysis of crystallographic data..	30
8.	Percentage volumne change upon alloying................	31
9.	ΔH versus temperature parameters...............	35
10.	ΔH versus $\frac{1}{T}$ parameters............	36
11.	Comparative observations of nucleation and growth rates of alpha tin..	39
12.	Critical values of the coefficient of determination....	40

- - - - - - - - - - - - -

CHAPTER I

RELATED STUDIES ON TIN

Introduction

Beta Tin exists in a Body Centered Tetragonal, (A5), crystal lattice. It's lattice dimensions are given as a=5.831 and c=3.182 at a temperature of 26^{o}c.(1) It is bonded by a non-directional metallic bond characterized by a coordination number of 8, an atomic packing factor of 0.55,(2) a relatively high, (3.022 Å), distance of closest approach,(3) and a ratio of .72 atoms with electrons in the $5s^2 5p^2$ level to .32 atoms with electrons in the $5s5p^3$ level. This condition is corraborated by Mossbauer studies on the phase transformation.(3)

Alpha Tin is a low temperature form of the element that exists below a temperature of approximately 13.5^{o}c. It exists in the Diamond Cubic, (A4), crystal lattice with the dimension a=6.489 at 25^{o}c.(4) It is bonded by a tetravalent covalent bond. This high energy bond is stereospecific, with an angle of 109.5^{o} between neighbouring bonds.(5)

Footnote:

[1] C.S. Barrett and T.B. Massalski, Structure of Metals (New York: McGraw-Hill, 1966), p. 631.

[2] Van Vlack, p. 63.

[3] Ibid. p. 631.

[4] C.S. Barrett and T.B. Massalski, Structure of Metals (New York: McGraw-Hill, 1966), p. 631.

[5] L.H. Van Vlack, Materials Science for Engineers (Reading, Mass.: Addison-Wesley, 1970), p. 41

It is characterised by a coordination number of 4, an atomic packing factor of .34,[6] and a low, (2.81 Å), distance of closest approach.[7] In this form, all the atoms have valence electrons in the $5s5p^3$ level.[8]

Another significant difference between beta and alpha tin is in electrical properties. The entire group IVa elements are referred to as the semi-metals, but only tin exists both as a metal in the beta phase, and as a semiconductor in the alpha phase. The semiconducting properties include an energy gap of .08 ev, which is the lowest value for all semiconductors.[9] Electrons can be excited across this gap by any wavelength of light lower than 15,540 Å, making it an excellent material for infrared photoconduction.[10] The electron mobility is .2 m^2/sec. volt, hole mobility is .1 m^2/sec. volt, and the intrinsic conductivity is 10^6 $ohm^{-1} m^{-1}$, the highest value of all the semiconductors.[11]

Footnote:

[6] Ibid.

[7] C.S. Barrett and T.B. Massalski, Structure of Metals (New York:McGraw-Hill, 1966), p. 631.

[8] V.N. Panyushkin, "Shift of the Mossbauer Line of Beta Tin During it's Phase Transformation under Pressure." Soviet Physics-Solid State, v. 10, no. 6, (Dec., 1968), p. 1515.

[9] L.H. Van Vlack, Materials Science for Engineers (Reading, Mass,:Addison-Wesley, 1970), p. 299.

[10] J.H. Becker, "On the Quality of Gray Tin Crystals and Their Rate of Growth." Journal of Applied Physics, v. 29, no. 7, (July 1958), p. 110.

[11] L.H. Van Vlack, Materials Science for Engineers (Reading, Mass.:Addison-Wesley, 1970), p. 299.

Recent attempts have been made by Jaros to describe the general non-spherical charge density in semiconductors, but with little success in the case of alpha tin.(12)(13)

The transformation of beta to alpha tin is sometimes referred to as Tin Disease, and is described as a Polymorphic transformation. It is perhaps the oldest known phase transformation, since both Aristotle and Plutarch were aware of its existance. The reaction seems to be a nucleation and growth type process. Attempts have been made as to the nature of the nucleation but with little success. It seems to occur at random places when allowed to self nucleate, and deformation seems to reduce the time required for nucleation.(14) Precipitation from solution via chemical reactions had no success, whereas precipitation from a mercury solution has shown promising results. Nucleation from the solid Beta phase seems to be promoted by physical contact with other semiconducting materials such as Alpha Tin, Silicon, Germanium, Indium-Antimony (InSb), and other isomorphous, semiconducting compounds.(15)

Footnote:

[12] M. Jaros, "Covalent Effects in -Sn." Solid State Communications, v. 7, (1969) p.p. 521-523.

[13] M. Jaros, "On the Theory of Covalent Bonding in Solids", Physica, v. 50, no. 3, (Dec. 7, 1970), p.p. 356-364.

[14] V.K. Lohberg and P. Presche, "Beitrag zur -Umwandlung des Zinns." Z. Metallkunde, v. 59, no. 1, (Jan., 1968) p.

[15] J.H. Becker, "On the Quality of Gray Tin Crystals and Their Rate of Growth." Journal of Applied Physics, v. 29, no. 7. (July, 1958), p.p. 1120-1121.

Growth of the alpha tin regions has been of major interest in most studies on the transformation. The maximum growth rate of 1.5 mm/hr. occurs at approximately 238°K.[16] This temperature is not affected by alloying additions.[17] The growth rate of spherical regions has been treated by Burgers and Groen utilizing Avrami's Equation in three dimensions,[18] by Becker and Cagle with little success,[19] and also by Bykhovskii from a kinetics approach.[20] Some work has been done on the growth rate susceptibility to impurities and alloying additions,[21][22] a summary of which is shown in table 1.

Footnote:

[16] V.K. Lohberg and P. Presche, "Beitrag zur -Umwandlung des Zinns." Z. Metallkunde, v. 59, no. 1, (Jan., 1968), p.

[17] J.H. Becker, "On the Quality of Gray Tin Crystals and Their Rate of Growth." Journal of Applied Physics, v. 29, no. 7, (July, 1958), p.

[18] W.G. Burgers and L.J. Groen, "Mechanism and Kinetics of the Allotropic Transformation of Tin." Disc. Faraday Soc., v. 23, no. 183, p.p. 183-195.

[19] J.H. Becker, "On the Quality of Gray Tin Crystals and Their Rate of Growth." Journal of Applied Physics, v. 29, no. 7, (July, 1958), p.p. 1110-1121.

[20] F.Wm. Cagle and Henry Eyring, "An Application of the Absolute Rate Theory to Phase Changes in Solids", Journal of Physical Chemistry, v. 57, (1953), p.p. 942-946.

[21] A.I. Bykhovskii, et al, "Growth Mechanism of -modification Centers in High Purity Tin.", Soviet Physics-Crystallography, v. 12, no. 3, (Nov.-Dec., 1967), p.p. 460-462.

[22] J.H. Becker, "On the Quality of Gray Tin Crystals and Their Rate of Growth.", Journal of Applied Physics, v. 29, no. 7, (July, 1958), p.p. 1120-1121.

There is no noticible change in the growth rate when the interface crosses a grain boundary.[23] The transformation has also been investigated via Laue back reflection studies on single crystals and has shown no orientation correspondence between the two phases, and thus bears no resemblence to a martensitic reaction.[24] Both the activation energy E_A,[25][26][27] and the transformation temperature are in considerable doubt.[28][29]

Table 1.

ALLOYING EFFECTS ON THE GROWTH RATE OF ALPHA TIN*.

Solute	Concentration (atomic percent)	Growth Rate(mm/hr)	Temp. (^{o}K)
Pure Sn	100	1.5	238
Sulphur	.5	.95	238
Selenium	.5	.60	238
Magnesium	.5	.01	238
Tellurium	.1	.6	238
Tellurium	1.0	.5	238
Tellurium	2.3	.3	238
Tellurium	5.0	.05	238

Footnote:

23 W.G. Burgers and L.J. Groen, "Mechanism and Kinetics of the Allotropic Transformation of Tin." Disc. Faraday Soc., v. 23, no. 183, p.p. 183-195.

24 Ibid.

25 Ibid.

26 R.R. Hultgren, Selected Values of Thermodynamic Properties of Metals and Alloys, (Metals Park, Ohio: ASM, 1973) p.

27 W.G. Burgers and L.J. Groen, "Mechanism and Kinetics of the Allotropic Transformation of Tin." Disc. Faraday Soc., v. 23, no. 183, p.p. 183-195; disc. Dr. J.W. Dunning, p. 222.

28 R.R. Hultgren, Selected Values of Thermodynamic Properties of Metals and Alloys, (Metals Park, Ohio : ASM, 1973) p.

29 G.V. Raynor and R.W. Smith, "Transition Temperature of the Transition between Grey and White Tin.", Proceedings of the Physics Society, v. 70B, p.p. 1135-1143.

One well observed property of the reaction is a 21.4% volumne increase, found through micrographic studies.[29][30]

The reverse alpha to beta transformation is also considered to be a nucleation and growth process with the formation of small domains of beta being constant and sudden.[31] With the addition of .06 atomic percent Germanium, nucleation was inhibited, with no domains formed after thirty minutes at 43°C.[32] Growth of the domains to final size occurred in 5 to 30 seconds due to the breakup of the alpha phase from the volumne contraction.[33] Growth is also characterized by a discontinuous release of stored energy by cleavage of the alpha phase.[34] Rate determinations have yeilded values of .003 mm/sec. at 30°c, and .002 mm/sec. at 36°c, which is low compared to martensitic reactions, and the actual rate determining reaction is the number of domains formed and not the growth rate.[35]

Footnote:

[30] R.G. Wolfson, et. al., "Transformation Studies of Grey Tin Single Crystals," Journal of Applied Physics, v. 31, no. 11, (Nov. 1960) p.p. 1973-1977.

[31] W.G. Burgers and L.J. Groen, "Mechanism and Kinetics of the Allotropic Transformation of Tin." Disc. Faraday Soc., v. 23, no. 183, p.p. 183-195.

[32] Ibid.

[33] Ibid.

[34] R.G. Wolfson, et. al., "Transformation Studies of Grey Tin Single Crystals." Journal of Applied Physics, v. 31, no. 11, (Nov., 1960), p.p. 1973-1977.

[35] W.G. Burgers and L.J. Groen, "Mechanism and Kinetics of the Allotropic Transformation of Tin." Disc. Faraday Soc., v. 23, no. 183, p.p. 183-195.

The temperature of the transformation is increased by the addition of Lead, Bismuth, and Antimony, decreased by Tellurium, and remains unchanged by Zinc and Aluminium. However Zinc and Aluminium accelerate the transformation rate.[36] These results are believed to be due to the presence of strains in the beta phase that affect the transformation.[37][38]

In this investigation, attempts were made to study the X-Ray and Thermodynamic properties of the transformation in pure tin, and the effects of solute additions in dilute concentrations, (.05 to .8 atomic percent) on the X-Ray and Thermodynamic parameters. The crystal structures and lattice parameters were determined for both the alpha and beta phases at various temperatures, (i.e. 274,286,297, and 394^{o}K), and the enthalpy of pure tin and the alloys were determined in the temperature range of 343 to 396^{o}K. From these results, some morphology of the phase transformation in pure tin and the effects of alloying elements on the lattice parameters and enthalpy were studied. Some observations regarding the phase transformation are also reported herein.

Footnote:

[36] G.V. Raynor and R.W. Smith, "Transition Temperature of the Transition between Grey and White Tin.", Proceedings of the Physics Society, v. 70B, p.p. 1135-1143.

[37] Ibid.

[38] R.G. Wolfson, et al, "Transformation Studies of Grey Tin Single Crystals." Journal of Applied Physics v. 31, no. 11, (Nov., 1960), p.p. 1973-1977.

- - - - - - - - - - - - -

CHAPTER II

GENERAL SAMPLE PREPARATION

Materials and Equiptment

All samples were prepared from 99.9998% pure tin purchased from the Materials Research Corporation. Elemental analysis data on which is provided in table 2.

Table 2.
Impurity Concentrations of As Recieved Tin,*

C	O	H	N	B	Al	Mg	Ca	Ti	Fe	Cu	Si	Cr	Ni	Mo	Ag	Pb
10	43	1	1	10	10	3	1	10	10	5	10	10	10	10	10	10

*Analysis in (PPM)

Alloys of 35 grams each were prepared by weighing the alloys on a Mettler analytical balance within ± .01 miligram tolerances. The composition of each specimen is given in table 3.

Table 3.
Specimen Compositions of Sn base alloys

Solute	Ag	Cd	In	Sb	Te	Zr
Atomic	.05	.05	.05	.05	.05	.05
Percent	.10	.10	.10	.10	.10	.10
Solute	.30	.30	.30	.30	.30	.30
	.50	.50	.50	.50	.50	.50
	.80	.80	.80	.80	.80	.80

All alloying additions were of spectral grade to minimize the chance of any tertiary solid solutions.

After weighing, all samples were sealed in fused quartz tubes of 1.5cm. inside diameter and sealed under a minimum vacuum of 5 times 10^{-6} torr to reduce the effects of oxidation at high temperatures.

Samples with solute additions of low melting points, i.e. Cadmium and Indium, were melted in a standard furnace at 560 degrees Kelvin and aggitated several times during the thirty minute molten period. Samples with solute additions of high melting points, i.e. Silver, Antimony, Tellurium and Zirconium were melted at $1000^{o}K$ and aggitated several times during the thirty minute molten period. This procedure for the high temperature alloys was necessary in order to insure complete solution of the high melting point elements. After this treatment, the high temperature alloys were returned to $560^{o}K$ and aggitated several times at this temperature to farther homogenize and remove any vaporized tin condenset. All samples were then furnace cooled to roomtemperature, reheated to $425^{o}K$, and allowed to anneal for eighteen hours followed by a furnace cool to room temperature.

Sample tubes were checked with an ionization gun to ensure that vacuum was maintained during the melting and annealling processes. Once this was determined, the tubes were broken, and the samples were weighed to ensure that the final composition was equal to the initial composition. All samples exhibited good correlation in this respect.

The tops of all samples were cut off manually with a hacksaw in order to utilize the top portions for x-ray analysis and the bottom portion for calorimetric experimentation. After cutting, all samples were thoroughly cleaned with acetone and ether. Separate procedures were then necessary for preparation of the x-ray and calorimetric samples.

X-RAY SAMPLE PREPARATION

The top sections of the castings were used for X-Ray sample preparation. These top sections were filed to obtain 200 mesh powder for use in the x-ray analysis of the beta phase. The solid portions of the samples were placed in a freezer at $-35^{o}C$ and seeded with specimens of alpha tin to initiate the formation of nuclei of the alpha phase in the specimens. Once the alpha phase was visible, the seeds were removed and the nuclei were allowed to grow until the specimen was completely transformed to a cracked and crumbling specimen of the alpha phase. These specimens were then roughly ground in a glass mortor and pestle to reduce the particle size. Portions of the sample transformed back to the beta phase during the deformation process. In order to revert the portions of beta back to alpha, the samples were replaced in the freezer and allowed to transform. It was observed that the transformation occurred at a higher rate following this treatment. This cycle was repeated until enough 200 mesh powder was obtained to use in the analysis.

It should be noted that various degrees of difficulty were encountered when trying to nucleate and grow the regions of alpha tin. These difficulties can be catagorized according to the various alloy groups, but in general, nucleation and growth was inhibited in various degrees for all the alloying elements in comparison to pure tin. A more complete discussion may be found in the miscellaneous observations section.

DESCRIPTION OF X-RAY APPARATUS

The general laboratory settup is shown in figure 1. A Norelco difractometer was used along with Philips Electronic X-Ray generating and counting apparatus. A Materials Research Corporation high and low temperature diffractometer attachment was utilized that provided for analysis to be performed under a helium atmosphere to prevent oxidation and water condensating the samples during the high and low temperature experimental runs.

Temperatures were maintained utilizing a Thermo-Electric Off-On controller connected to a Materials Research Corporation Variable power supply to heat the carbon sample stage. Cooling of the same stage was performed utilizing tap water that was passed through a makeshift heat exchanger utilizing a cooling medium of approximately 75% Antifreexe in water solution maintained at -40°C. Temperature was monitored to the controller by the use of an Iron-Constanton thermocouple immersed in the X-Ray specimen. By operating both the heating and cooling systems simultaneously, the temperature of the sample could be held to within one degree centigrade in the temperature range of 3 to 150°c.

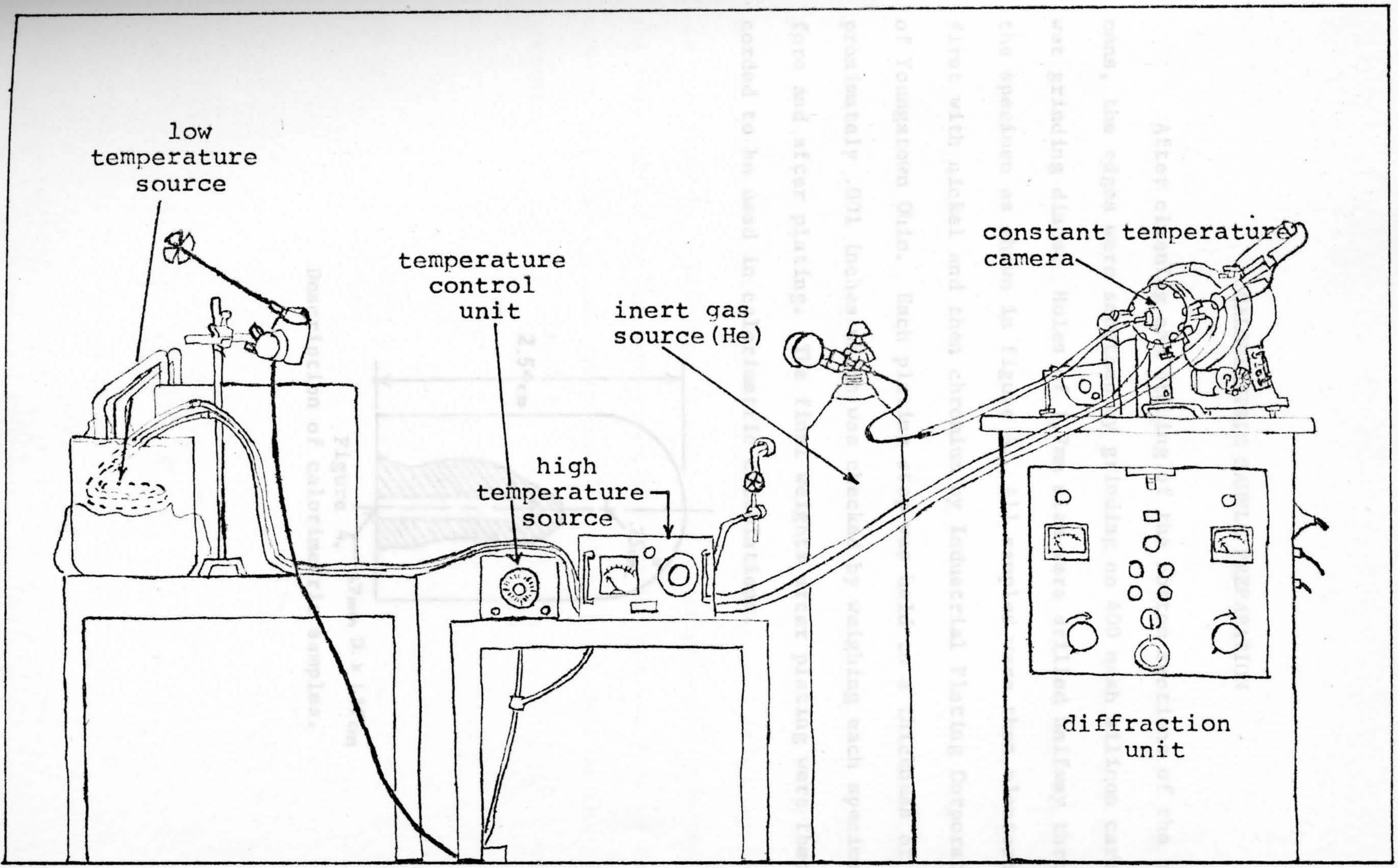

Figure 1. X-ray Diffraction Unit with constant thermal environment supply apparatus.

CALORIMETRIC SAMPLE PREPARATION

After cleaning and etching of the bottom sections of the specimens, the edges were smoothed by grinding on 400 mesh silicon carbide wet grinding discs. Holes of 1.7mm size were drilled halfway through the specimen as shown in figure 4. All samples were then electorplated first with nickel and then chromium by Industrial Plating Corporation of Youngstown Ohio. Each plating step was held to a thickness of approximately .001 inches which was checked by weighing each specimen before and after plating. The final weights after plating were then recorded to be used in calorimetric calculations.

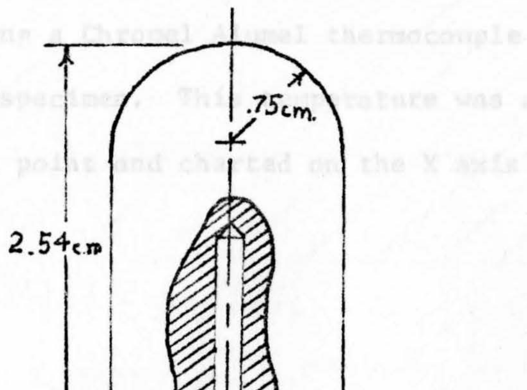

Figure 4.
Description of calorimetric samples.

DESCRIPTION OF CALORIMETER

A modified Olsen Calorimeter constructed at Youngstown State University was utilized in the experiments. A diagram of the apparatus is shown in figure 5. Isopropyl Alcohol of spectral quality was used as a media. Temperature of the media was minitored by six Chromel Alumel thermocouples connected in series, converted by an electric ice point, and charted on the Y axis of an X-Y recorder. Temperatures were double checked using a quartz thermometer equiped with a digital display in degrees Centigrade. The media was aggitated by using a magnetic stirrer also shown in figure 2. Temperature of the specimen was monitored by utilizing a Chromel Alumel thermocouple inserted in the hole drilled in the specimen. This temperature was also converted through the electric ice point and charted on the X axis of the X-Y recorder.

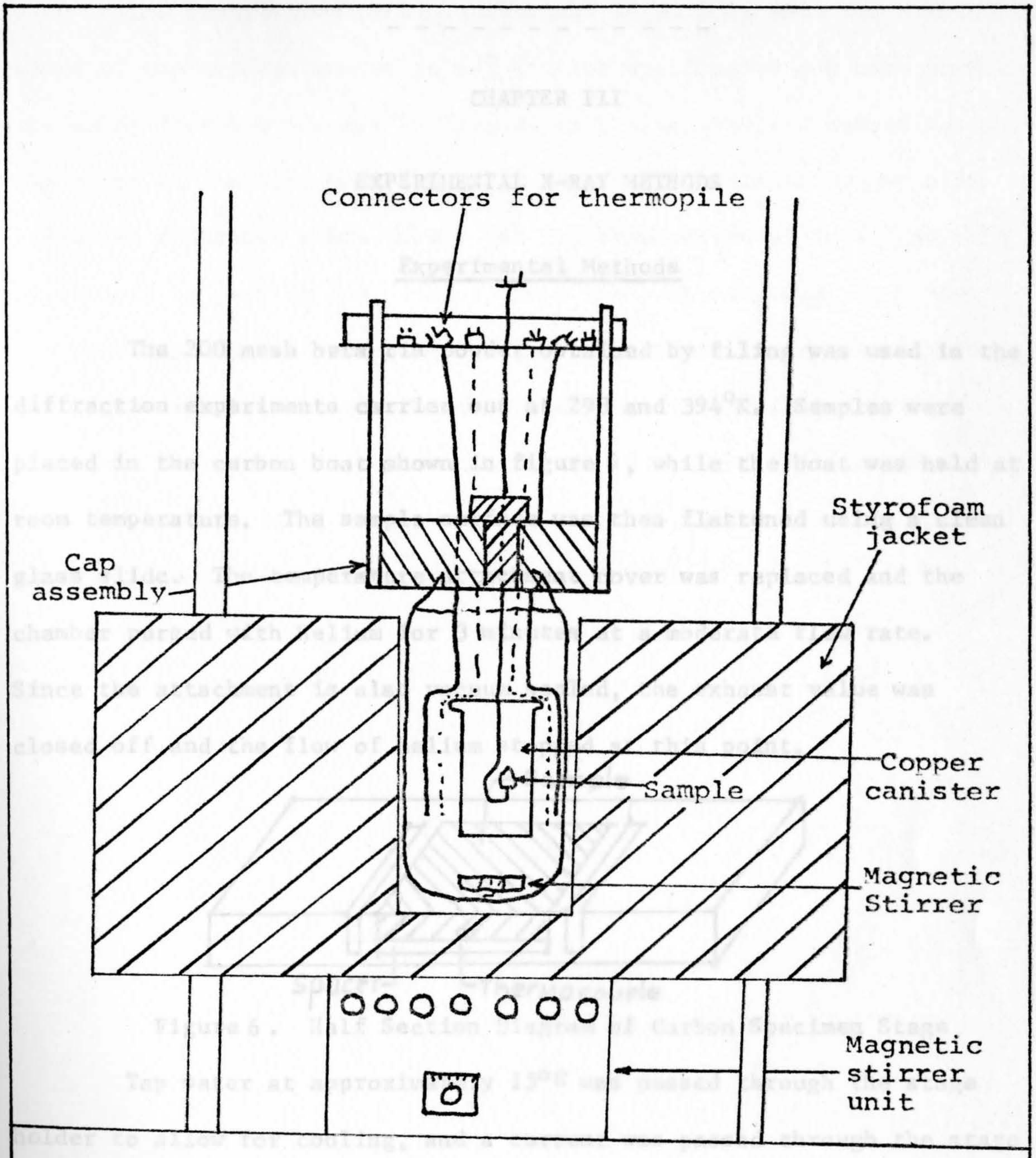

Figure 5. The calorimeter.

- - - - - - - - - - - - -

CHAPTER III

EXPERIMENTAL X-RAY METHODS

Experimental Methods

The 200 mesh beta tin powder obtained by filing was used in the diffraction experiments carried out at 298 and 394°K. Samples were placed in the carbon boat shown in figure 6, while the boat was held at room temperature. The sample surface was then flattened using a clean glass slide. The temperature attachment cover was replaced and the chamber purged with Helium for 3 minutes at a moderate flow rate. Since the attachment is also vacuum sealed, the exhaust value was closed off and the flow of helium stopped at this point.

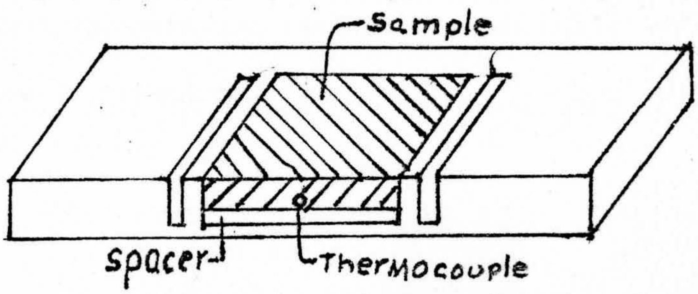

Figure 6. Half Section Diagram of Carbon Specimen Stage

Tap water at approximately 15°C was passed through the stage holder to allow for cooling, and a current was passed through the stage to heat the specimen. The temperature of the run was set on the temperature controller and the sample was given fifteen minutes at temperature before the run was initiated. Diffraction peaks were obtained for 2 theta range of 28 to 90 degrees for all specimens at both 298° and 394°K temperatures.

Low temperature data was obtained by cooling down the carbon stage of the diffractometer to 40° C. The specimen of 200 mesh powder was taken from the freezer and immediately placed in the carbon boat. The cover of the attachment was replaced and the chamber purged with helium as described previously. The low temperature of the stage was maintained by passing tap water through the heat exchanger and into the mounting bloch of the attachment. Temperature control was facilitated through the use of the temperature controller that supplied heat when needed to the carbon stage. In this case, diffraction peaks were obtained in the 2 theta range of 20 to 90 degrees for the specimens at both 273 and 286°K temperatures.

X-RAY CALCULATIONS

Lattice parameters were determined utilizing a procedure described in detail by Klug and Alexander.(39) It is an extrapolation of the lattice parameters to a zero value of $\sin^2 2\theta\left(\frac{1}{\sin\theta}+\frac{1}{\theta}\right)$. Diffraction peaks used were in the range of $30^\circ < \theta < 90^\circ$. The extrapolation was accomplished by a least squares analysis in three unknowns, (A, C, and D), commonly known as Cohen's Method. The D values are referred to as the drift constants, and are representative of the amount of scatter or error in the experimental θ values. The calculations were carried out by fortran batch processing on an IBM 360 computer system. A sample program and readout for the cubic and tetragonal systems are shown in Appendix A.

Figure 7. Photograph of Constant Temperature - Atmosphere Camera Attachment.

Footnote:

[39]Harold P. Klug and Leroy E. Alexander, X-Ray Diffraction Procedures, John Wiley and Sons, Inc., (New York, 1962) p.p. 485-487.

CALORIMETRIC METHODS

The calorimeter cooling medium was prepared by cooling of the as recieved isopropyl alcohol with dry ice to a temperature of 286 degrees kelvin and then weighed out to 1200 grams on a Mettler Analytical balance. The thermos section of the calorimeter was then placed in the apparatus and the thermopile replaced. The calorimeter was then ready to recieve the specimen.

The beta specimens described previously were placed on the sample thermocouple and heated to 448 degrees kelvin in a conventional muffle furnace. When removed from the furnace, the sample was immediately encapsulated in the Copper cannister shown in figure 5., and immersed in the cooling medium.

CALORIMETRIC CALCULATIONS

Thermodynamic calculations were carried out assuming negligible calorimetric equivalency and heat gain from the surroundings. These assumptions made possible the use of a simplified heat balance, $\Delta Hm + \Delta Hs = 0$ with heat being transferred from the sample to the media. The enthalpy change of the sample was calculated through the use of the formula.

$$\Delta Hs = -\Delta Hm = -Wm \times \Delta Tm \times Cpm$$

where, ΔHs=enthalpy change of sample
ΔHm=enthalpy change of media
Wm=weight of media
ΔTm=temperature change of media
Cpm=specific heat of media

The X-Y recorder graphs obtained in the experiments were converted from millivolts to temperature by the use of the IPTS 1968 standards for type K thermocouples in the case of the sample temperature, and by a calibration curve obtained by corresponding the thermopile millivolt readings with the digital readout of a quartz thermometer immersed in the media in the case of the media temperature change. The temperature changes were determined, recorded, and specific heat values for the isopropyl alcohol were assigned according to the values obtained by Andon, Counsell, and Martin.[40]

Footnote:

[40] R.J.L. Andon, J.F. Counsell, and J.F. Martin, "Thermodynamic Properties of Organic Oxygen Compounds." Transactions of the Faraday Society, vol. 59, (1963), p. 1556.

The free energy change, (ΔF), of the samples has been calculated by utilization of a linear regression analysis on the values of the enthalpy change, (ΔH), with respet to inverse temperature, ($\frac{1}{T_i}$). From the equations obtained, it was possible to assume that the area under the resulting curve, ($\Delta H d(\frac{1}{T})$), was equal to the area of a right triangle, as seen by the equation,

$$A_i = \int_{T_o}^{T_i} \Delta H d(\frac{1}{T}) = (1/2)\Delta H_i (\frac{1}{T_i} - \frac{1}{T_o})$$

where:

A_i=area under H versus $\frac{1}{T}$ curve at point t,
ΔH=enthalpy change,
ΔH_i=enthalpy change at point i,
T_i=temperature, and
T_o=401.2^{o}K=reference state.

At this point, the free energy change, (ΔF), was calculated by,

$$\Delta F = F_{Ti} - F_{401.2} = T_i A_i$$

where;

F_T=free energy at T_i, and
$F_{401.2}$=reference free energy.

- - - - - - - - - - - - - - - - -

CHAPTER IV

EXPERIMENTAL RESULTS

CRYSTALLOGRAPHIC RESULTS

The crystallographic results obtained from the computor programs are given in Table 4. In the case of the tetragonal structures, the lattice parameters, (a and c), the unit cell volumne, (v), and the calculated axial ratio, (c/a), are presented at the respective experimental temperature. Much difficulty was encountered when trying to obtain suitable specimens of the alpha phase, therefore Table 6 is incomplete for the many alloy compositions that did not transform for periods up to six months. The only systems that transformed completely at all compositions were Silver and Zirconium, whereas Indium, Cadmium, and Tellurium were transformed at some compositions.

Since the lattice parameters of the tetragonal alloys were determined for two temperatures, the coefficients of lattice thermal expansion for the unit cell parameters a, c, and volumne were calculated, tabulated in Table 5, and plotted in figures 22 thru 43 located in Appendix B. Table 6 contains the results of a least squares, linear regression analysis performed on the unit cell parameters as a linear function of atomic percent. The graphical representation of the functions are contained in Appendix B, figures 10 thru 21 . Also in Appendix B. figures 8 thru 9 , are the graphical representation of the variation in the cubic lattice parameter, a, as a function of alloy composition and temperature for the Silver and Zirconium alloys.

TABLE 4.

Experimental X-Ray Results

Alloy	Temp. (^ok)	Lattice Parameters a	c	volumne	c/a
SN	276	6.488		273.13	
SN	286	6.472*		271.13*	
SN	286	6.496		274.14	
SN	286	5.833	3.180	108.19	.5452
SN	286	5.836*	3.191*	108.66*	.5468
SN	297	5.831	3.182	108.20	.5457
SN	394	5.846	3.197	109.27	.5469
.05Ag	276	6.502		274.86	
.05Ag	286	6.495		273.96	
.05Ag	297	5.832	3.182	108.22	.5456
.05Ag	380	5.844	3.187	108.83	.5453
.1Ag	276	6.508		275.69	
.1Ag	286	6.495		273.97	
.1Ag	297	5.832	3.182	108.22	.5456
.1Ag	394	5.838	3.190	108.72	.5464
.3Ag	276	6.491		273.43	
.3Ag	286	6.481		272.26	
.3Ag	297	5.832	3.182	108.21	.5456
	394	5.843	3.202	109.33	.5480
.5Ag	276	6.488		273.12	
	286	6.483		272.45	
	296	5.833	3.181	108.21	.5453
.8Ag	276	6.482*		272.37*	
.8Ag	286	6.495*		273.94*	
.8Ag	286	6.481*		272.26*	
.8Ag	286	5.835*	3.180*	108.27*	.5450
.8Ag	297	5.833	3.182	108.25	.5455
.8Ag	394	5.853	3.200	109.62	.5467
.05Cd	297	5.833	3.183	108.29	.5457
.05Cd	394	5.844	3.196	109.15	.5469
.1Cd	276	6.493		273.73	
.1Cd	286	6.499		274.48	
.1Cd	297	5.832	3.182	108.25	.5456
.1Cd	394	5.841	3.193	108.93	.5467
.3Cd	297	5.831	3.182	108.19	.5457
.3Cd	394	5.845	3.196	109.18	.5468
.5Cd	297	5.833	3.182	108.24	.5455
.5Cd	394	5.842	3.192	108.96	.5464
.8Cd	297	5.832	3.182	108.23	.5456
.8Cd	394	5.844	3.191	108.98	.5460

TABLE 4. (continued)

Experimental X-Ray Results

Alloy	Temp. (^{o}k)	Lattice Parameters			
		a	c	volumne	c/a
.05In	276	6.484		272.60	
.05In	286	6.490		273.34	
.05In	297	5.833	3.182	108.25	.5455
.05In	394	5.845	3.191	109.02	.5459
.1In	276	6.501		274.79	
.1In	286	6.495		274.03	
.1In	297	5.833	3.182	108.28	.5455
.1In	394	5.844	3.193	109.07	.5464
.3In	297	5.832	3.181	108.20	.5454
.3In	394	5.845	3.200	109.33	.5475
.5In	297	5.832	3.181	108.20	.5454
.5In	394	5.856	3.200	109.74	.5464
.8In	297	5.830	3.181	108.12	.5456
.8In	394	5.847	3.195	109.22	.5464
.05Sb	297	5.841	3.183	108.58	.5449
.05Sb	394	5.845	3.191	109.05	.5459
.1Sb	297	5.842	3.189	108.83	.5459
.1Sb	394	5.846	3.155	107.83	.5397
.3Sb	297	5.836	3.185	108.45	.5458
.3Sb	394	5.840	3.192	108.88	.5466
.5Sb	297	5.840	3.184	108.57	.5452
.5Sb	394	5.837	3.193	108.76	.5470
.8Sb	297	5.839	3.184	108.55	.5453
.8Sb	394	5.849	3.196	109.34	.5464
.05Te	297	5.833	3.181	108.23	.5453
.05Te	394	5.840	3.195	108.99	.5471
.1Te	276	6.483		272.52	
.1Te	286	6.501		274.76	
.1Te	297	5.840	3.186	108.67	.5455
.1Te	394	5.842	3.190	108.86	.5460
.3Te	297	5.834	3.181	108.27	.5453
.3Te	394	5.850	3.196	109.38	.5463
.5Te	297	5.838	3.187	108.62	.5459
.5Te	394	5.846	3.195	109.17	.5465
.8Te	297	5.838	3.187	108.60	.5459
.8Te	394	5.848	3.197	109.32	.5467

TABLE 4. (continued)

Experimental X-Ray Results

Alloy	Temp. (^{o}k)	Lattice Parameters a	c	volumne	c/a
.05Zr	276	6.493*		273.68*	
.05Zr	286	6.492*		273.63*	
.05Zr	276	5.832*	3.181*	108.17*	.5454
.05Zr	286	5.832*	3.185*	108.33*	.5461
.05Zr	297	5.832	3.182	108.23	.5456
.05Zr	394	5.861	3.202	109.99	.5463
.1Zr	276	6.500*		274.62*	
.1Zr	286	6.497*		274.22*	
.1Zr	297	5.840	3.188	108.75	.5459
.1Zr	394	5.849	3.191	109.18	.5456
.3Zr	276	6.496		274.08	
.3Zr	286	6.497		274.22	
.3Zr	297	5.834	3.185	108.42	.5459
.3Zr	394	5.846	3.193	109.09	.5462
.5Zr	276	6.497		274.27	
.5Zr	286	6.488		273.15	
.5Zr	297	5.833	3.183	108.29	.5457
.5Zr	394	5.841	3.191	108.89	.5463
.8Zr	276	6.482*		272.33*	
.8Zr	286	6.484*		272.66*	
.8Zr	297	5.836	3.185	108.48	.5458
.8Zr	408	5.850	3.197	109.43	.5465

*-Indicates values from diffraction patterns containing both alpha and beta phases.

TABLE 5.

COEFFICIENTS OF THERMAL EXPANSION

Alloy	v	a	c
Sn(α)	1.010 10^{-1}	3.000 10^{-4}	
Sn(β)	1.103 10^{-2}	1.546 10^{-4}	1.546 10^{-4}
.05Ag(α)	-9.000 10^{-2}	-7.000 10^{-4}	
(β)	7.349 10^{-3}	1.446 10^{-4}	6.024 10^{-5}
.10Ag(α)	-1.720 10^{-1}	-1.300 10^{-3}	
(β)	5.155 10^{-3}	6.186 10^{-5}	8.247 10^{-5}
.3Ag(α)	-1.170 10^{-1}	-1.000 10^{-3}	
(β)	1.155 10^{-2}	1.134 10^{-4}	2.062 10^{-4}
.5Ag(α)	-6.700 10^{-2}	-5.000 10^{-4}	
(β)	N/A	N/A	N/A
.8Ag(α)	-1.100 10^{-2}	-1.000 10^{-4}	
(β)	1.412 10^{-2}	2.062 10^{-4}	1.856 10^{-4}
.05Cd(β)	8.866 10^{-3}	1.134 10^{-4}	1.340 10^{-4}
.1Cd(α)	7.500 10^{-2}	6.000 10^{-4}	
(β)	7.010 10^{-3}	9.278 10^{-5}	1.134 10^{-4}
.3Cd(β)	1.021 10^{-2}	1.443 10^{-4}	1.443 10^{-4}
.5Cd(β)	7.423 10^{-3}	9.278 10^{-5}	1.031 10^{-4}
.8Cd(β)	7.732 10^{-3}	1.237 10^{-4}	9.278 10^{-5}
.05In(α)	7.400 10^{-2}	6.000 10^{-4}	
(β)	7.938 10^{-3}	1.237 10^{-4}	9.278 10^{-5}
.1In(α)	-7.600 10^{-2}	-6.000 10^{-4}	
(β)	8.144 10^{-3}	1.134 10^{-4}	1.134 10^{-4}
.3In(β)	1.165 10^{-2}	1.340 10^{-4}	1.959 10^{-4}
.5In(β)	1.588 10^{-2}	2.474 10^{-4}	1.959 10^{-4}
.8In(β)	1.134 10^{-2}	1.753 10^{-4}	1.443 10^{-4}
.05Sb(β)	4.845 10^{-3}	4.124 10^{-5}	8.247 10^{-5}
.1Sb(β)	-1.031 10^{-2}	4.124 10^{-5}	-3.505 10^{-4}
.3Sb(β)	4.433 10^{-3}	4.124 10^{-5}	7.216 10^{-5}
.5Sb(β)	1.959 10^{-3}	-3.093 10^{-5}	9.278 10^{-5}
.8Sb(β)	8.144 10^{-3}	1.031 10^{-4}	1.237 10^{-4}
.05Te(β)	7.835 10^{-3}	7.216 10^{-5}	1.443 10^{-4}
.1Te(α)	2.240 10^{-1}	1.800 10^{-3}	
(β)	1.959 10^{-3}	2.062 10^{-5}	4.124 10^{-5}
.3Te(β)	1.144 10^{-2}	1.649 10^{-4}	1.546 10^{-4}
.5Te(β)	5.670 10^{-3}	8.247 10^{-5}	8.247 10^{-5}
.8Te(β)	7.423 10^{-3}	1.031 10^{-4}	1.031 10^{-4}
.05Zr(α)	-5.000 10^{-3}	-1.000 10^{-4}	
(β)	1.814 10^{-2}	2.990 10^{-4}	2.062 10^{-4}
.1Zr(α)	-4.000 10^{-2}	-3.000 10^{-4}	
(β)	4.433 10^{-3}	9.278 10^{-5}	3.093 10^{-5}
.3Zr(α)	1.400 10^{-2}	1.000 10^{-4}	
(β)	6.907 10^{-3}	1.237 10^{-4}	8.247 10^{-5}
.5Zr(α)	-1.120 10^{-1}	-9.000 10^{-4}	
(β)	6.186 10^{-3}	8.247 10^{-5}	8.247 10^{-5}
.8Zr(α)	3.300 10^{-2}	2.000 10^{-4}	
(β)	8.559 10^{-3}	1.261 10^{-4}	1.081 10^{-4}

TABLE 6.

REGRESSION FORMULAE OF EXPERIMENTAL ALLOY SYSTEMS.

Alloy System	Temp. ^oK	Formula	(r^2)
Sn-Ag	297	a=5.832+.0021(a/o) c=3.182+-.0004(a/o) v=108.21+.04(a/o)	r^2=.75 r^2=.12 r^2=.5
	394	a=5.8437+.0099(a/o) c=3.1986+.0030(a/o) v=109.24+.45(a/o)	r^2=.61 r^2=.23 r^2=.95
Sn-Cd	297	a=5.8318+.0005(a/o) c=3.1823+-.0005(a/o) v=108.24-.02(a/o)	r^2=.03 r^2=.15 r^2=.02
	394	a=5.8450+-.0024(a/o) c=3.1969+-.0077(a/o) v=109.22-.35(a/o)	r^2=.28 r^2=.88 r^2=.74
Sn-In	297	a=5.8325+-.0024(a/o) c=3.1819+-.0015(a/o) v=108.25-.14(a/o)	r^2=.41 r^2=.73 r^2=.65
	394	a=5.8454+.0015(a/o) c=3.1985+-.0033(a/o) v=109.17+.36(a/o)	r^2=.38 r^2=.27 r^2=.19
Sn-Sb	297	a=5.8323+.0106(a/o) c=3.1829+.0021(a/o) v=108.26+.45(a/o)	r^2=.78 r^2=.30 r^2=78
	394	a=5.8459+-.0182(a/o) c=3.1941+-.0038(a/o) v=109.18-.90(a/o)	r^2=1.00 r^2=.11 r^2=.88
Sn-Te	297	a=5.8319+.0087(a/o) c=3.1810+.0080(a/o) v=108.20+.57(a/o)	r^2=86 r^2=72 r^2=.82

TABLE 6. CONT.

	394	a=5.8470+.0012(a/o) c=3.1964+-.0003(a/o) v=109.29-2.94 10^{-3}(a/o)	r^2=.04 r^2=.01 r^2=1.24 10^{-4}
Sn-Zr	297	a=5.8315+.0053(a/o) c=3.1823+.0034(a/o) v=108.22+.30(a/o)	r^2=.83 r^2=.55 r^2=.67
	394	a=5.8482+-.0119(a/o) c=3.1948+-.0081(a/o) v=109.27-.72(a/o)	r^2=.63 r^2=.41 r^2=.97

In addition to this, a multiple regression analysis by the least squares method was performed on the experimental data in order to determine a second degree polynomial in two independent, and one dependent variable that would describe the combined effects of temperature and alloy composition upon the unit cell volumnes of the tetragonal alloys. The results of this analysis is presented in Table 7, where the coefficients, A,B1,B2,B3, and B4 correspond to the general equation

$$V=A+B1(C)+B2(T)+B3(C^2)+B4(T^2)$$

where;

C=composition in atomic percent
T=temperature in degrees Kelvin
V=unit cell volumne
A,B1,B2,B3,B4-Constants

The percentage volumne change upon alloying, $(\Delta V/V)\%$ has been calculated from the crystallographic data, and may be found in Table 8 along with the theoretical or calculated lattice volume change obtained by the equation;

$$\left(\frac{\Delta V}{V}\right)\%=100\ \frac{(1-F)(A.R._{Sn})+(F)(A.R._{A})}{(A.R._{Sn})}$$

where;

F=atomic fraction of alloying element.
$A.R._{Sn}$=atomic radii of Tin.
$A.R._{A}$=atomic radii of the alloying addition.

In Table 8, many different atomic radii available were used to calculate the theoretical volumne expansion upon alloying. They are listed by the columnes as:

E = Experimental Value
G = Goldschmidt Radii
D = ½ Distance of Closest Approach
M = Mott and Jones
A = Atomic Radius (Coordination Number = 4)
C = Covalent Radius

Table 7.

MULTIPLE REGRESSION ANALYSIS OF CRYSTALLOGRAPHIC DATA

Alloy System	Polynomial Coefficients					Index of Determination
	A	B1	B2	B3	B4	
Sn-Ag	124.191	-.121429	-.102512	.586981	1.6338×10^{-4}	.896369
Sn-Cd	146.09	-.293831	-.229492	.208808	3.44276×10^{-4}	.960535
Sn-In	190.932	1.03913	-.49707	-1.19559	7.34806×10^{-4}	.928397
Sn-Sb	70.0053	-.758557	.224976	1.37248	-3.20792×10^{-4}	.245442
Sn-Te	80.2448	.542037	.159912	-.235299	-2.20299×10^{-4}	.844779
Sn-Zr	106.746	-1.16547	3.60107×10^{-3}	1.25947	8.06525×10^{-6}	.765401

Table 8.

PERCENTAGE VOLUMNE CHANGE UPON ALLOYING

Solute	Comp. a/o	(°K) Temp	$(\frac{\Delta V}{V})$% Beta E	G	D	M	A	C
Ag	.05	297	.018	-.0044	-.0022	-.0073	-.0056	N/A
		394	N/A	----	----	----	----	N/A
	.1	297	.018	-.0089	-.0044	-.0145	-.0111	N/A
		394	-.503	----	----	----	----	N/A
	.3	297	.009	-.0266	-.0133	-.0435	-.0333	N/A
		394	.055	----	----	----	----	N/A
	.5	297	.009	-.0443	-.0222	-.0726	-.0555	N/A
		300	N/A	----	----	----	----	N/A
	.8	297	.046	-.0709	-.0355	-.1161	-.0888	N/A
		394	.320	----	----	----	----	N/A
Cd	.05	297	.083	-.0019	-.0007	-.0035	-.0025	N/A
		394	-.110	----	----	----	----	N/A
	.1	297	.046	-.0038	-.0014	-.0070	-.0049	N/A
		394	-.311	----	----	----	----	N/A
	.3	297	-.009	-.0114	-.0043	-.0210	-.0148	N/A
		394	-.082	----	----	----	----	N/A
	.5	297	.037	-.0190	-.0071	-.0349	-.0247	N/A
		394	-.284	----	----	----	----	N/A
	.8	297	.028	-.0304	-.0114	-.0559	-.0395	N/A
		394	-.265	----	----	----	----	N/A
In	.05	297	.046	-.0003	.0038	-.0005	.0012	N/A
		394	-.229			----	----	N/A
	.1	297	.074	-.0006	.0075	-.0011	.0025	N/A
		394	-.183		----	----	----	N/A
	.3	297	0	-.0019	.0226	-.0032	.0074	N/A
		394	.055	----	----	-----	----	N/A
	.5	297	0	-.0032	.0377	-.0054	.0123	N/A
		394	.430	----	----	----	----	N/A
	.8	297	-.074	-.0051	.0604	-.0086	.0198	N/A
		394	-.046	----	----	----	----	N/A
Sb	.05	297	.351	.0009	-.0020	.0019	-.0009	N/A
		394	-.201	----	----	----	----	N/A
	.1	297	.582	.0019	-.0039	.0038	-.0019	N/A
		394	-1.318	----	----	----	----	N/A
	.3	297	.231	.0057	-.0118	.0113	-.0056	N/A
		394	-.357	----	----	----	----	N/A
	.5	297	.342	.0095	-.0197	.0188	-.0093	N/A
		394	-.467	----	----	----	----	N/A
	.8	297	.323	.0152	-.0315	.0301	-.0148	N/A
		394	.064	----	----	----	----	N/A

Table 8 Cont.

PERCENTAGE VOLUMNE CHANGE UPON ALLOYING

Solute	Comp a/o	(^{o}K) Temp	$(\frac{\Delta V}{V})$% Beta					
			E	G	D	M	A	C
Te	.05	297	.028	.0038	-.0020	N/A	-.0006	N/A
		394	-.256	----	----	----	----	N/A
	.1	297	.434	.0076	-.0039	N/A	-.0012	N/A
		394	-.375	----	----	----	----	N/A
	.3	297	.065	.0228	-.0118	N/A	-.0037	N/A
		394	.101	----	----	----	----	N/A
	.5	297	.388	.0380	-.0197	N/A	-.0062	N/A
		394	-.092	----	----	----	----	N/A
	.8	297	-.370	.0608	-.0315	N/A	-.0099	N/A
		394	.046	----	----	----	----	N/A
Zr	.05	297	.028	.0006	.0024	-.0040	0	N/A
		394	.659	----	----	----	----	N/A
	.1	297	.508	.0013	.0049	-.0081	0	N/A
		394	-.082	----	----	----	----	N/A
	.3	297	.203	.0038	.0147	-.0242	0	N/A
		394	-.165	----	----	----	----	N/A
	.5	297	.083	.0063	.0245	-.0403	0	N/A
		394	-.348	----	----	----	----	N/A
	.8	297	.259	.0101	.0392	-.0645	0	N/A
		394	N/A	----	----	----	----	N/A
			$(\frac{\Delta V}{V})$% Alpha Base					
Ag	.05	276	.633	----	.0014	----	----	-.0025
		286	-.066	----	----	----	----	----
	.1	276	.937	----	.0028	----	----	-.0050
		286	-.062	----	----	----	----	----
	.3	276	.110	----	.0083	----	----	-.0149
		286	-.686	----	----	----	----	----
	.5	276	-.004	----	.0139	----	----	-.0248
		286	-.616	----	----	----	----	----
	.8	276	-.278	----	.0222	----	----	-.0397
		286	-.073,-.686	----	----	----	----	----
In	.05	276	-.194	----	.0078	----	----	.0011
		286	-.292	----	----	----	----	----
	.1	276	.608	----	.0157	----	----	.0021
		286	-.040	----	----	----	----	----
Te	.1	276	-.223	----	.0021	----	----	-.0035
		286	.226	----	----	----	----	----

Table 8 Cont.

PERCENTAGE VOLUMNE CHANGE UPON ALLOYING

Solute	Comp a/o	(^{o}K) Temp	(ΔV/V)% Alpha Base					
			E	G	D	M	A	C
Zr	.05	276	.201		.0064			.0014
		286	-.186					
	.1	276	.546		.0128			.0028
		286	.029					
	.3	276	.348		.0384			.0085
		286	.029					
	.5	276	.417		.0641			.0142
		286	-.361					
	.8	276	-.293		.1025			.0227
		286	-.540					

THERMODYNAMIC RESULTS

The results of the thermodynamic calculations are presented in Tables 9 and 10 and in Appendix C. Table 9 contains the results of linear regression analysis that was performed on the values of ΔH obtained experimentally. Graphical representation of this data may be found in Appendix C, figures 44 thru 60. In order to determine the Free Energy change, ΔF, the Enthalpy values, ΔH, were plotted as a function of $\frac{1}{T}$ in Appendix E. A linear regression analysis was performed on these curves and is presented in Table 10. Since the curves are linear the free energy change was then calculated and plotted as a function of temperature in Appendix F.

Table 9.

ΔH VERSUS TEMPERATURE PARAMETER

Alloy	ΔH versus T, (^oK) Equation	Coefficient of Determination, (r^2)
Sn	$\Delta H=7515.8-18.8T$	.998
.05Ag	$\Delta H=12195.3-30.0T$	.996
.1Ag	$\Delta H=8980.0-22.1T$	.958
.3Ag	$\Delta H=7811.4-19.5T$	.998
.05Cd	$\Delta H=8290.8-20.4T$	.998
.1Cd	$\Delta H=8606.8-21.3T$	.998
.3Cd	$\Delta H=8423.5-20.7T$	.992
.05In	$\Delta H=8496.2-21.2T$	.996
.1In	$\Delta H=8682.4-21.6T$	.998
.3In	$\Delta H=14115.1-35.1T$	1.000
.05Sb	$\Delta H=8086.1-20.2T$	.996
.1Sb	$\Delta H=8003.5-20.0T$	1.000
.3Sb	$\Delta H=13107.7-32.7T$	.996
.05Te	$\Delta H=8108.3-19.5T$	.994
.1Te	$\Delta H=8657.3-19.9T$	.998
.3Te	$\Delta H=8195.2-20.4T$	1.000
.05Zr	$\Delta H=8043.3-20.2T$	.996
.1Zr	$\Delta H=8634.7-21.3T$	.996
.3Zr	$\Delta H=8084.0-20.2T$	.996

TABLE 10.

ΔH VERSUS $(\frac{1}{T})$ PARAMETERS

Alloy	ΔH versus $(\frac{1}{T})$ equation	Coefficient of Determination, (r^2)
Sn	$\Delta H=2{,}486{,}170.91(\frac{1}{T})-6181.08$	$r^2=.99$
.05Ag	$\Delta H=4{,}089{,}276.25(\frac{1}{T})-9993.67$	$r^2=.97$
.1Ag	$\Delta H=3{,}029{,}255.42(\frac{1}{T})-7414.97$	$r^2=.99$
.3Ag	$\Delta H=2{,}677{,}461.64(\frac{1}{T})-6664.85$	$r^2=1.00$
.05Cd	$\Delta H=2{,}784{,}701.81(\frac{1}{T})-6769.14$	$r^2=1.00$
.1Cd	$\Delta H=2{,}911{,}437.65(\frac{1}{T})-7139.15$	$r^2=1.00$
.3Cd	$\Delta H=2{,}827{,}288.76(\frac{1}{T})-6876.31$	$r^2=.99$
.05In	$\Delta H=2{,}899{,}717.58(\frac{1}{T})-7185.74$	$r^2=1.00$
.1In	$\Delta H=2{,}961{,}856.69(\frac{1}{T})-7339.48$	$r^2=1.00$
.3In	$\Delta H=4{,}805{,}489.24(\frac{1}{T})-11879.29$	$r^2=1.00$
.05Sb	$\Delta H=2{,}763{,}285.59(\frac{1}{T})-6853.26$	$r^2=1.00$
.1Sb	$\Delta H=2{,}738{,}126.60(\frac{1}{T})-6804.10$	$r^2=1.00$
.3Sb	$\Delta H=4{,}480{,}298.71(\frac{1}{T})-11125.78$	$r^2=1.00$
.05Te	$\Delta H=2{,}826{,}387.59(\frac{1}{T})-6766.48$	$r^2=.98$
.1Te	$\Delta H=3{,}216{,}750.58(\frac{1}{T})-7470.30$	$r^2=.96$
.3Te	$\Delta H=2{,}789{,}913.57(\frac{1}{T})-6892.20$	$r^2=1.00$
.05Zr	$\Delta H=2{,}762{,}853.00(\frac{1}{T})-6892.65$	$r^2=1.00$
.1Zr	$\Delta H=2{,}918{,}952.26(\frac{1}{T})-7154.84$	$r^2=1.00$
.3Zr	$\Delta H=2{,}819{,}245.98(\frac{1}{T})-7017.08$	$r^2=1.00$

MISCELLANEOUS OBSERVATIONS

The observations that came about during the course of experimentation may be catagorized into three major areas, nucleation of alpha precipitates, growth of the alpha regions, and precipitation of secondary phases at low temperatures.

Nucleation of the pieces of alpha was accomplished by seeding with small specimens of alpha tin. However the alloys exhibited various rates of nucleation depending upon the solute type and composition ranges. Pure tin was nucleated most readily, with this nucleation enhanced by using a specimen of beta that was quenched from the liquid state in ice water. The silver alloys were next, followed closely by the zirconium alloys. There was then a rate gap before the tellurium alloys showed signs of nucleation, with the indium and cadmium following in descending order. The antimony alloys showed no signs of nucleation even after one year of treatment.

Growth of the alpha phase nuclei was observed to proceed not in a true three dimensional manner, but by proceeding along the free surface of the specimen until it was completely covered, and then proceeding into the center of the specimen. Once again, the silver and then zirconium alloys followed pure tin in the rate of growth, followed by another rate gap untill the tellurium and indium alloys were found. The slowest rate of growth was found in the cadmium alloys, since no growth could be observed in the unnucleated antimony specimens. In all cases however, the growth rate was found to be proportioned to alloy composition. Indium demonstrated this phenomena most effectively, since up to .1 atomic percent Indium, growth was exhibited while after .1 atomic percent, the growth of the alpha phase was inhibited to a large degree, depending upon the amount of solute addition, For the relative rates of nucleation and growth refer to Table 13.

Only one experimental alloy showed the precipitation of a secondary phase during the low temperature x-ray analysis. This occurred in the .8 atomic percent zirconium alloy at the low temperature x-ray patterns. It was observed that the orthorhombic, (c54), structure of $ZrSn_2$ was precipitated out of the alpha solution at 273°C and decreased in concentration at 286°C, indicating a true solubility limit in alpha tin.

Table 11.

COMPARATIVE OBSERVATIONS OF NUCLEATION AND GROWTH RATES OF ALPHA TIN

Solute Addition	Percentage (a/o)	Nucleation Rate	Growth Rate
Sn	Pure	10	10
Ag	.05	9	9
	.1	9	9
	.3	8	8
	.5	8	8
	.8	7	7
Cd	.05	5	2
	.1	5	2
	.3	4	1
	.5	4	1
	.8	3	1
In	.05	8	3
	.1	7	2
	.3	6	1
	.5	5	0
	.8	4	0
Sb	.05	0	
	.1	0	
	.3	0	
	.5	0	
	.8	0	
Te	.05	5	5
	.1	5	5
	.3	4	4
	.5	3	4
	.8	2	4
Zr	.05	8	8
	.1	8	8
	.3	7	7
	.5	7	7
	.8	6	6

- - - - - - - - - - - - - -

CHAPTER V

DISCUSSION

In this investigation, it is necessary to determine a basis for decisionmaking on the experimental results obtained. The index of determination has been chosen for this purpose since it is an indicative value of the scatter that is exhibited in the data as compared to the equation obtained in a regression analysis. In order to base a decision on the validity of the equation, it is necessary to establish a confidence interval for this value. In this case, a 95 percent confidence interval was chosen, and critical values of the index of determination were obtained.[41]

These values are presented in Table 12. If the experimental index of determination exceeds this value, which is dependent upon the number of data points, (n), then the equation obtained is statistically significant. If the experimental value should fall below the critical value then the equation is statistically insignificant and must be rejected. The individual results obtained for the crystallographic and thermodynamic data will be reviewed in this manner.

In reviewing the crystallographic results, it is readily seen that none of the equations obtained for the lattice parameter, "C", versus atomic percent at any temperature are applicable since in all

---

Footnote:

[41] J.E. Freund, Statistics, <u>A First Course</u> (Englewood Cliffs, N.J.: Prentice Hall, 1970), p. 312.

Table 12.

CRITICAL VALUES OF THE COEFFICIENT OF DETERMINATION r^2*

n	$r^2_{.025}$	$r^2_{.005}$
3	.994	
4	.903	.998
5	.771	.920
6	.658	.841
7	.569	.766
8	.500	.696
9	.444	.637
10	.399	.585

*This table calculated from Table VI of J.E. Freund, Statistics, A First Course, Prentice-Hall, Inc. Englewood Cliffs, N.J., 1970.

cases, the index of determination is below the critical value. In the lattice parameter "A" versus atomic percentage, only the Tellurium and Zirconium systems at 297°K and the Antimony at 394°K are significant. However the equations obtained for unit cell volume versus percent have faired somewhat better, with the Tellurium at 297°K, Zirconium at 394°K, Antimony at 297° and 394°K, and the Silver at 394°K being significant. In all alloy groups, no significant change in the c/a ratio was observed, indicating substitutional alloying has taken place, which in the case of the silver alloys, contradics theories set forth by T.R. Anthony and D. Turnbull on interstitial solutions of silver in tin [42]. The coefficients of lattice thermal expansion are in considerable doubt

Footnote:

[42] T.R. Anthony and D. Turnbull, "On the theory of Interstitial Solutions of the Noble Metals in Lead, Tin, Thalliu, Indium, and Cadmium." Applied Physics Letters, v. 8, no. 5, (March, 1966) pp. 120, 121.

since they are derived from only two data points. The $\Delta v/v$ values in Table 8 reflect a much greater increase due to alloying additions than expected. This is possible due to the highly covalent character of the bond and subsequent balance of the electrons being upset by the addition of elements of different electron structure.

The exceptionally high specific heats of the samples found in the equations in Table 9 indicate that much heat was absorbed into the calorimeter medium during the course of the experimental runs. These equations could be corrected by determining a heat gain factor for the temperature region in question. It can also be noted in Table 9 that the change in specific heats are not consistant with the amounts of alloying additions. This is believed to be due to problems encountered in the electrical monitoring of the experiments. Much of the difficulty encountered in the course of this investigation was centered around the controversy as to what type of reaction was exhibited by tin. Specifically, whether the reaction proceeded martensitically or by a nucleation and growth type process. The following discussion is based upon the observations encountered in this study and the general characteristics of both types of reactions.

Martensitic reactions are essentially isothermal and independent of time with a thermally assisted nucleation process. The amount of transformation is dependent upon temperature, with the spontaneous initiation at a temperature M_s, and completion at a temperature M_f. Within this temperature range, the velocity of the reaction is independent of temperature. The reactions are generally reversible, with a single crystal of the initial phase transformable to many crystals of the second phase and upon transforming back will result in an identical single crystal of the initial phase. There is a temperature hysteresis associated with the reverse transformation, indicating a discreet potential energy barrier associated with the process. Plastic stress in the transformation region will increase the temperature hysterisis loop, and out of the region will inhibit the transformation. There is no composition change associated with the transformation, and the volumne change is small. The product phase is usually in the form of flat plates or thin, parrallel sided bands formed on the habit plane of the original lattice, resulting in a definite orientation or twin relationship between the product and original lattices. Stabilization may take place by cooling to a temperature within the transformation hysterisis loop, stopping, and then proceeding again to a lower temperature. In this case, the transformation will not start immediately, and the amount of transformation will be less than when no stoppage has taken place. In fact, new plates will be formed instead of growth of old ones.

Nucleation and Growth reactions are athermal processes that are dependent upon time. The temperature dependence is due to the fact that as the temperature decreases, the free energy of formation of nuclei of critical size will decrease faster than the thermal energy. In the solid state, other terms will contribute to the energy necessary to cross the boundary. Thus, the reaction rate will increase with decreasing temperature to a maximum value and then will decrease again as the thermal energy decreases past the energy necessary to cross the boundary. Therefore it is possible to quench the reaction by passing through the temperature range faster than the time required to form a critically sized nuclei.

At constant temperature, the amount of material transformed will increase with time to completion due to the effect of atomic diffusion. This type of transformation is irreversible both crystallographically and thermodynamically since the critically sized nuclei for the different phases are of different size and structure. The reaction is accelerated by cold work prior to transformation since the formation of vacant lattice sites increases the driving force, and decreases the free energy barrier. Compositions and atomic volumnes need not be related between the phases, and any orientation relationships that exist between the phases occurs only in the stages of nucleation and early growth. In the case of homogeneous changes, such as pure tin, the reaction velocity is characterized by the general equation.

$$R = Ae^{kt}$$

where; R = reaction rate
A = constant
k = constant
T = temperature.

CHAPTER VI

Conclusions

In reviewing the phase transformation in tin and the affects of alloying additions it is seen that the transformation is athermal, and time dependent with the amount of the product phase increasing to completion. There is no spontaneous initiation or completion of new phases, and the velocity of the reaction is time dependent. It is an irreversible reaction, since reversing the reaction does not result in identical grains of the original structure. There is no discreet energy barrier, since no single factor is predominant in the reaction. Plastic Stress will increase the reaction rate to a marked degree due to the creation of vacancies and the subsequent increase in atomic diffusion rates. The volumne change of the reaction is very large, with the alpha phase in the form of pustules with no direct orientation relationship encountered in this investigation. Furthermore, there is no stabilization of the reaction, i.e., if cooled into the transformation temperature range, stopped, and then cooled further, the original pustule will continue to grow, and no new nuclei are formed. The reaction rate is maximum at a value of $-35^{o}C$, but exists in a temperature range of $12.3^{o}C$ to $-60^{o}C$. It is also possible to quench the reaction. Finally, in work by Burgers and Groen[43] it

Footnote:

[43] W.G. Burgers and L.J. Groen, "Mechanism and Kinetics of the Allotropic Transformation of Tin." Disc. Faraday Soc., v. 23, no. 183, p.p. 183-195.

was found that the reaction rate, (R), was expressed by the general equation;

$$R = Ae^{kt}$$

where; R = reaction time
A = constant
k = constant
t = temperature.

This summary of the phase transformation in tin results in classifying this reaction as a nucleation and growth type process. The driving forces of the reaction are the change in the electron structure and the free energy of the formation of critically sized nuclei. The inhibiting forces are; the lack of thermal energy since the reaction occurs at such a low temperature, the large volumne change associated with the transformation, and the decrease in the coordination number between the beta and alpha phases necessitating large atomic diffusion. The transformation temperature is affected by the activation energy for atomic diffusion, the recrystallization temperature, the grain size of both phases, the thermal energy available, and the energy necessary for cleavage of atomic planes due to the large volumne change. The electron structure factors are the evident cause of the seeding qualities of the reaction.

The experimental results obtained in this investigation are intended to add to the information available to create a justifiable mathematical expression for the transformation and the affects of alloying elements. However, many more experimentally determined points are necessary in order to statistically justify the equations obtained.

The general affects of the alloying additions did however enlighten upon the large importance of the critical electron structure balance of the reaction. The addition of small amounts of Antimony will inhibit the reaction to a large degree. This could be helpful to increase the resistance of solders, tin plate, and tin alloys to Tin Disease at low service temperatures.

APPENDIX A

Calculation of X-Ray Results

PAGE

Calculation of Lattice Parameter"A" For Cubic Systems.............. 49

Sample Readout of Program For Cubic Systems.........................51

Calculation Of Lattice Parameters"A" and "C" For Tetragonal Systems.52

Sample Readout of Program For Tetragonal Systems.................. 55

STEP C CALCULATION OF LATTICE PARAMETER A FOR CUBIC SYSTEM

```
      DIMENSION THETA(40),J(40),K(40),L(40)
      N=9
      READ(5,1)(THETA(M),J(M),K(M),L(M),M=1,N)
    1 FORMAT(9(F5.2,3I1))
      DO 3NR=1,5
      WRITE(6,49)
   49 FORMAT('1',//,30X,'SN + 0.1 ZR')
      WRITE(6,50)
   50 FORMAT(4X,'THETA',4X,'PLANE',4X,'PLANE',6X,'COS',7X,'SIN',9X,'H2+'
     *)
      WRITE(6,51)
   51 FORMAT(5X,'IN',5X,'INDICES',2X,'SPACINGS',2X,'SQUARED',3X,'THETA
     +',7X,'K2+')
      WRITE(6,52)
   52 FORMAT(3X,'DEGREES',4X,'HKL',7X,'THETA',18X,'L2')
      A=0
      B=0
      C=0
      D=0
      E=0
      WL=1.54178
      DO 2 M=5,N
      P=(COS(.01745*THETA(M)))**2
      Q=J(M)**2+K(M)**2+L(M)**2
      S=(SIN(.01745*THETA(M)))
      DS=WL/(2*SIN(.01745*THETA(M)))
      SS=S*S
      QQ=Q*Q
      QSS=Q*SS
      PSSS=P*(S+(SS/(.01745*THETA(M))))
      QPSSS=Q*PSSS
      SPSSS=PSSS*PSSS
      SSPSSS=SS*PSSS
```

STEP C CALCULATION OF LATTICE PARAMETER A FOR CUBIC SYSTEM

```
      A=QPSSS+A
      B=SPSSS+B
      C=QSS+C
      D=SSPSSS+D
      E=QQ+E
2     WRITE(6,80)THETA(M),J(M),K(M),L(M),DS,P,S,Q
80    FORMAT(F9.2,5 ,3I1,F11.5,F9.4,F10.4,F12.2)
      Y=((C*A)-(D*E))/((A*A)-(B*E))
      X=((C*B)-(D*A))/((E*B)-(A*A))
      AP=SQRT(ABS(WL**2/(4.*X)))
      WRITE(6.100)
100   FORMAT(//,11X,'A',14X,'D',9X,'WAVELENGTH')
      WRITE(6,110)AP,Y,WL
110   FORMAT(3F15.5)
      VOL=AP**3
      WRITE(6,121)
121   FORMAT(//,20X,'VOLUME')
      WRITE(6,122)VOL
122   FORMAT(F25.4)
      WRITE(6,13)
      FORMAT(//,4X,'FROM MIXED ALPHA AND BETA SAMPLE')
3     WRITE(6,17)
17    FORMAT(//,10X,'276 DEGREES KELVIN')
      WRITE(6,200)
200   FORMAT('1')
      STOP
      END

  $ ENTRY
```

SAMPLE READOUT OF PROGRAM FOR CUBIC SYSTEMS

SN + 0.1 ZR

THETA IN DEGREES	PLANE INDICES HKL	PLANE SPACINGS D	COS SQUARED THETA	SIN THETA	H2+ K2+ L2
31.18	331	1.48924	0.7320	0.5176	19.00
35.58	422	1.32514	0.6616	0.5817	24.00
38.10	511	1.24954	0.6194	0.6169	27.00
42.18	440	1.14825	0.5493	0.6714	32.00
44.61	531	1.09786	0.5070	0.7022	35.00

A	D	WAVELENGTH
6.49994	0.00104	1.54178

VOLUME
274.6174

FROM MIXED ALPHA AND BETA SAMPLE
276 DEGREES KELVIN

STEP C CALCULATION OF LATTICE PARAMETERS A AND C AND DRIFT CONSTANT D

```
      DIMENSION THETA(30),J(30),K(30),L(30)
      N=12
      READ(5,1)(THETA(M),J(M),K(M),L(M),M=1,N)
    1 FORMAT(9(F5.2,3I1))
      DO 3 NR=1,5
      WRITE(6,49)
   49 FORMAT('1',//,30X,'SN + 0.3 CD')
      WRITE(6,50)
   50 FORMAT(4X,'THETA',4X,'PLANE',4X'PLANE',6X,'SIN',7X,'COS',5X,'HSQ
     +UARED')
      WRITE(6,51)
   51 FORMAT(5X,'IN',5X,'INDICES',2X,'SPACINGS',12X,'SQUARED
     +',6X,'PLUS')
      WRITE(6,52)
   52 FORMAT(3X,'DEGREES',4X,'HKL',7X,'D',7X,'THETA',5X,'THETA',4X,'
     +K SQUARED',2X,'L SQUARED')
      A=0
      B=0
      C=0
      D=0
      F=0
      G=0
      H=0
      V=0
      W=0
      WL=1.54178
      DO 2 M=6,N
      P=(SIN(.01745*THETA(M)))**2
      Q=J(M)**2+K(M)**2
      R=L(M)**2
      S=(COS(.01745*THETA(M)))**2
      DS=WL/(2*SIN(.01745*THETA(M)))
      PP=P*P
```

STEP C CALCULATION OF LATTICE PARAMETERS A AND C AND DRIFT CONSTANT D

```
      QQ=Q*Q
      RR=R*R
      SPPP=S*(P+(PP/(.01745*THETA(M))))

      QR=Q*R
      SPPPS=SPPP*SPPP
      QSPPP=Q*SPPP

      QPP=Q*PP
      RSPPP=R*SPPP
      RPP=R*PP

      PPSPPP=PP*SPPP
      A=QQ+A
      B=QR+B

      C=QSPPP+C
      D=QPP+D
      F=RR+F

      G=RSPPP+G
      H=RPP+H
      V=SPPPS+V

      W=PPSPPP+W
  2   WRITE(6,80)THETA(M),J(M),K(M),L(M),DS,P,S,Q,R
 80   FORMAT(F9.2,5X,3I1,F11.5,F9.4,F10.4,F12.2,F10.2)

      DEN=A*(F*V-G*G)-B*(B*V-G*C)+C*(B*G-F*C)
      XNUM=D*(F*V-G*G)-H*(B*V-G*C)+W*(B*G-F*C)
      YNUM=A*(H*V-W*G)-B*(D*V-W*C)+C*(D*G-H*C)

      ZNUM=A*(F*W-G*H)-B*(B*W-G*D)+C*(B*H-F*D)
      X=XNUM/DEN
      Y=YNUM/DEN

      Z=ZNUM/DEN
      AP=SQRT(ABS((WL**2)/(4.*X)))
      CP=SQRT(ABS((WL**2)/(4.*Y)))

      VOL=AP*AP*CP
      DTAVOL=VOL-107.9763
      WRITE(6,100)
```

STEP C CALCULATION OF LATTICE PARAMETERS A AND C AND DRIFT CONSTANT D

```
100 FORMAT(//,11X,'A',14X,'C',14X,'D')
    WRITE(6,110)AP,CP,Z
110 FORMAT(3F15.5)

    WRITE(6,101)
101 FORMAT(/,9X,'VOLUME',5X,'VOLUME CHANGE',4X,'WAVELENGTH')
    WRITE(6,110)VOL,DTAVOL,WL

3   WRITE(6,17)
17  FORMAT(//,10X,'394 DEGREES KELVIN
    WRITE(6,111)

111 FORMAT('1')
    STOP
    END

    $ ENTRY
```

SAMPLE READOUT OF PROGRAM FOR TETRAGONAL SYSTEMS

SN + 0.3 CD

THETA IN DEGREES	PLANE INDICES HKL	PLANE SPACINGS D	SIN THETA	COS SQUARED THETA	H SQUARED PLUS K SQUARED	L SQUARED
31.13	112	1.49139	0.5169	0.7328	2.00	4.00
31.81	400	1.46275	0.5270	0.7223	16.00	0.00
32.22	321	1.44610	0.5331	0.7158	13.00	1.00
36.13	420	1.30765	0.5895	0.6525	20.00	0.00
36.50	411	1.29621	0.5947	0.6463	17.00	1.00
39.61	312	1.20932	0.6375	0.5936	10.00	4.00
44.59	501	1.09825	0.7019	0.5073	25.00	1.00

A	C	D
5.84518	3.19568	-0.00044
VOLUME	VOLUME CHANGE	WAVELENGTH
109.18400	1.20772	1.54178

394 DEGREES KELVIN

APPENDIX B

Figures Of X-Ray Results

PAGES

Cubic Lattice Parameter "A" Versus Atomic Percent Figures........ 57,58

Unit Cell Volumnes Versus Atomic Percentage For Tetragonal Alloys..59-70

Lattice Parameter "A" Versus Temperature For Tetragonal Alloys.... 71-76

Lattice Parameter "C" Versus Temperature For Tetragonal Alloys.... 77-82

Unit Cell Volumne Versus Temperature For Tetragonal.............. 83-89

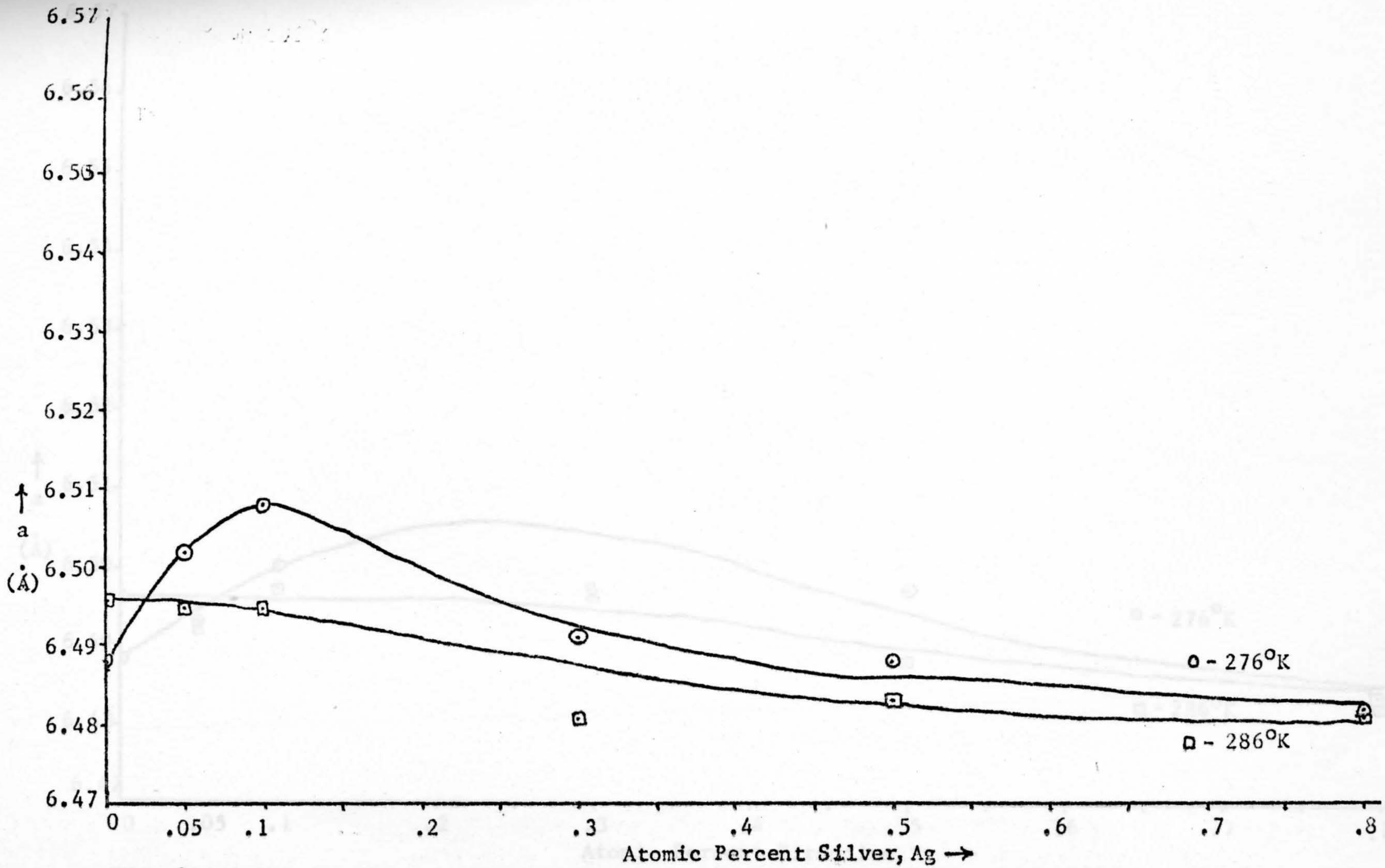

Fig. 8. Cubic lattice parameter, a, versus atomic percent Silver at both 276 and 286 degrees Kelvin.

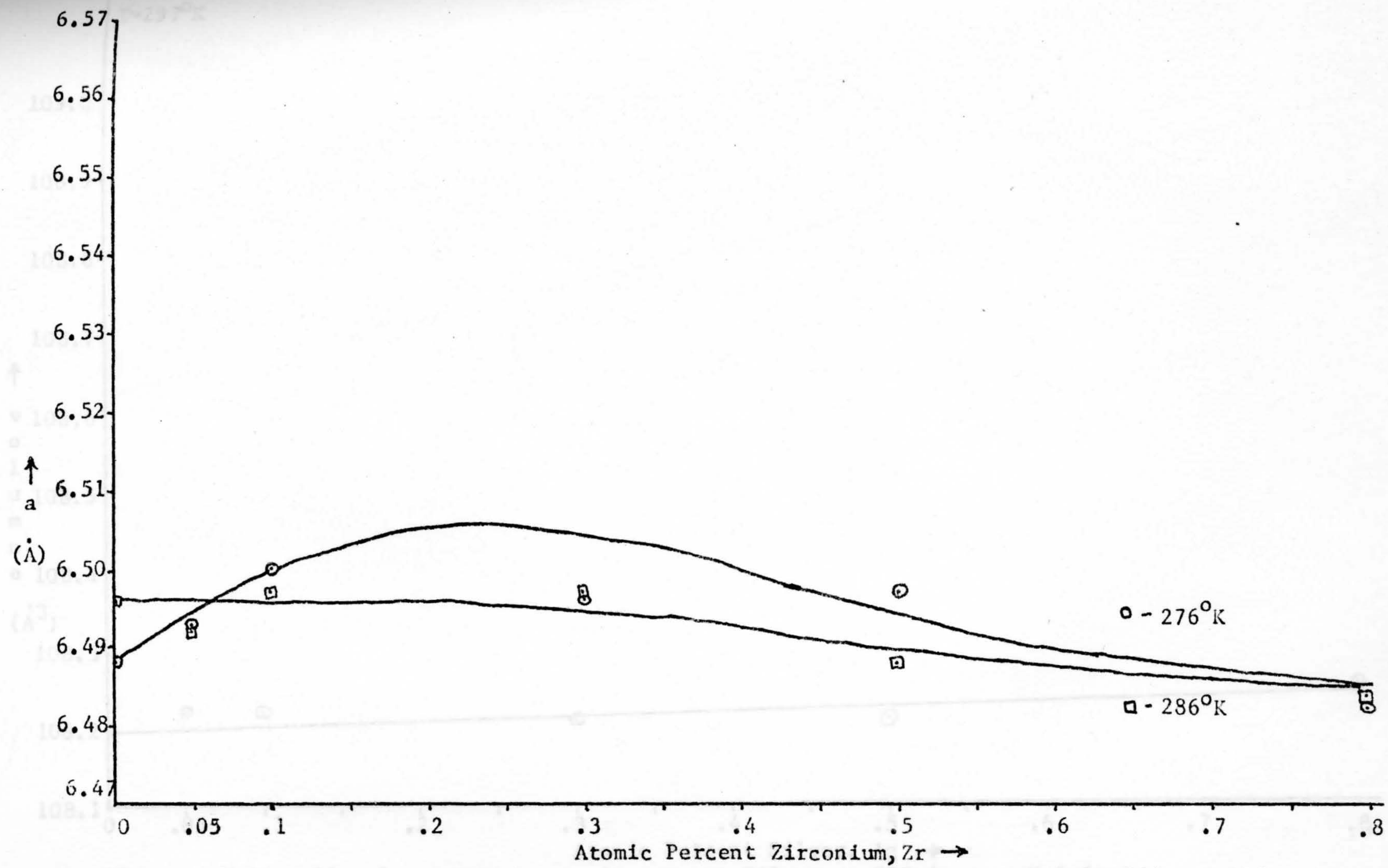

Fig. 9. Cubic lattice parameter, a, versus atomic percent Zirconium at both 276 and 286 degrees Kelvin.

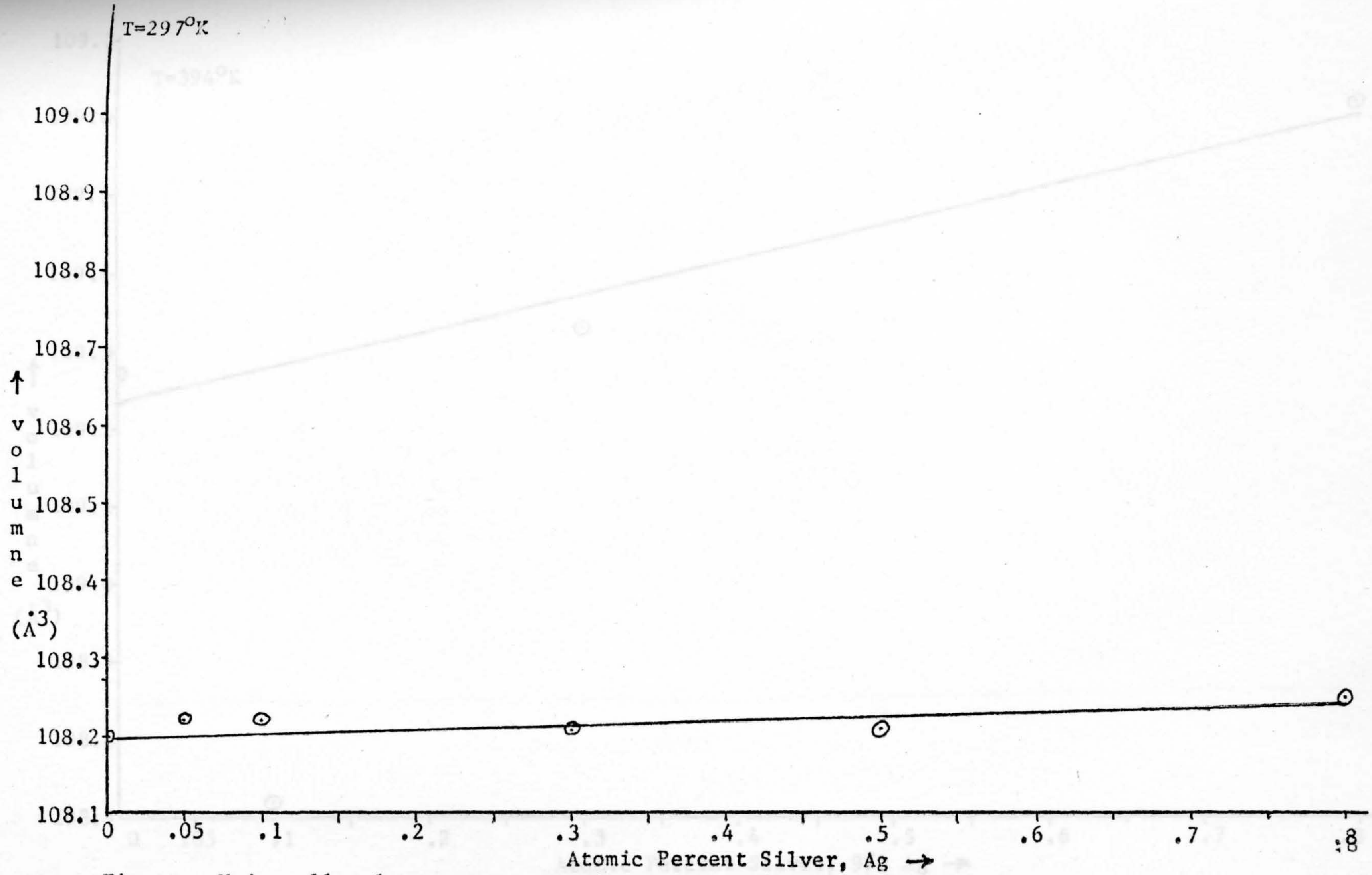

Fig. 10.--Unit cell volumne versus atomic percent Silver at 297 degrees Kelvin.

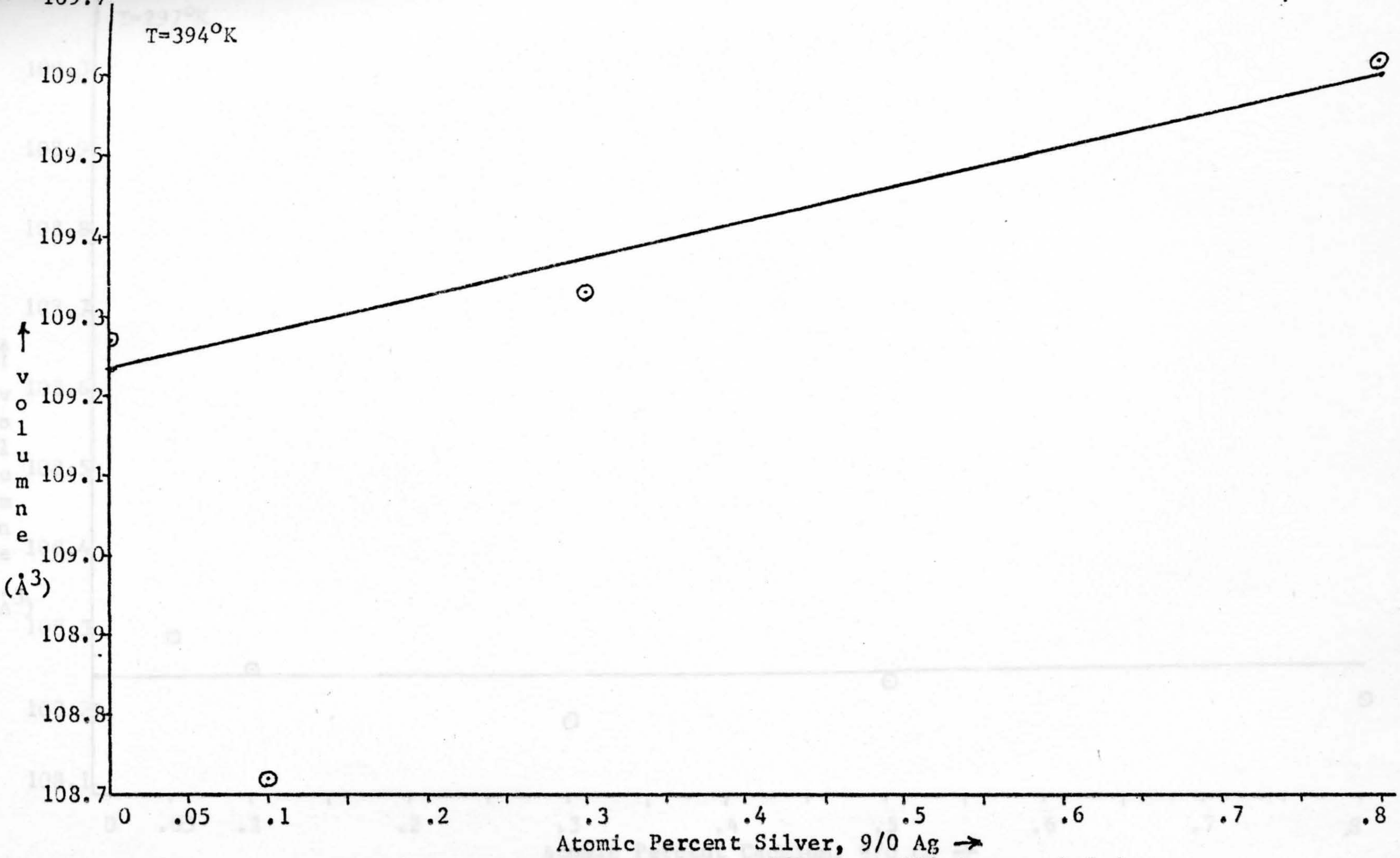

Fig. 11.--Unit cell volumne versus atomic percent Silver at 394 degrees kelvin.

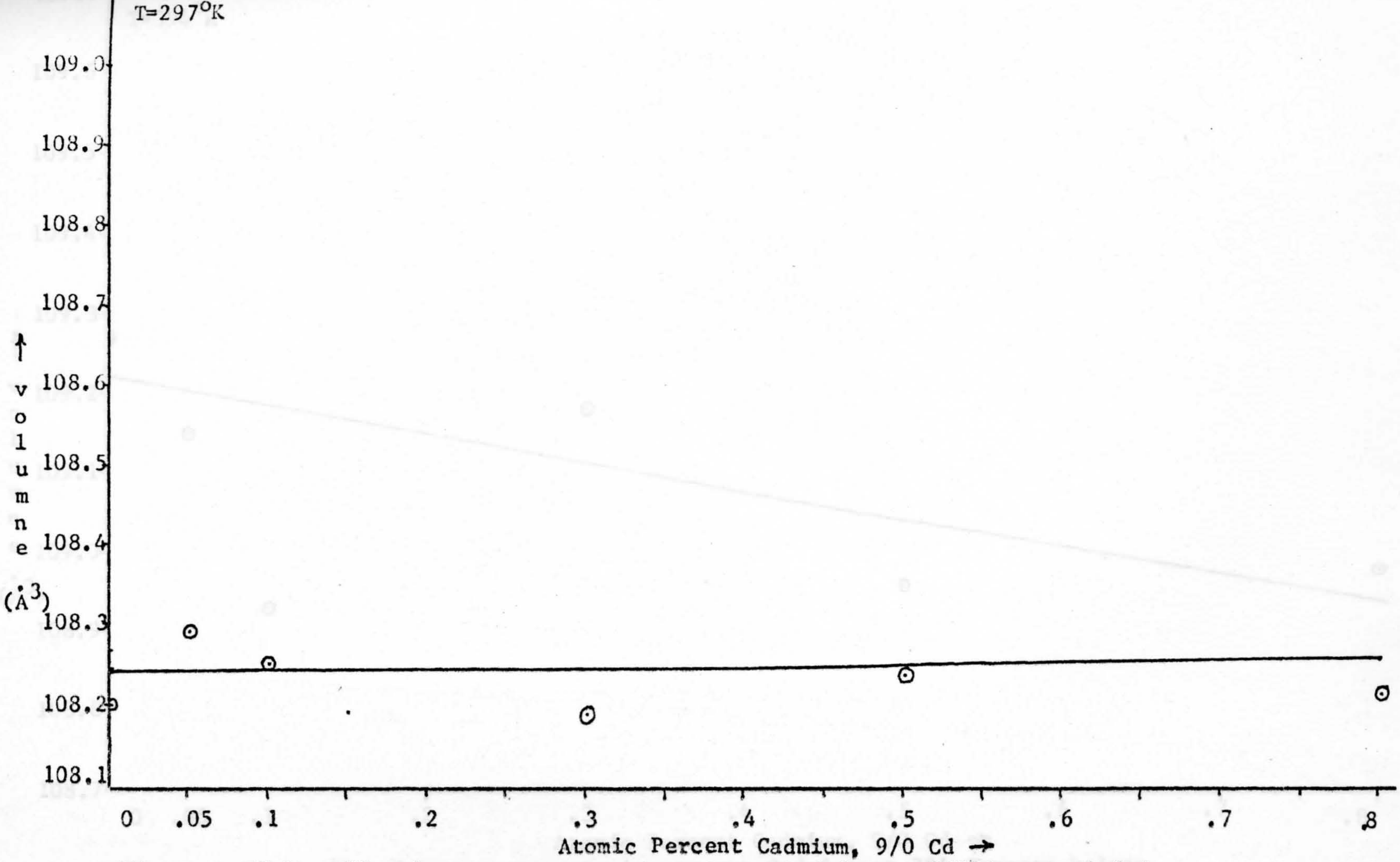

Fig. 12.--Unit cell volumne versus atomic percent Cadmium at 297 degrees kelvin.

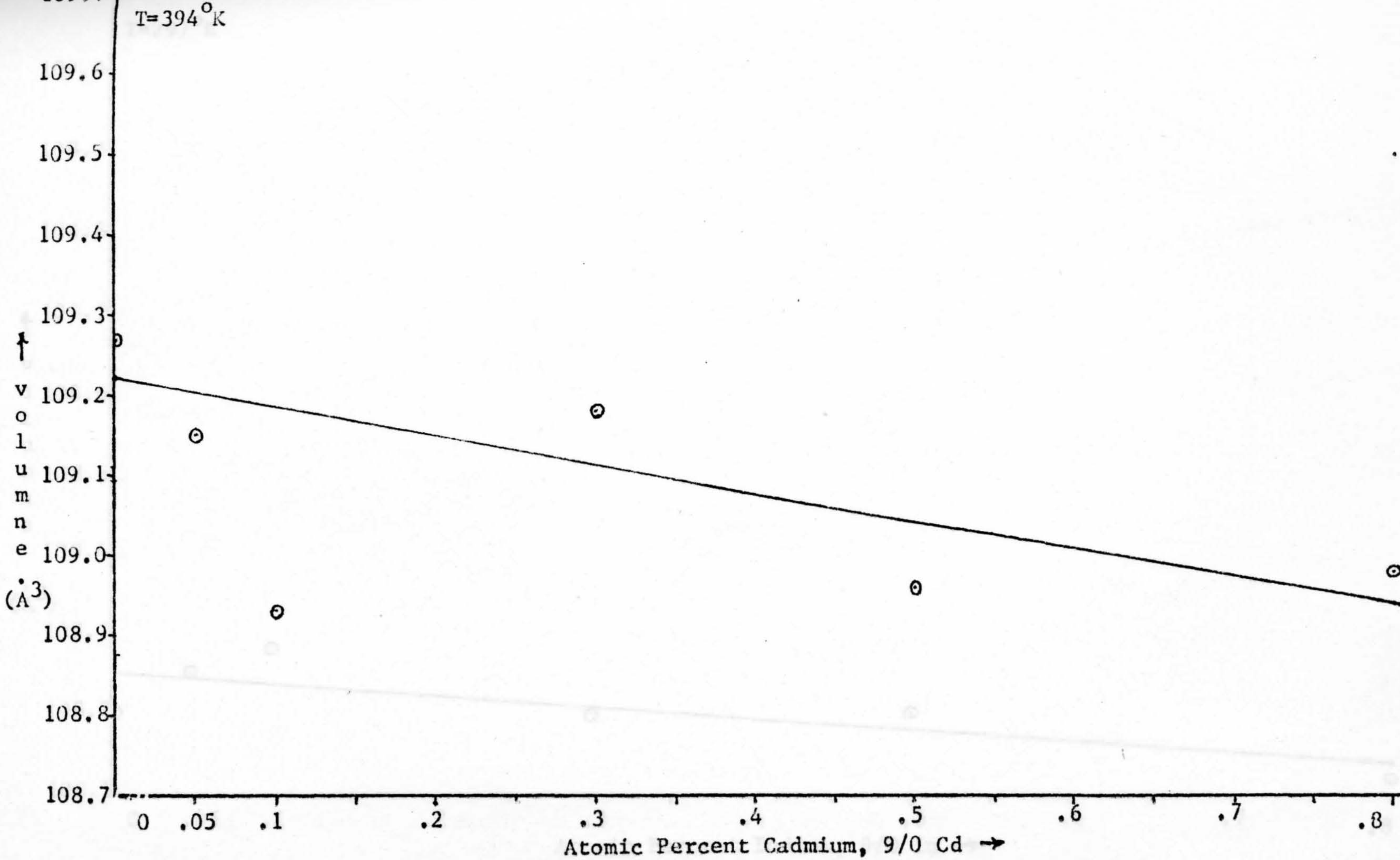

Fig.13.--Unit cell volumne versus atomic percent Cadmium at 394 degrees kelvin

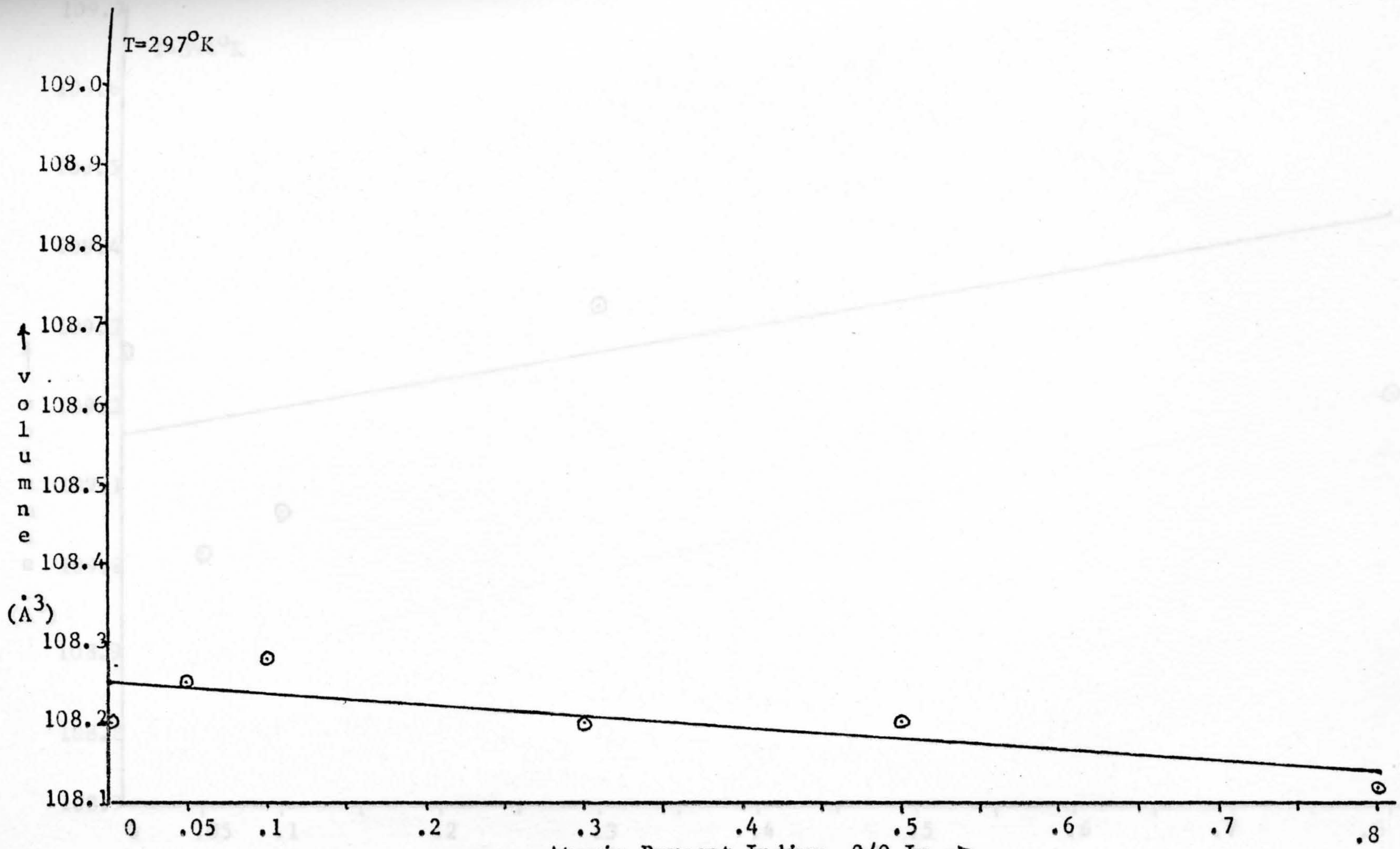

Fig.14.--Unit cell volumne versus atomic percent Indium 297 degrees kelvin.

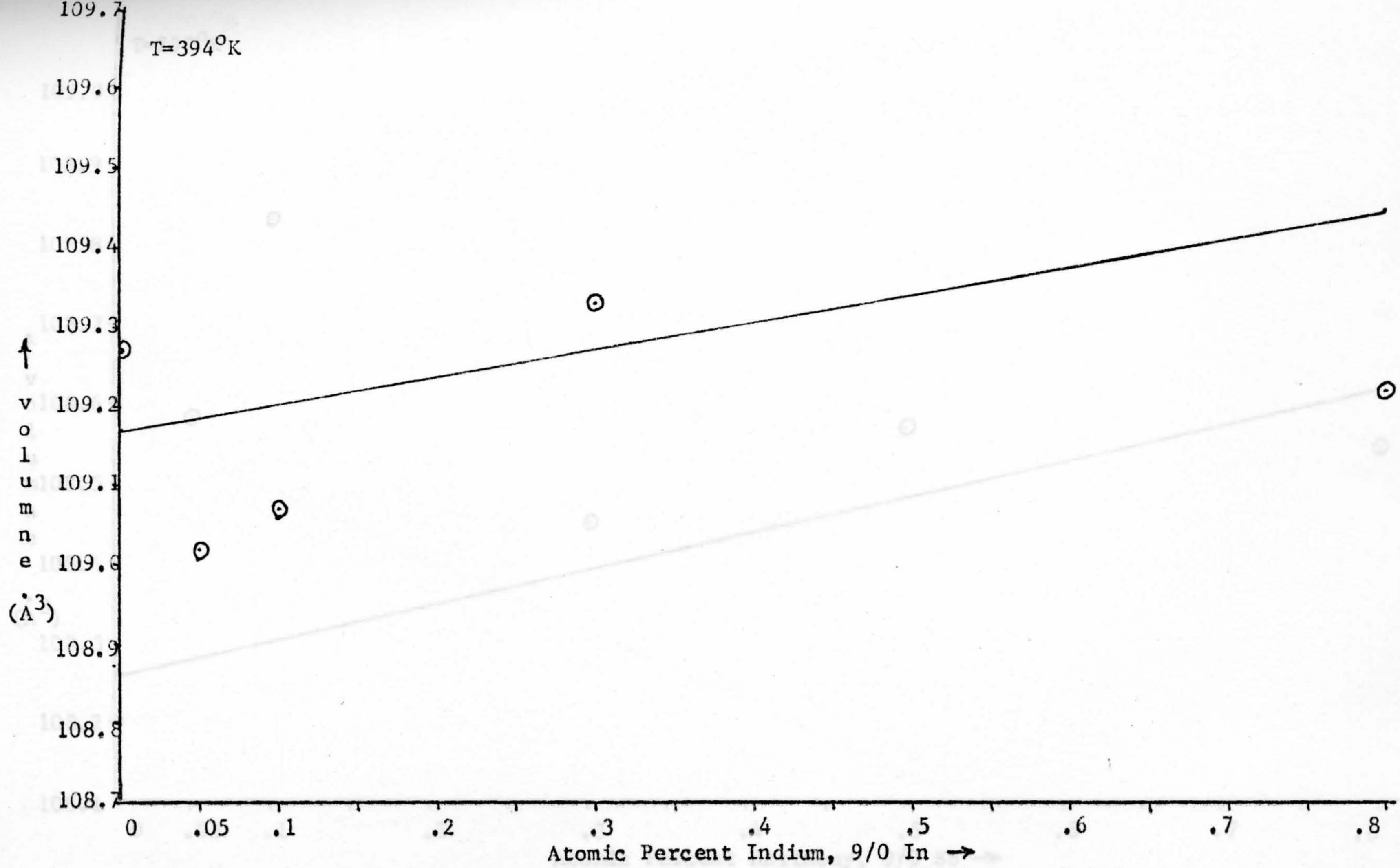

Fig. 15.--Unit cell volumne versus atomic percent Indium at 394 degrees kelvin.

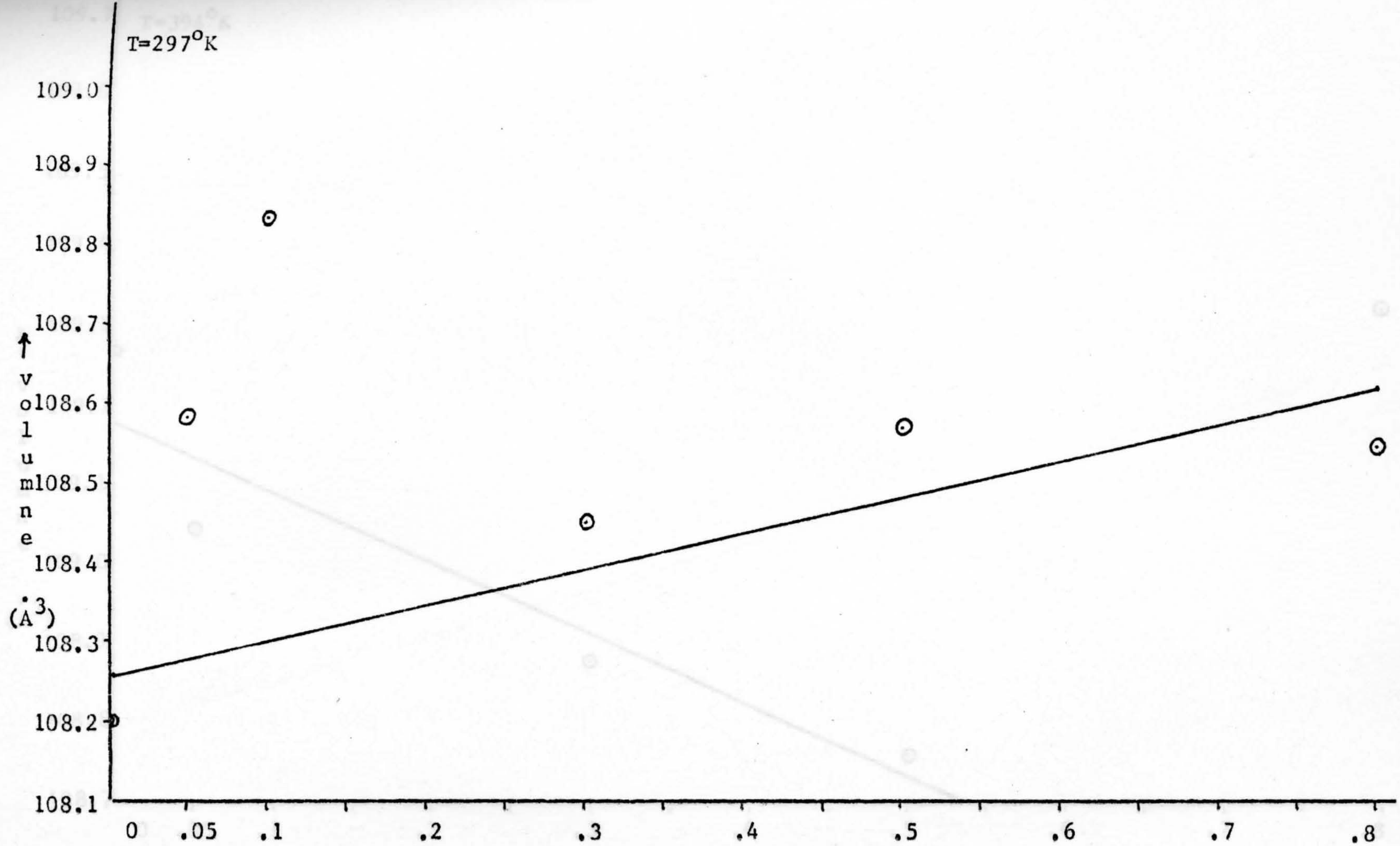

Fig.16.--Unit cell volumne versus atomic Antimony at 297 degrees kelvin.

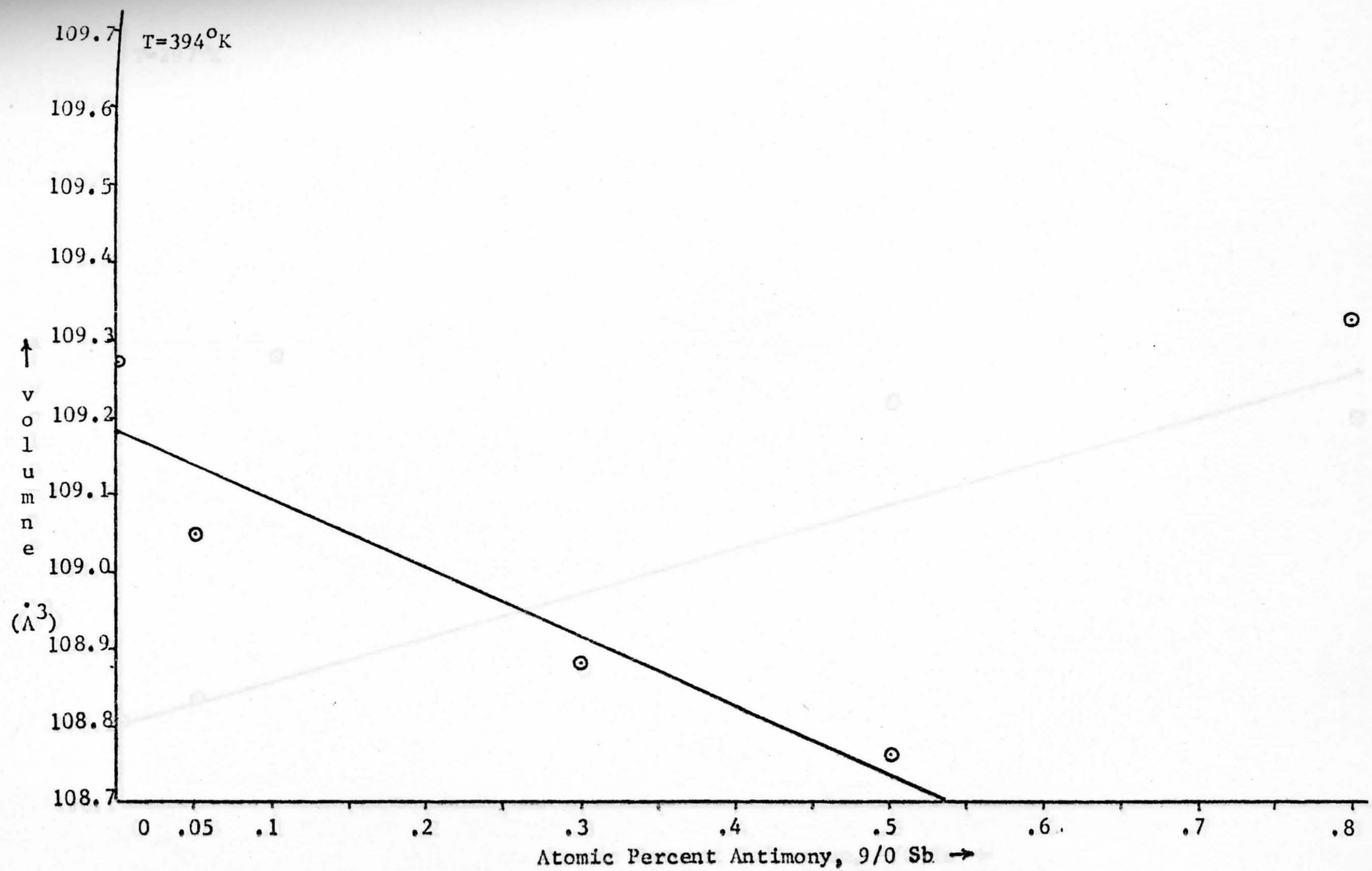

Fig. 17.--Unit cell volume versus atomic Antimony at 394 degrees kelvin.

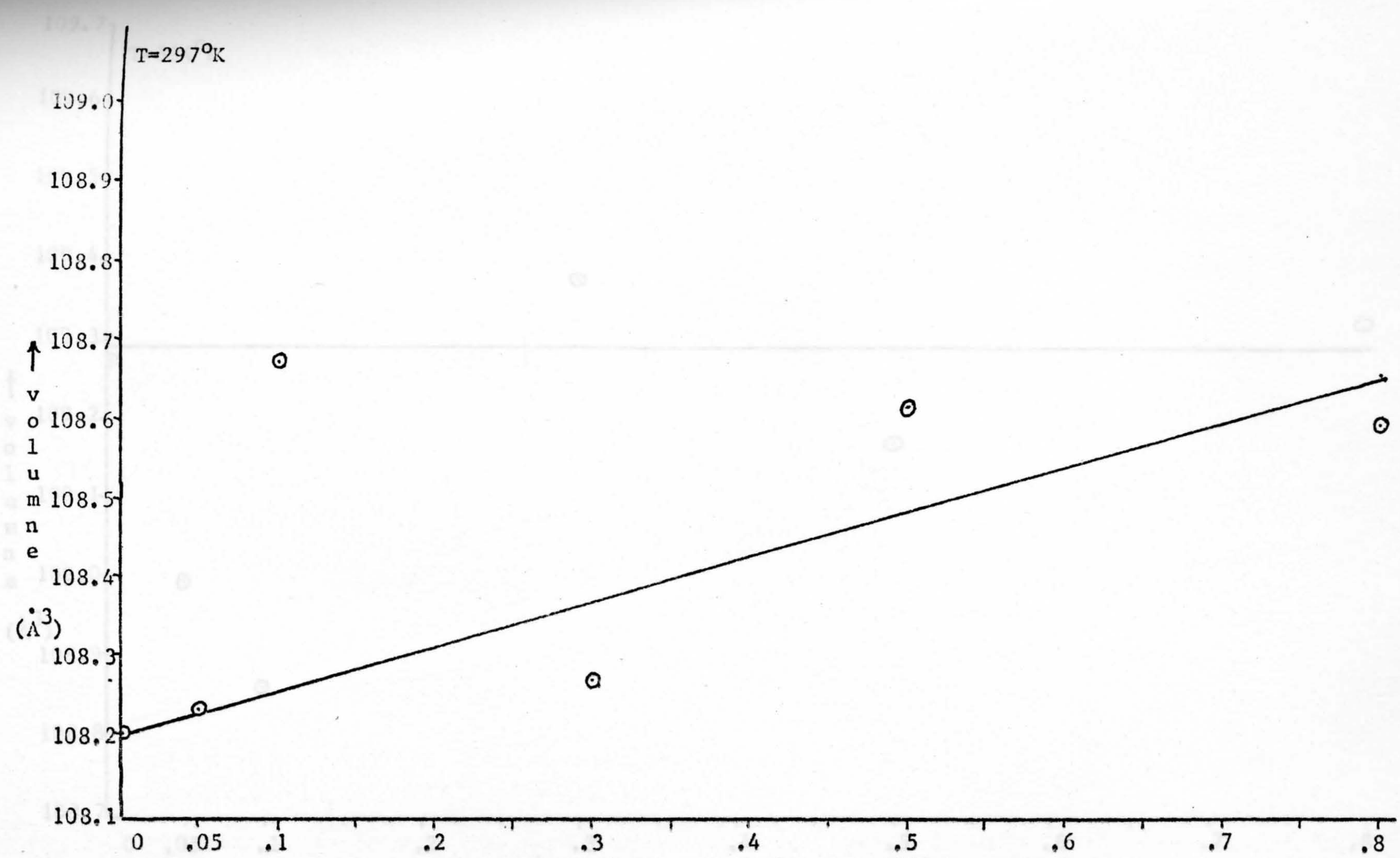

Fig. 18.--Unit cell volumne versus atomic Tellurium at 297 degrees kelvin.

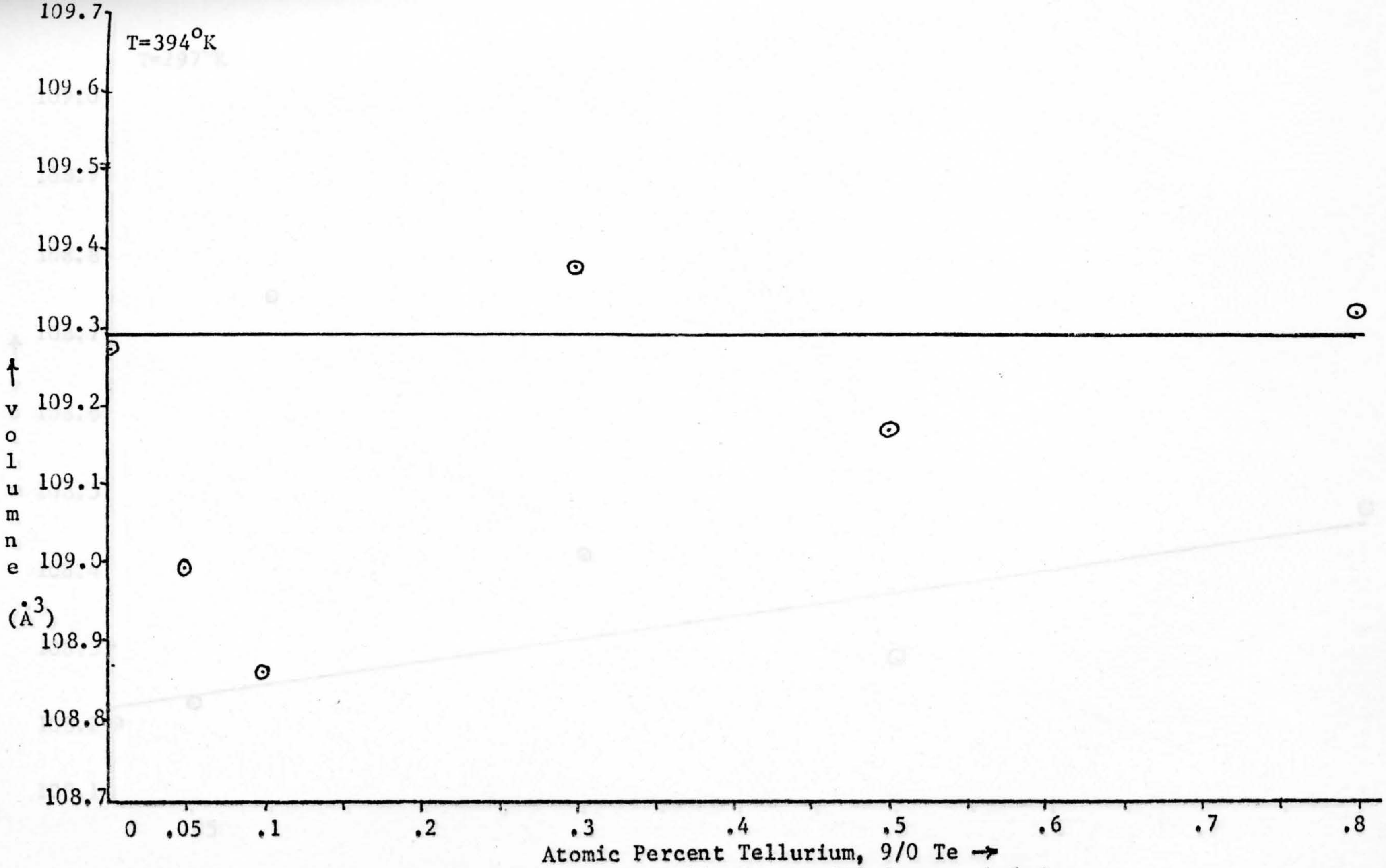

Fig.19.--Unit cell volumne versus atomic Tellurium at 394 degrees kelvin.

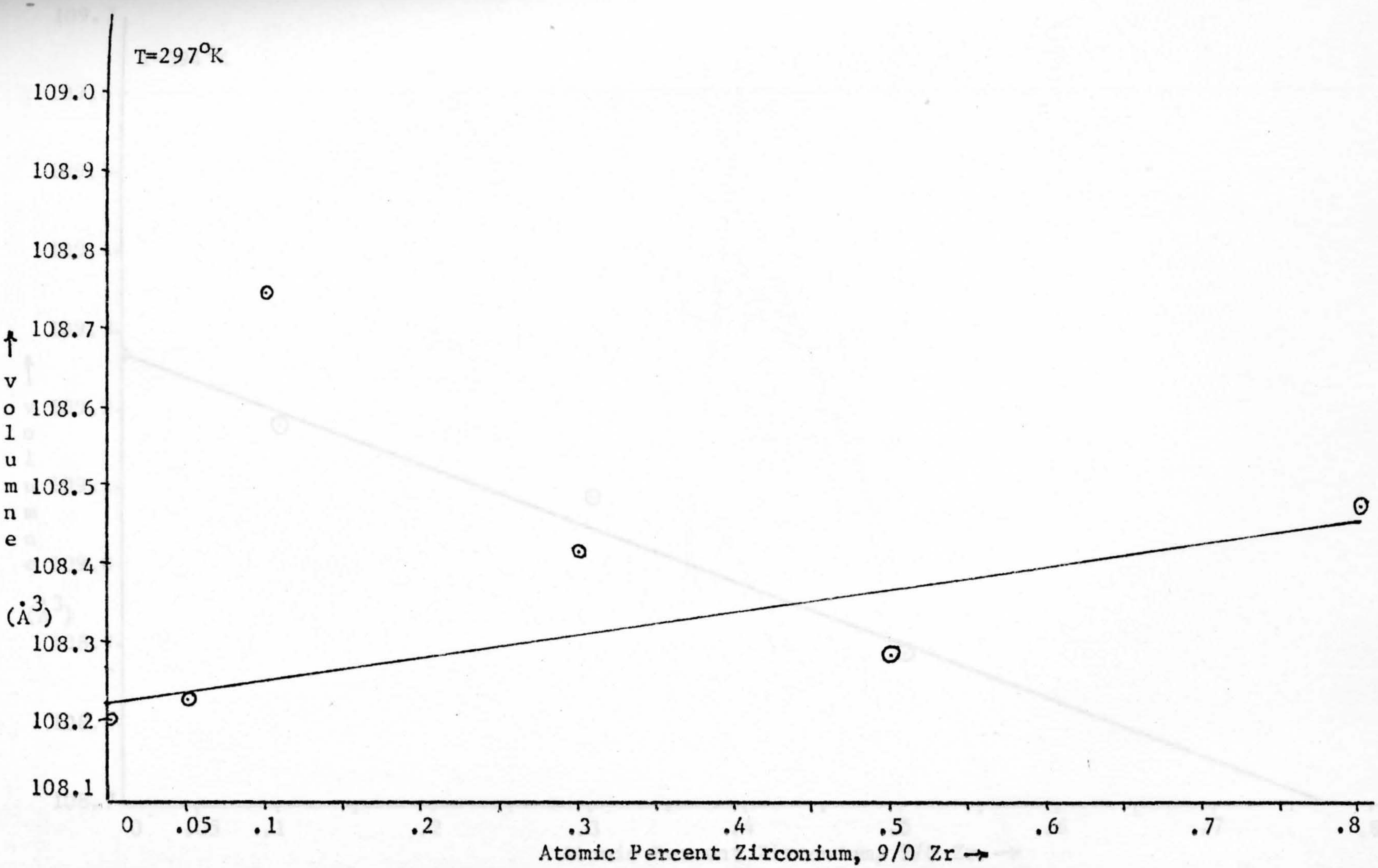

Fig. 20.--Unit cell volumne versus atomic Zirconium at 297 degrees kelvin.

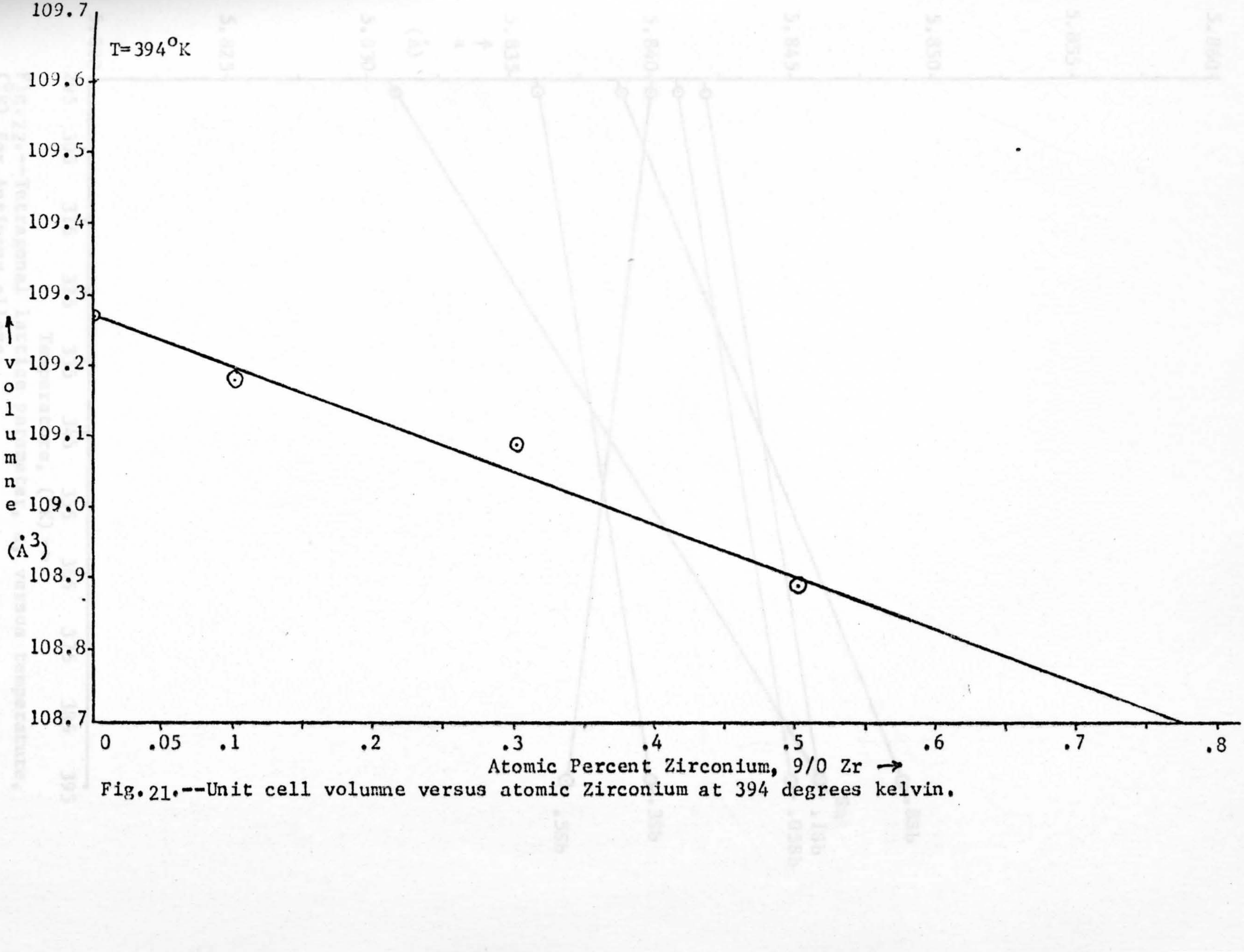

Fig. 21.--Unit cell volumne versus atomic Zirconium at 394 degrees kelvin.

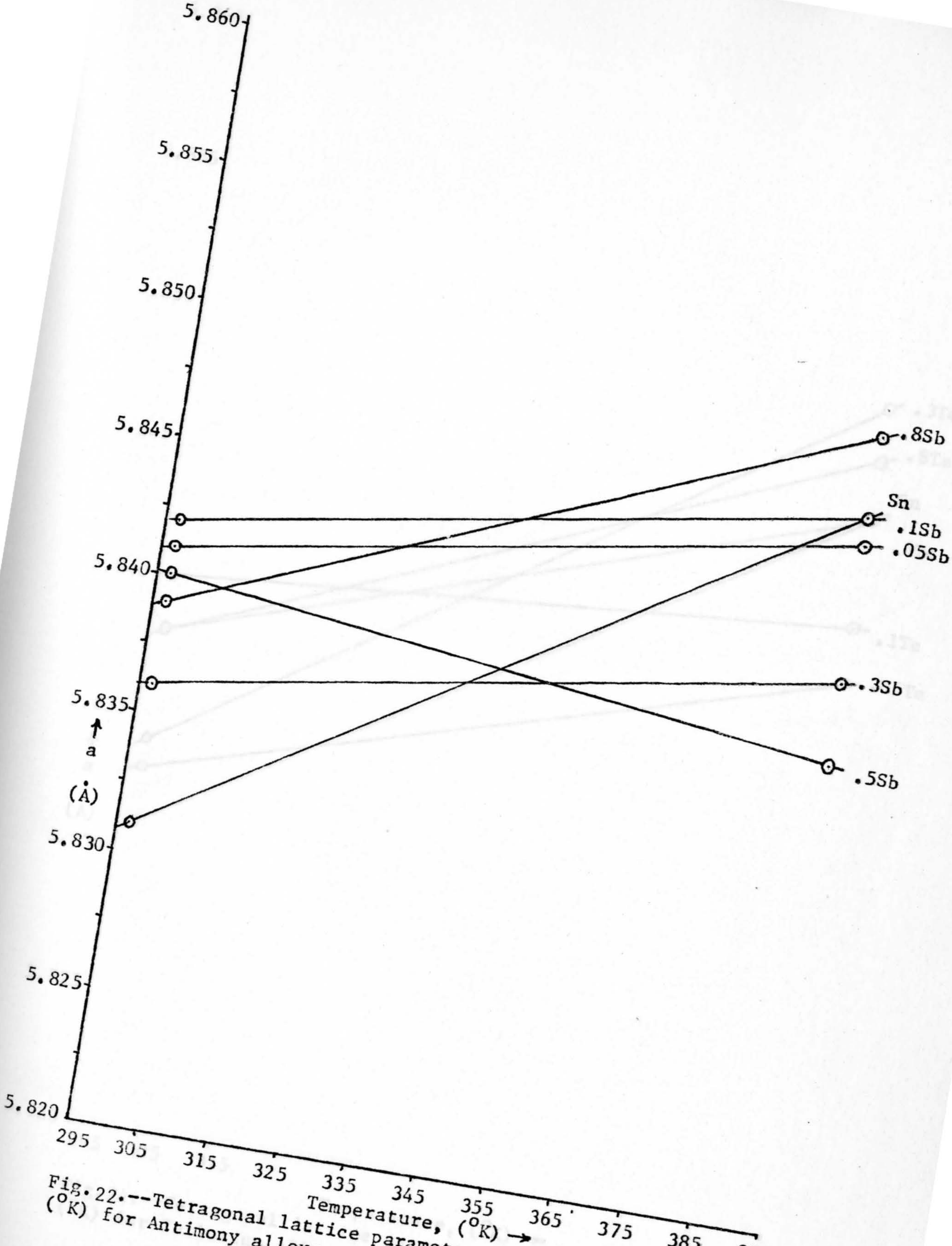

Fig. 22.--Tetragonal lattice parameter, a, versus temperature, (^{o}K) for Antimony alloys.

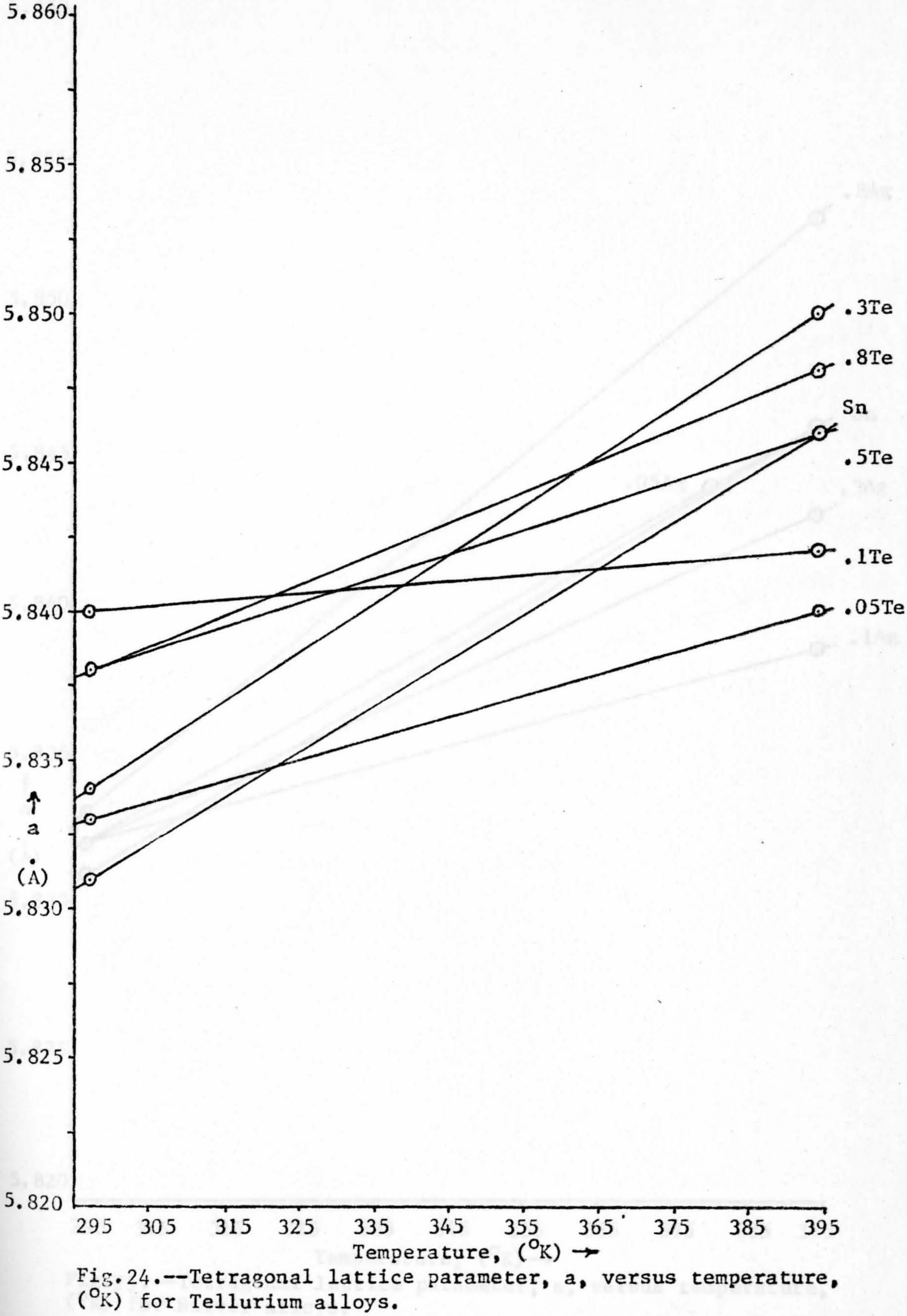

Fig. 24.--Tetragonal lattice parameter, a, versus temperature, (^oK) for Tellurium alloys.

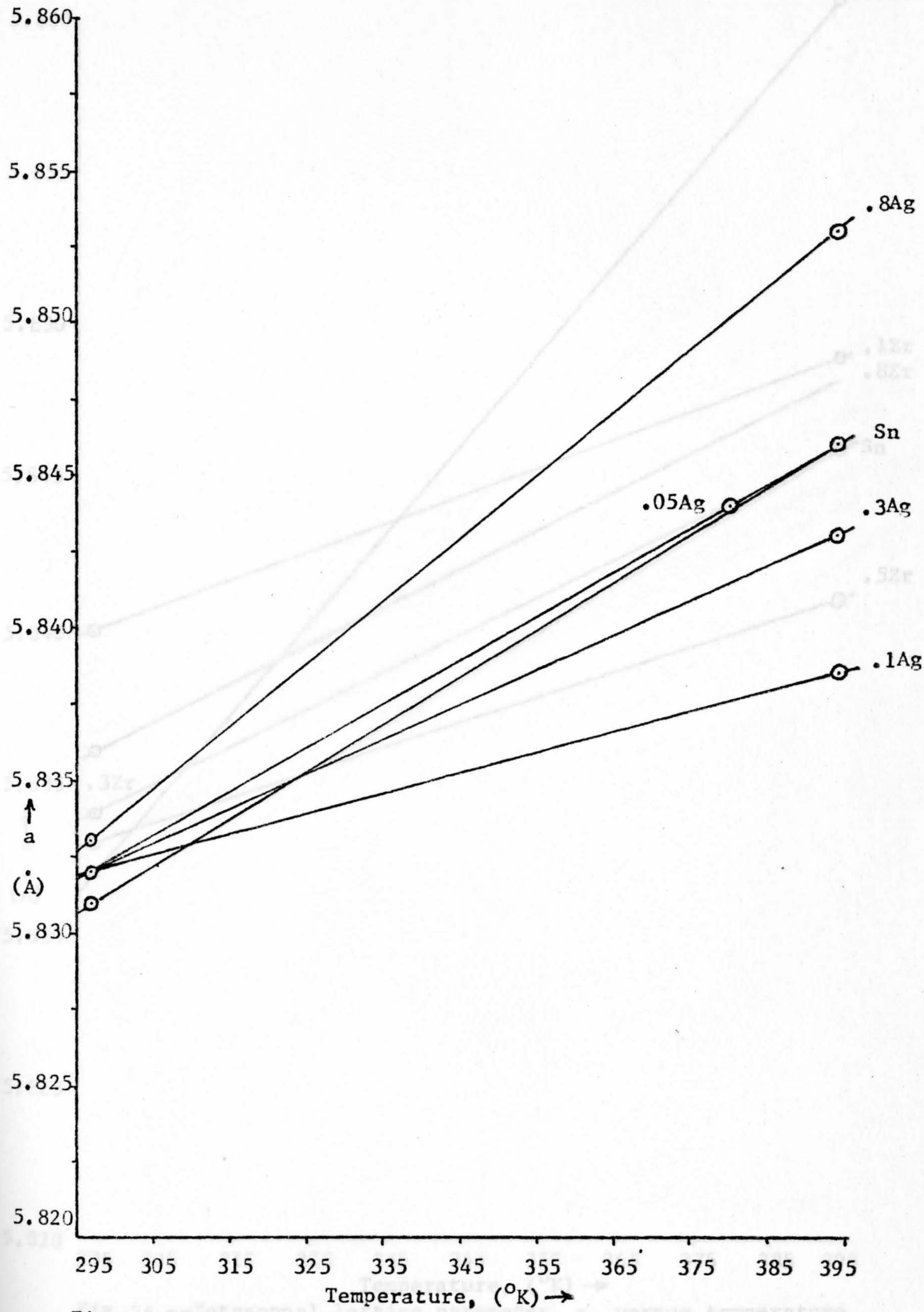

Fig.25.--Tetragonal lattice parameter, a, versus temperature, (°K) for Silver alloys.

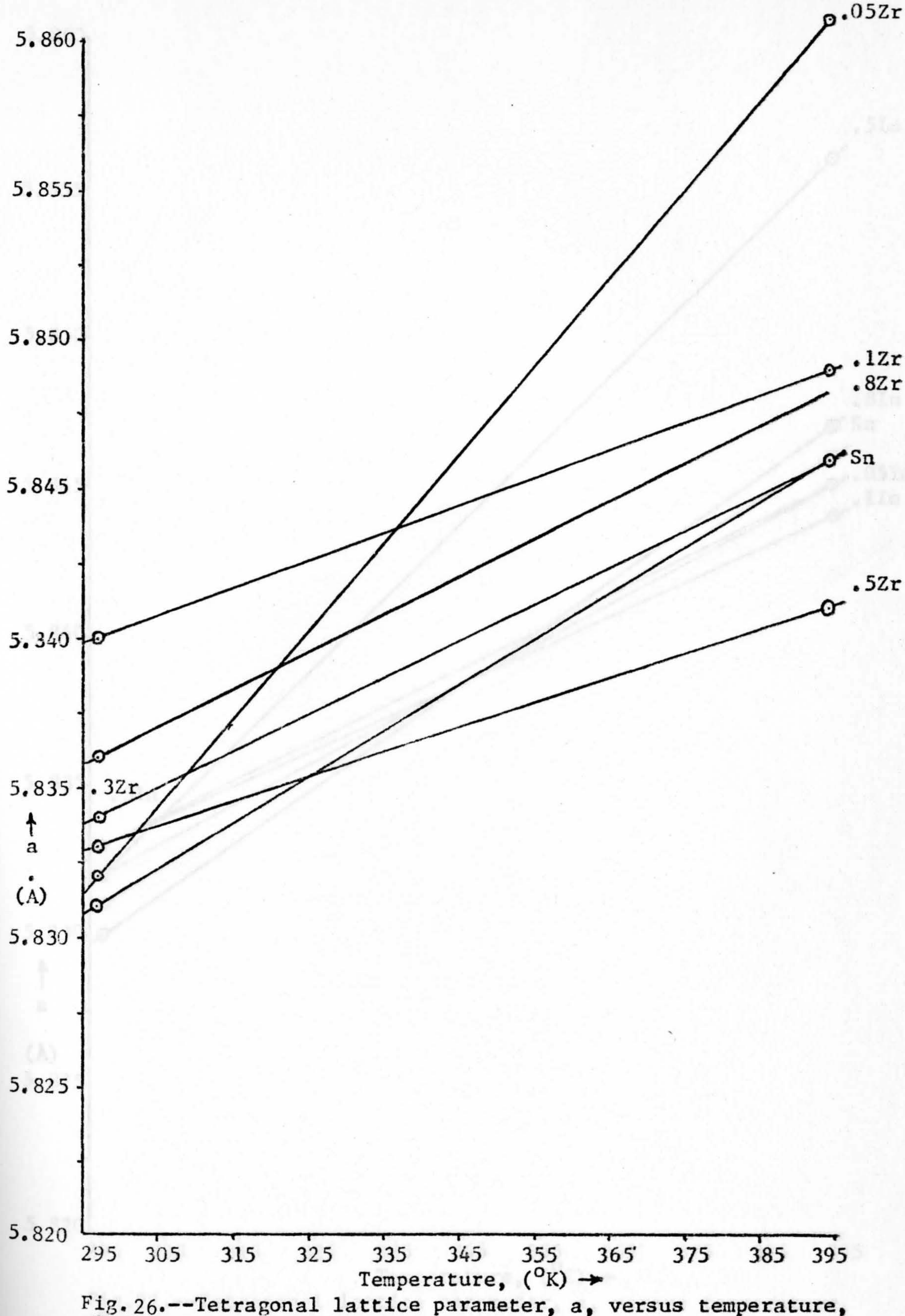

Fig. 26.--Tetragonal lattice parameter, a, versus temperature, (^oK) for Zirconium alloys.

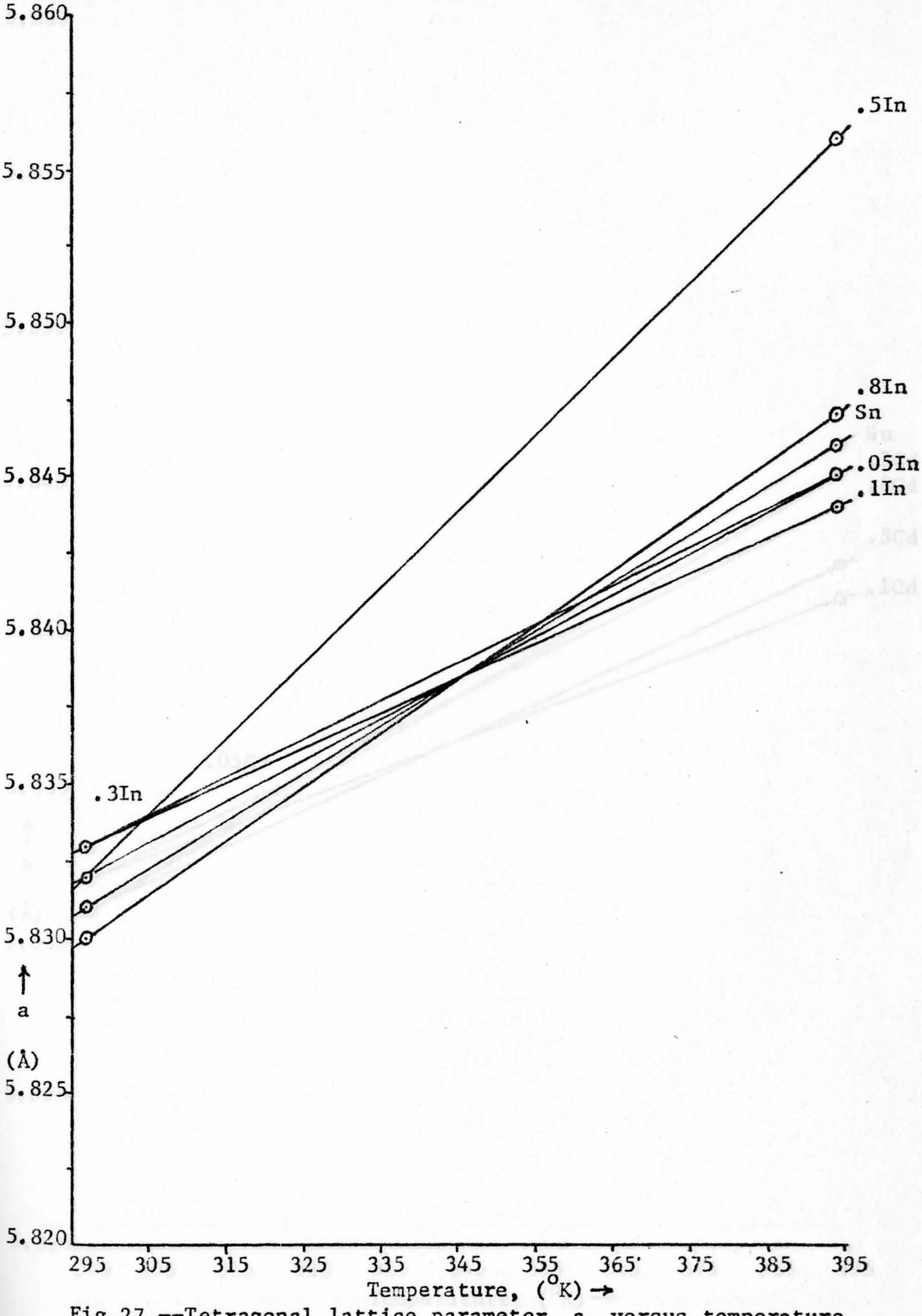

Fig.27.--Tetragonal lattice parameter, a, versus temperature, (°K) for Indium alloys.

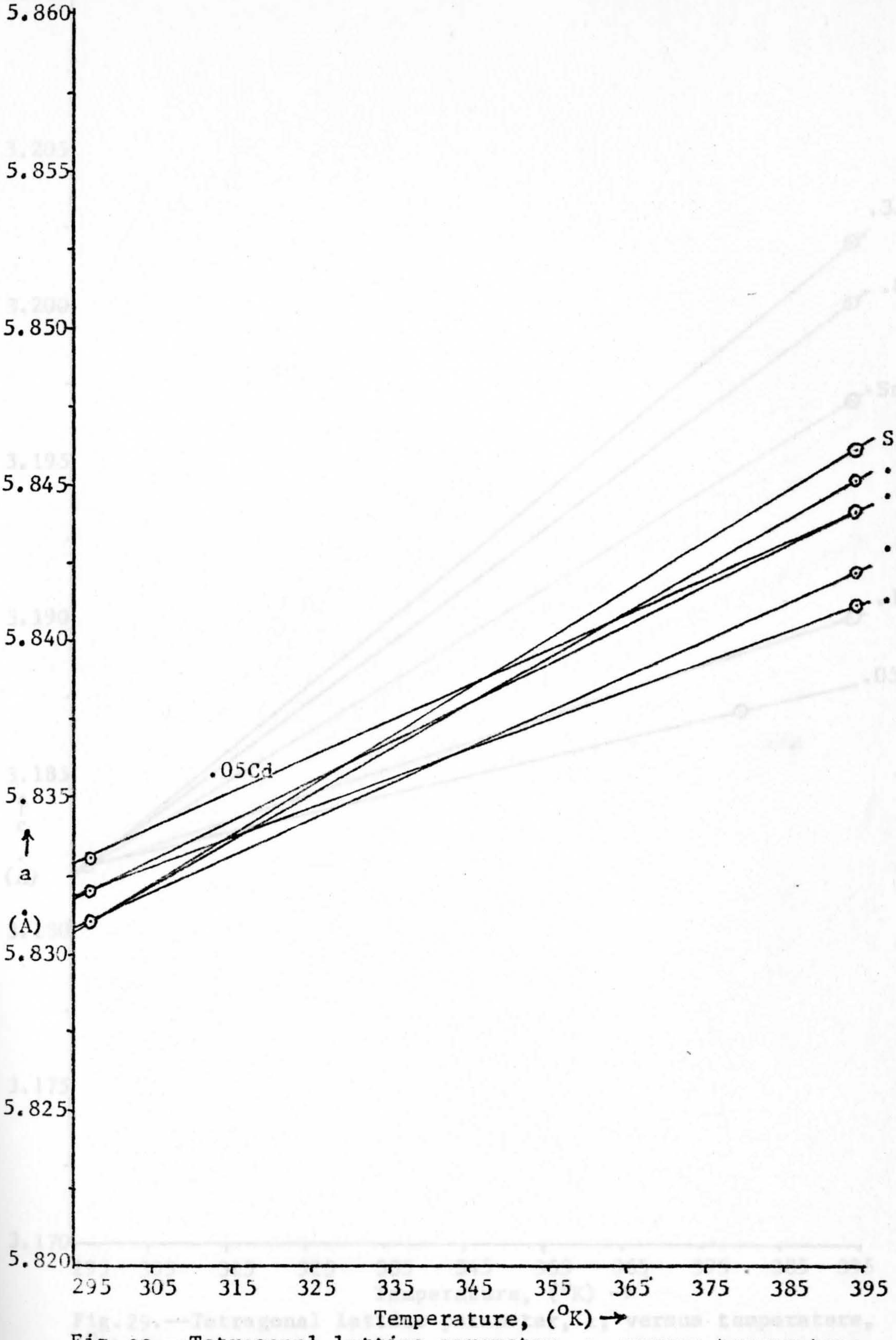

Fig. 28.--Tetragonal lattice parameter, a, versus temperature, (°K) for Cadmium alloys.

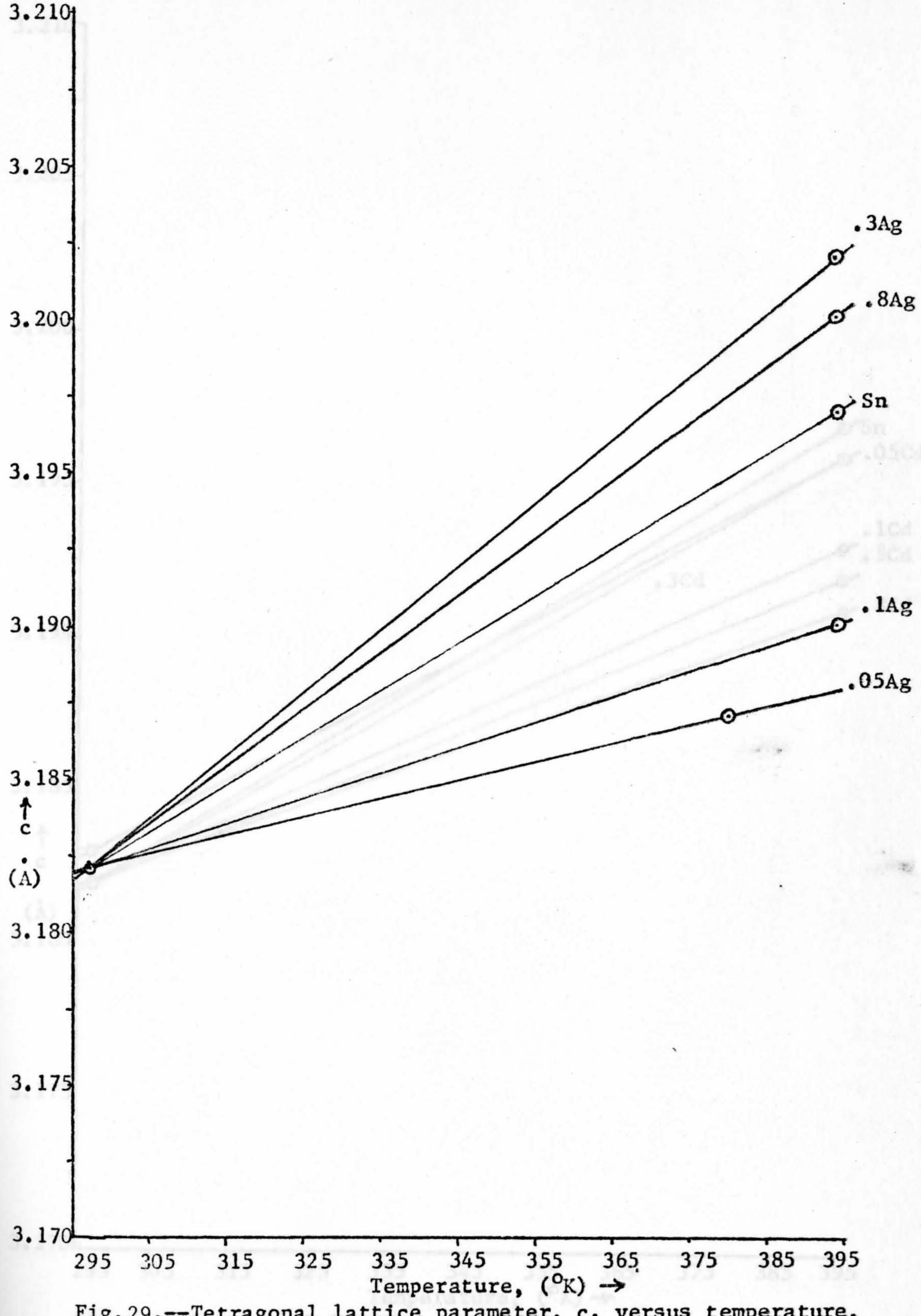

Fig. 29.--Tetragonal lattice parameter, c, versus temperature, (°K) for Silver alloys.

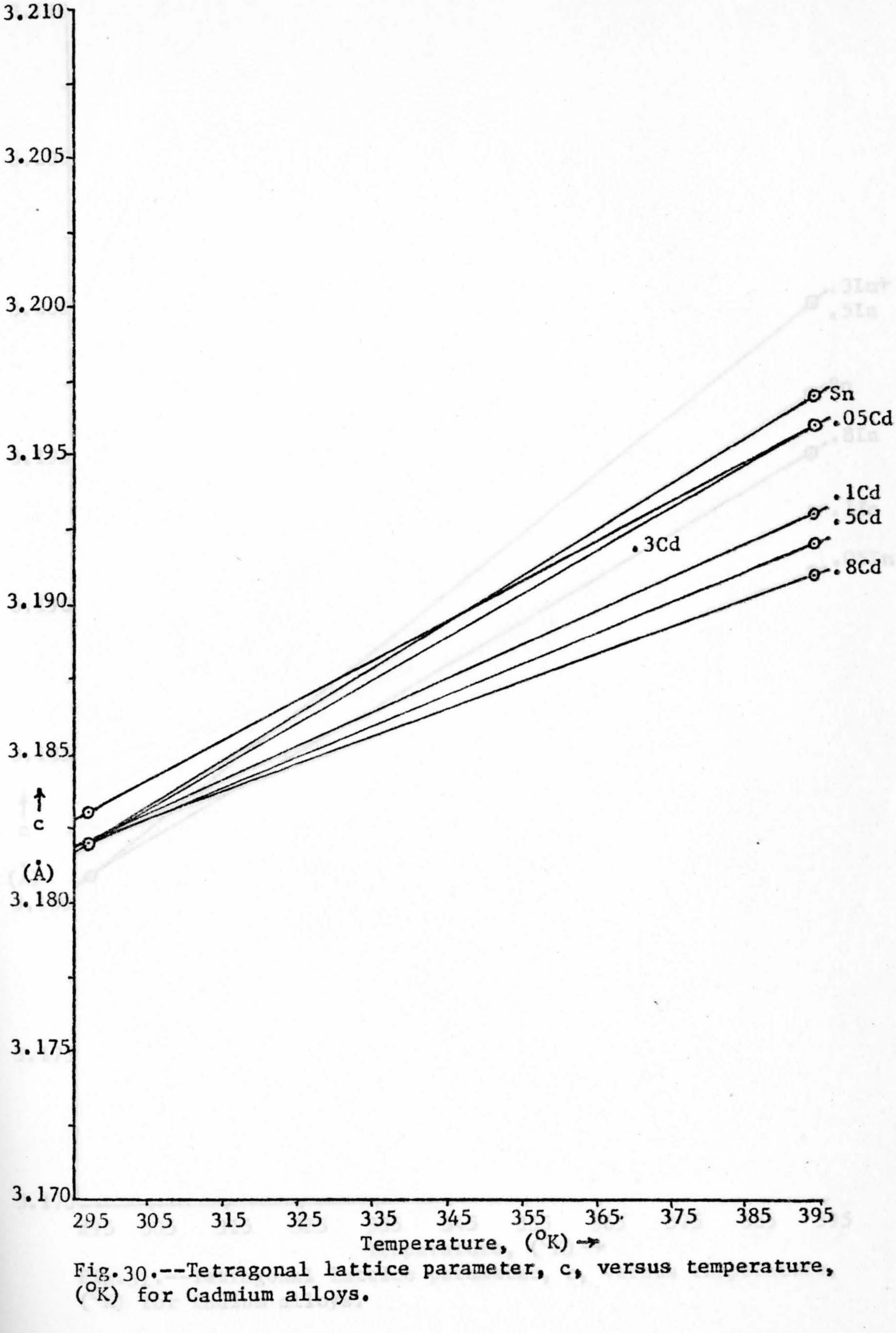

Fig. 30.--Tetragonal lattice parameter, c, versus temperature, (°K) for Cadmium alloys.

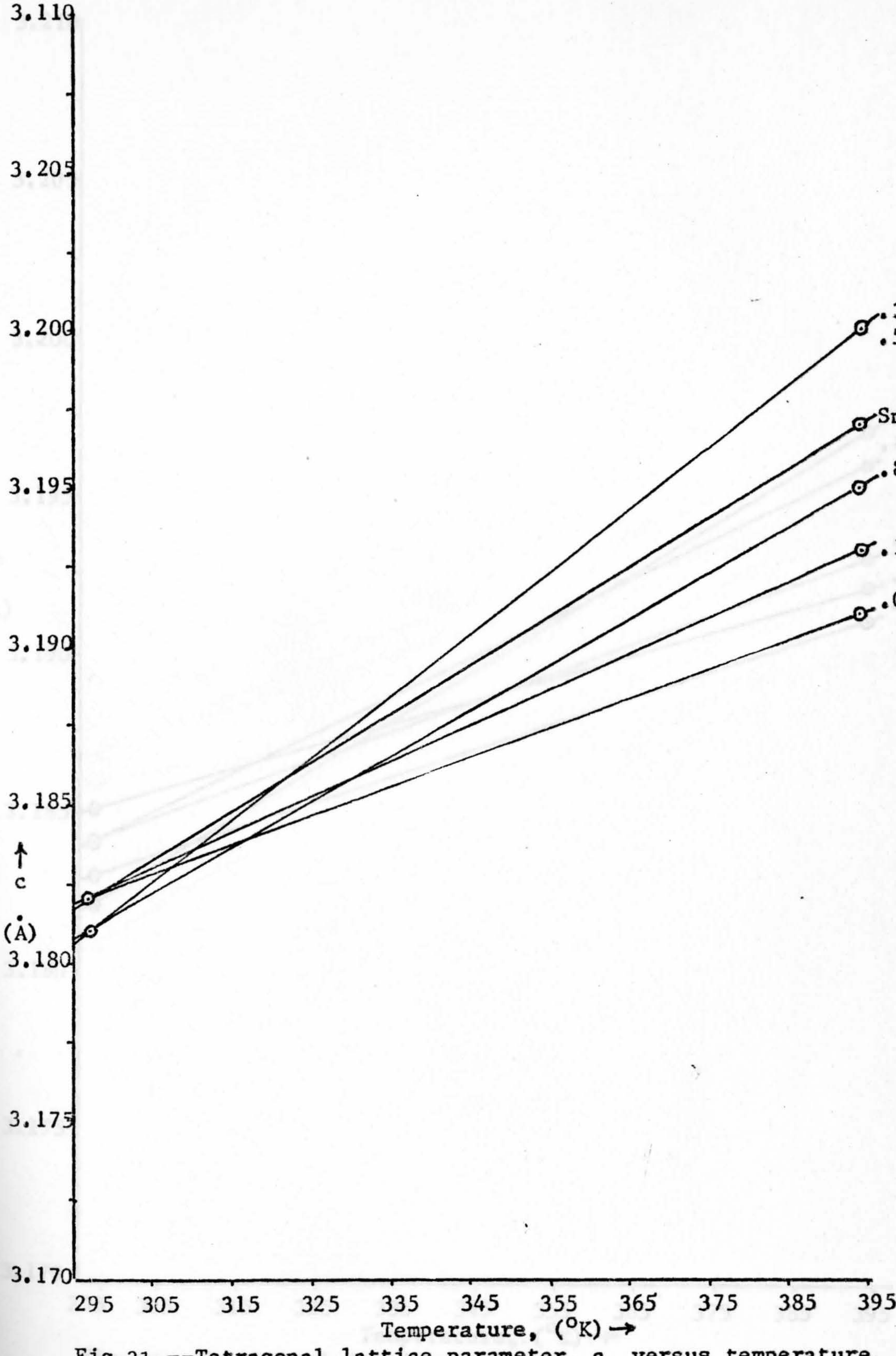

Fig.31.--Tetragonal lattice parameter, c, versus temperature, (°K) for Indium alloys.

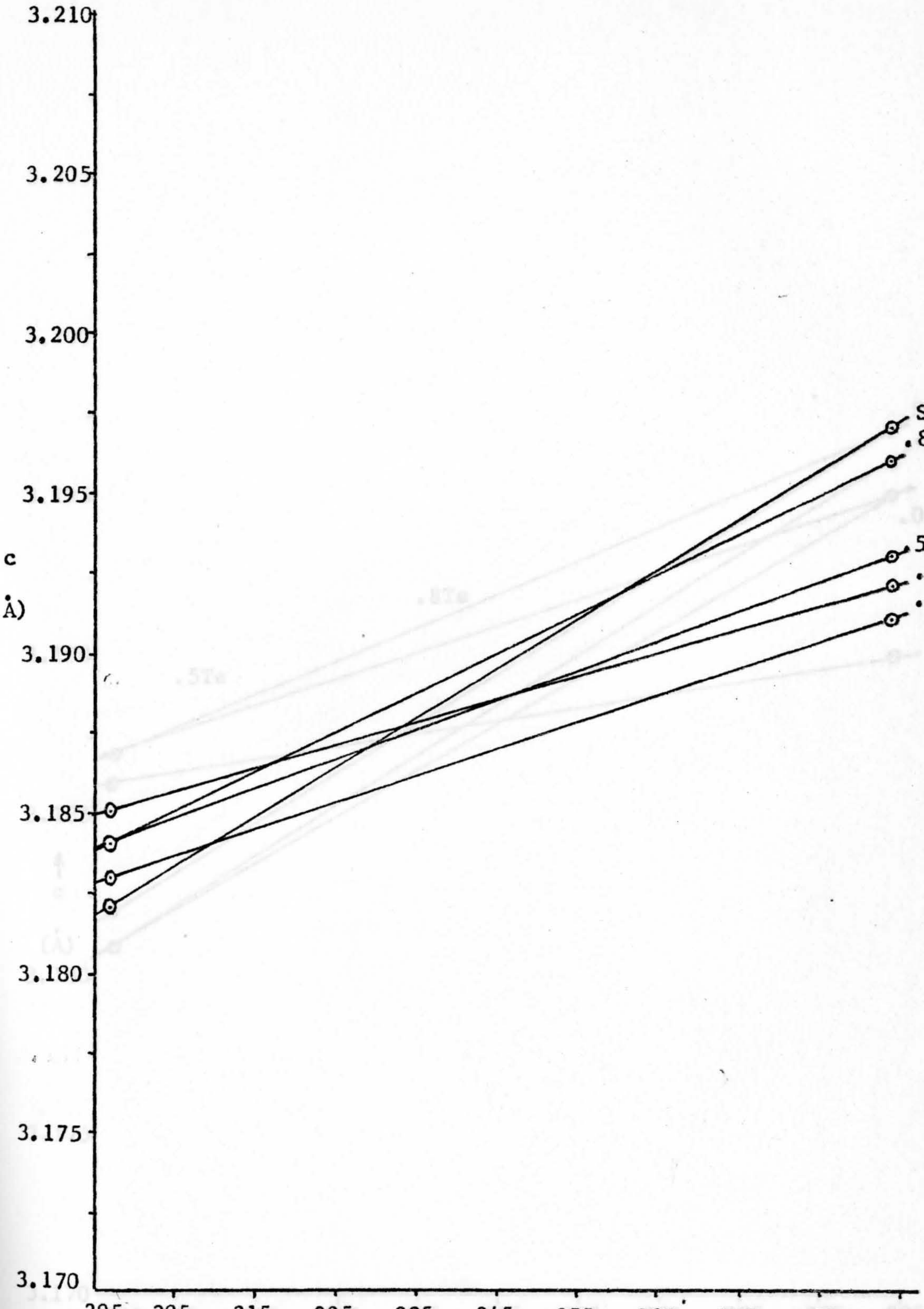

Fig. 32.--Tetragonal lattice parameter, c, versus temperature, (^oK) for Antimony alloys.

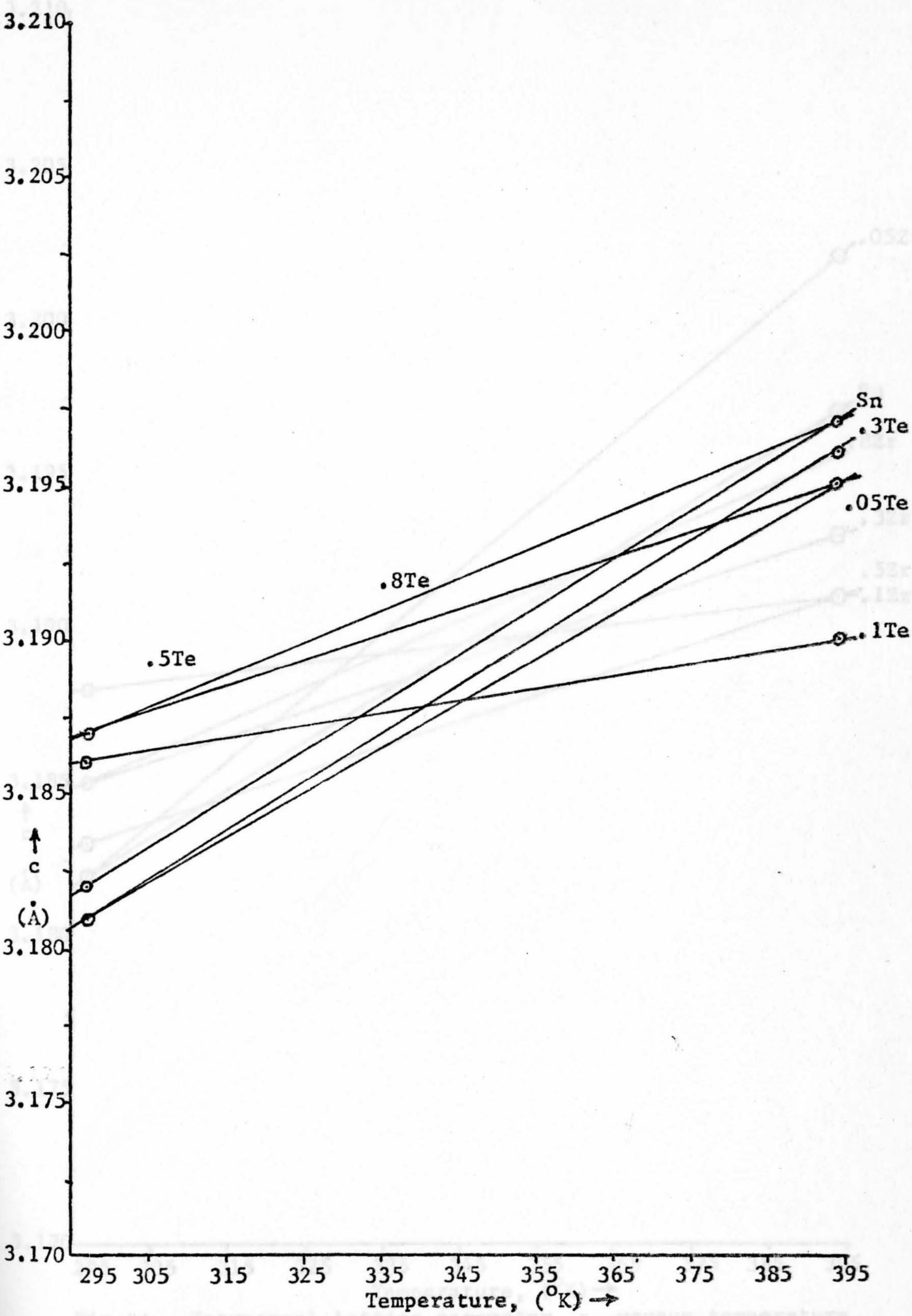

Fig. 33.--Tetragonal lattice parameter, c, versus temperature, (°K) for Tellurium alloys.

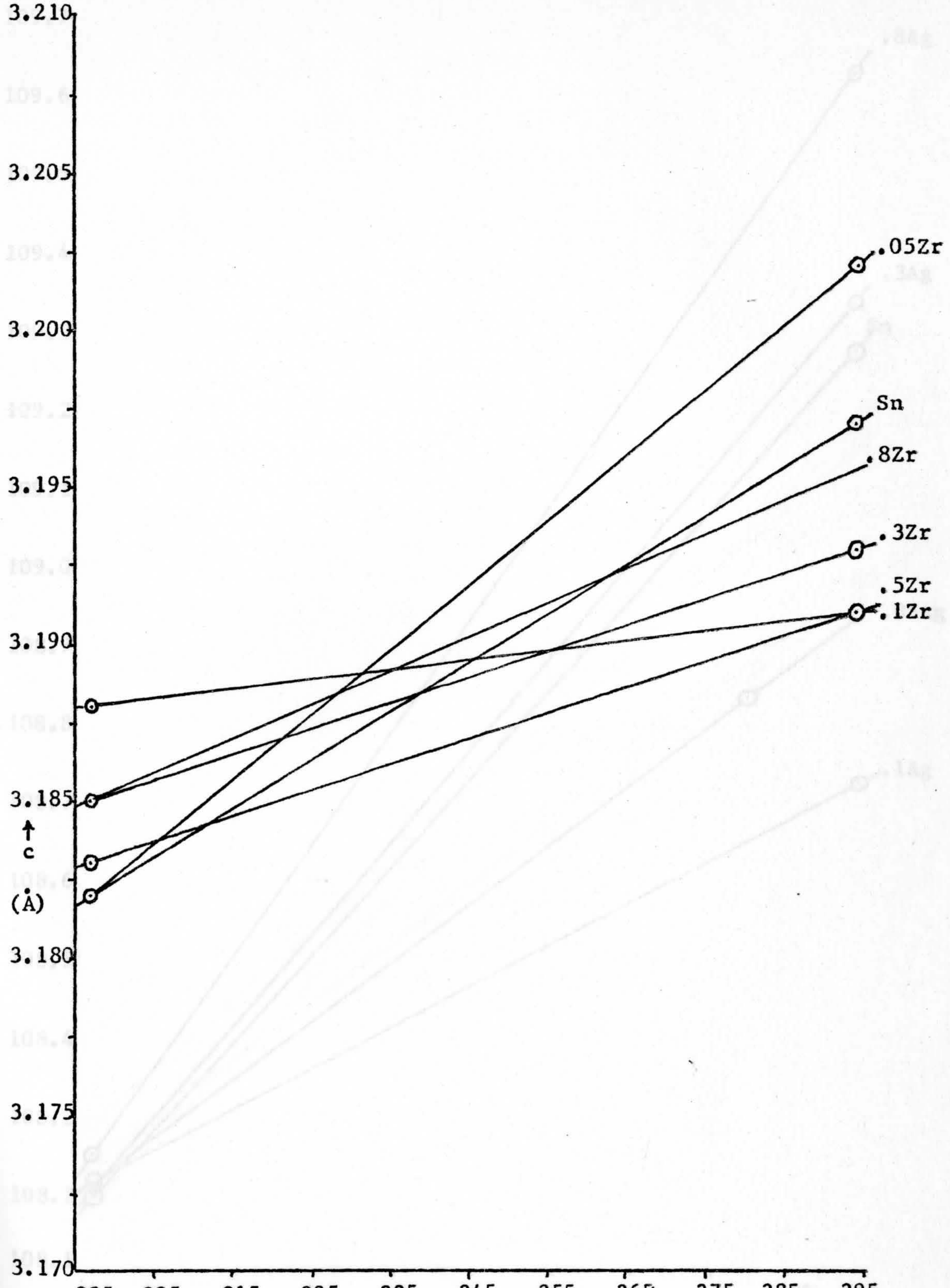

Fig. 34.--Tetragonal lattice parameter, c, versus temperature, (°K) for Zirconium alloys.

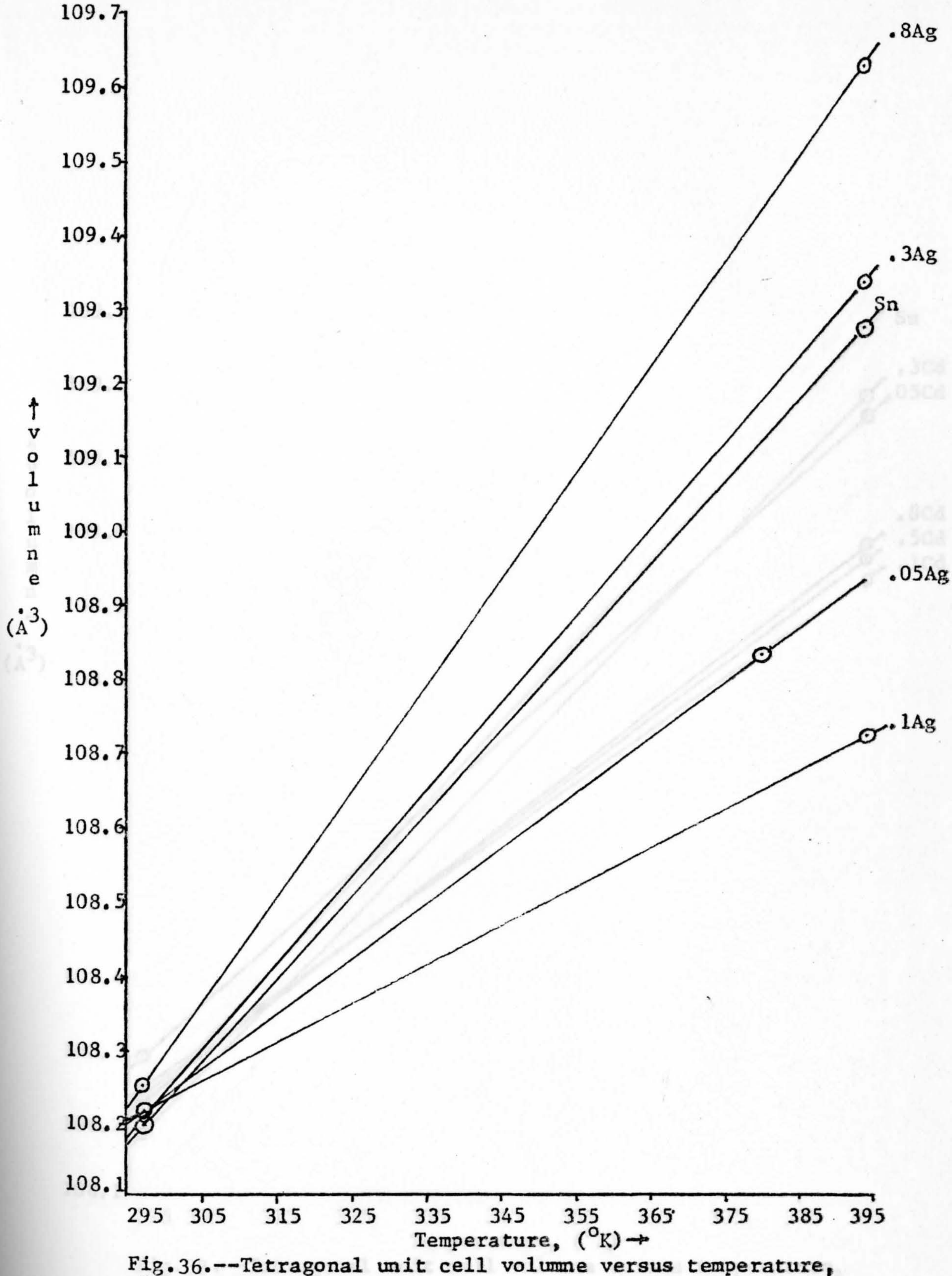

Fig. 36.--Tetragonal unit cell volumne versus temperature, (°K) for Silver alloys.

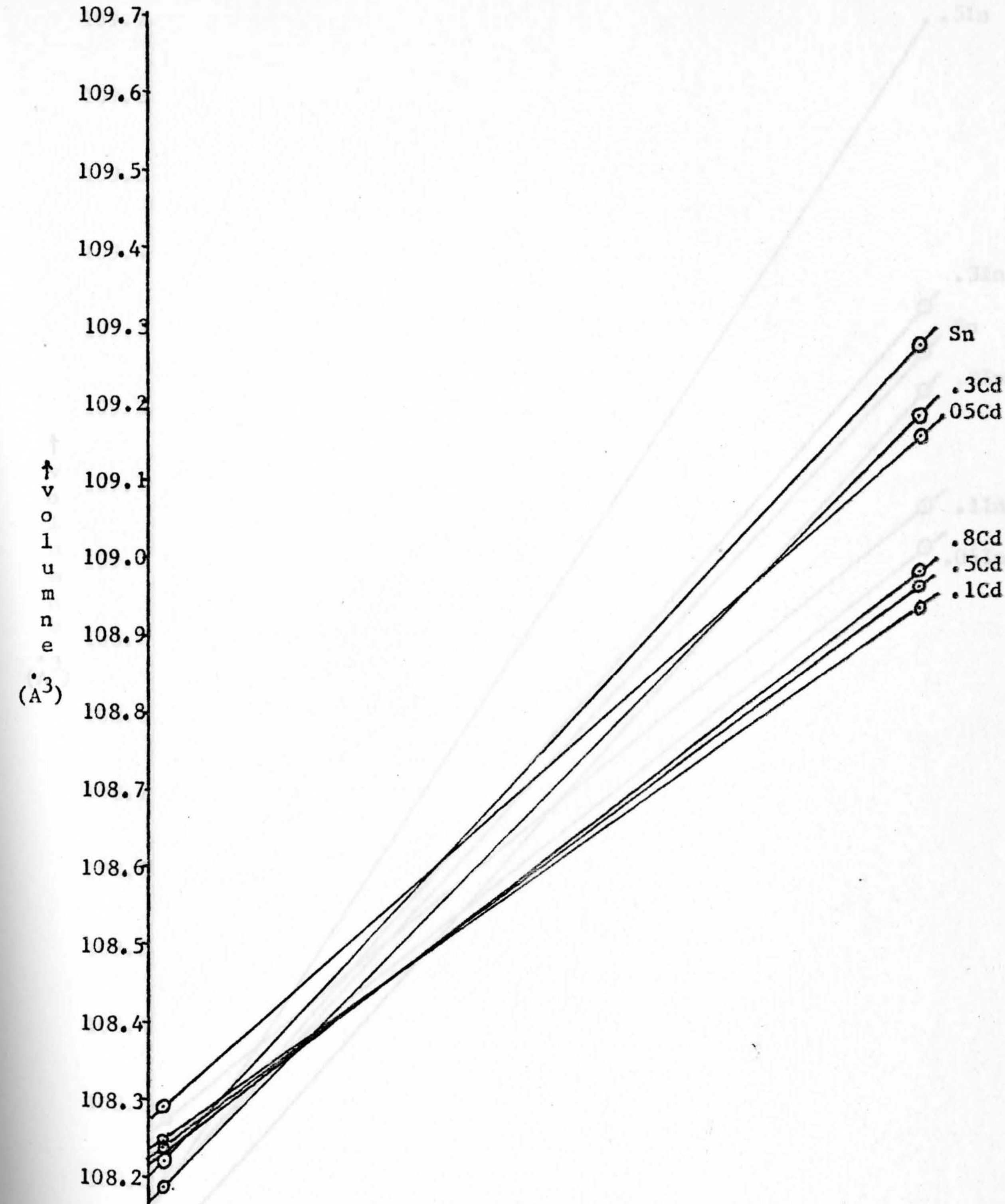

Fig.38.--Tetragonal unit cell volumne versus temperature, (°K) for Cadium alloys.

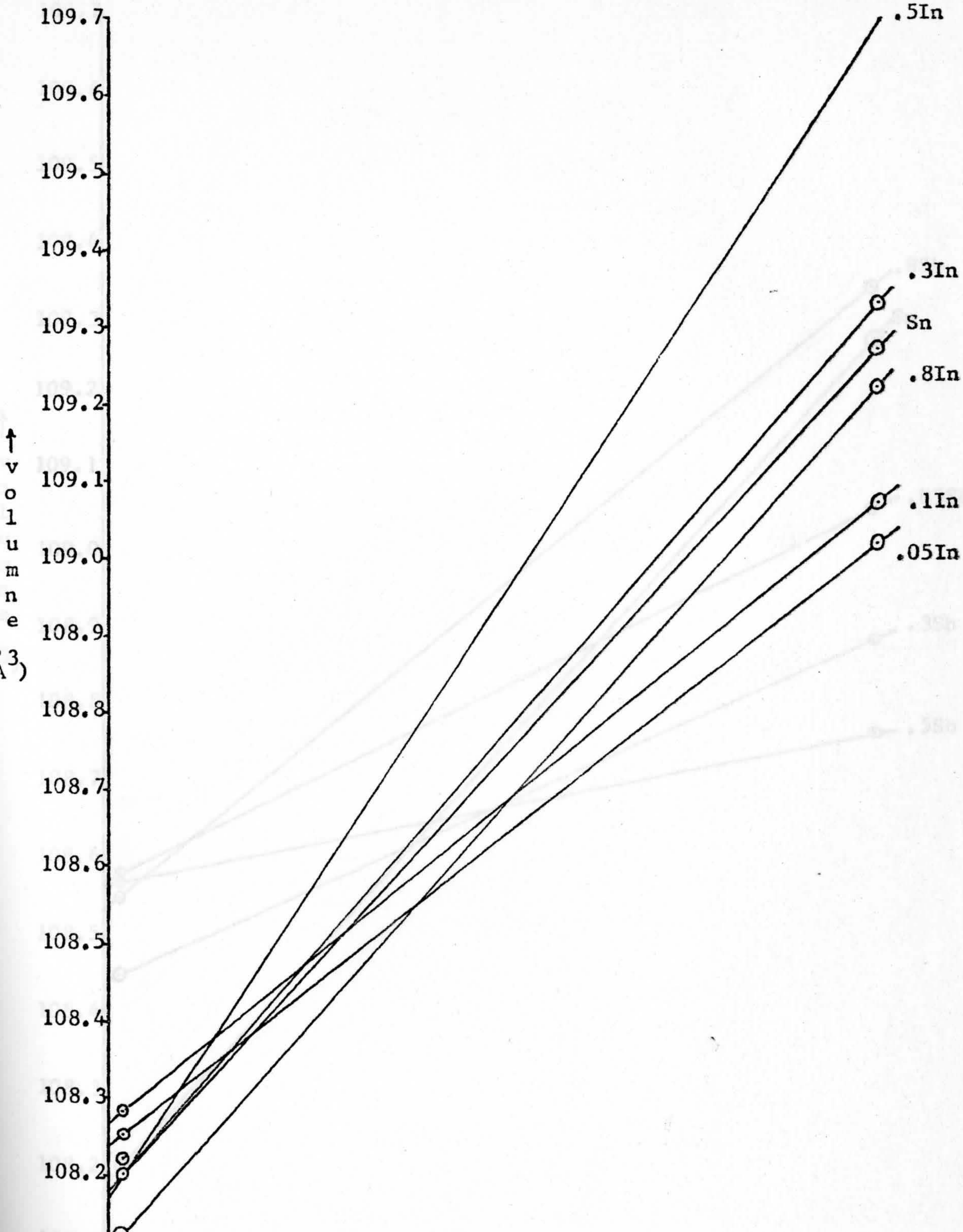

Fig.40.--Tetragonal unit cell volumme versus temperature, (^{o}K) for Indium alloys.

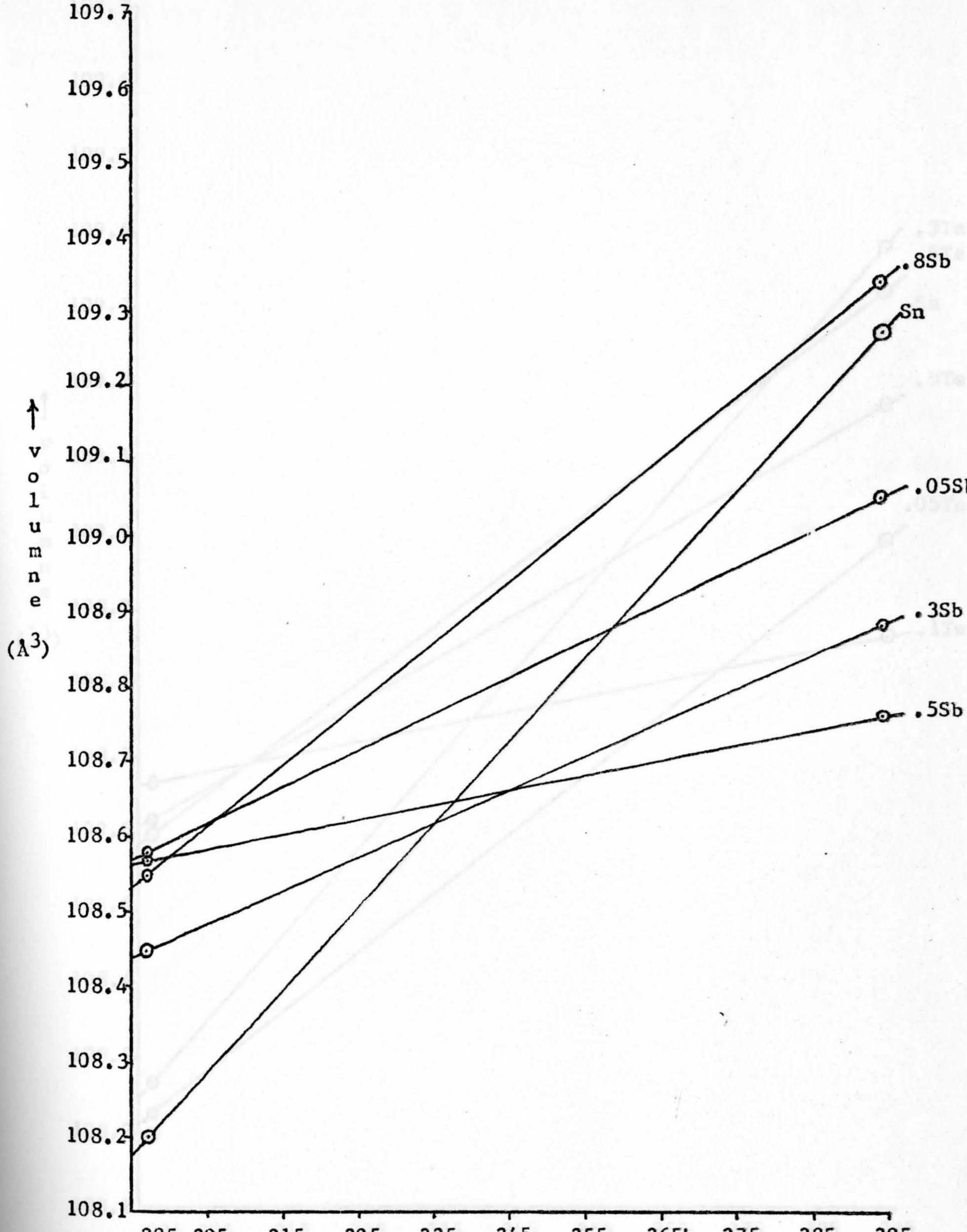

Fig. 41.--Tetragonal unit cell volume versus temperature, (°K) for Antimony alloys.

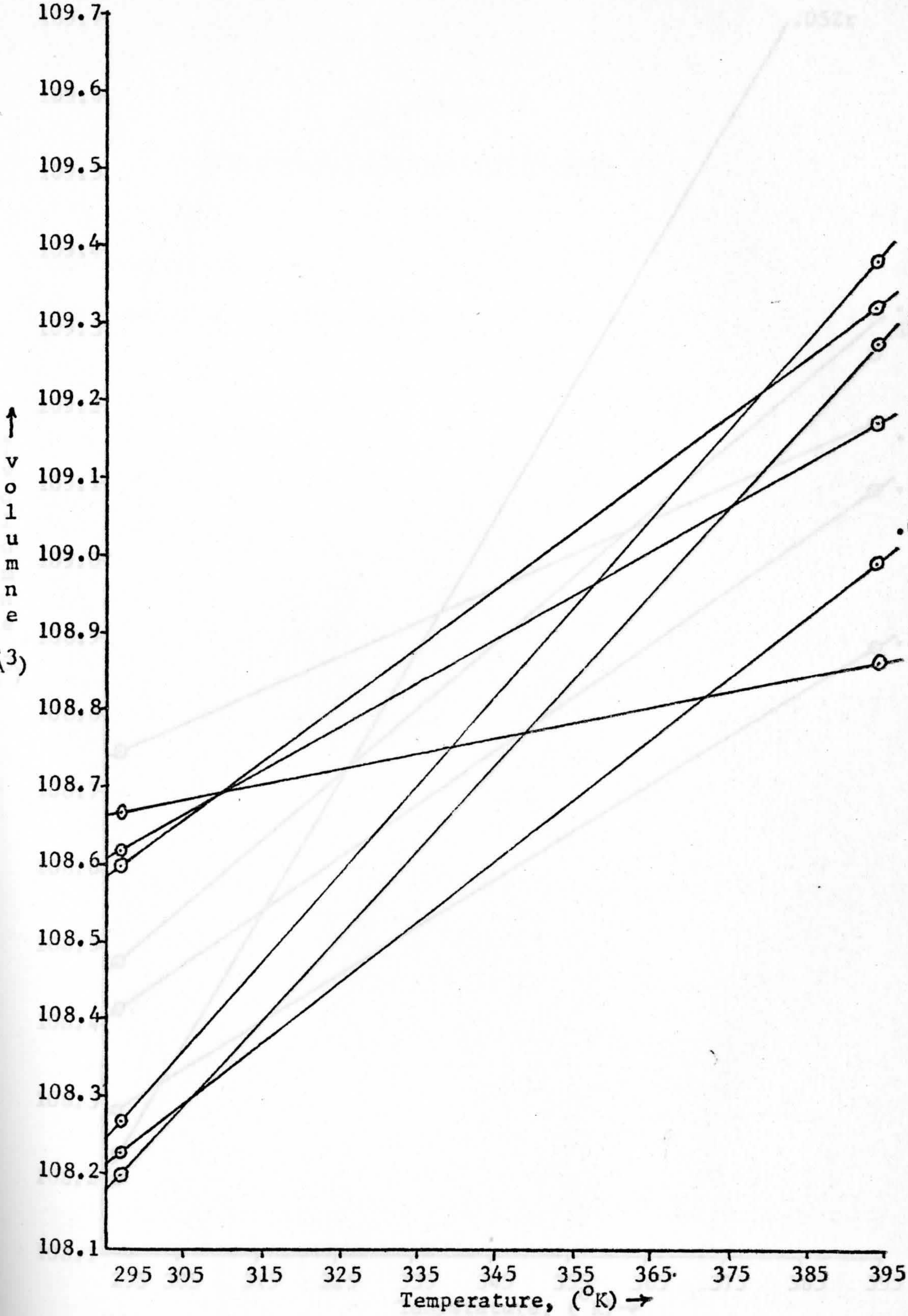

Fig.42.—Tetragonal unit cell volumne versus temperature, (°K) for Tellurium alloys.

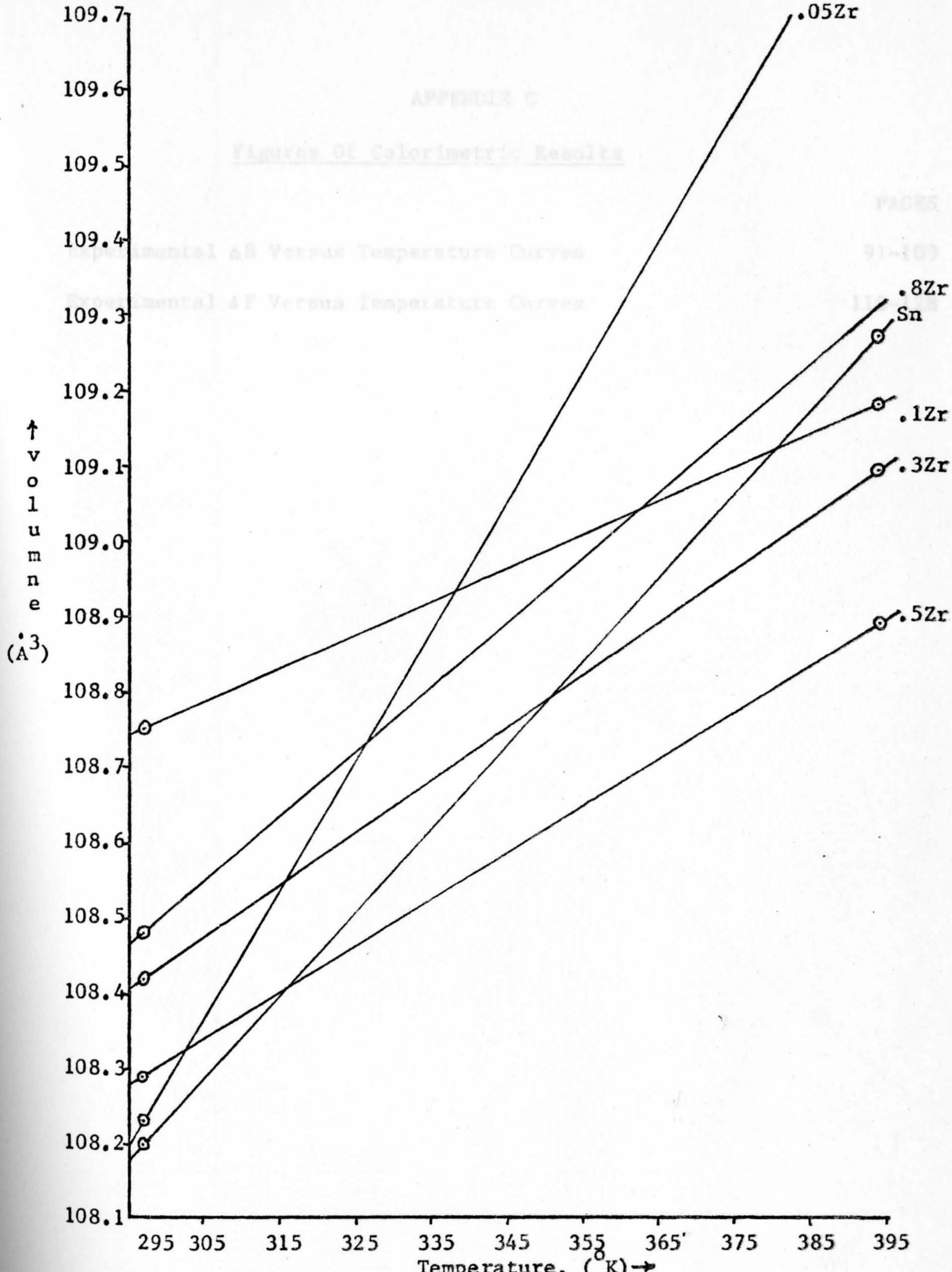

Fig.43.--Tetragonal unit cell volumne versus temperature, (°K) for Zirconium alloys.

APPENDIX C

Figures Of Calorimetric Results

	PAGES
Experimental ΔH Versus Temperature Curves	91-109
Experimental ΔF Versus Temperature Curves	110-128

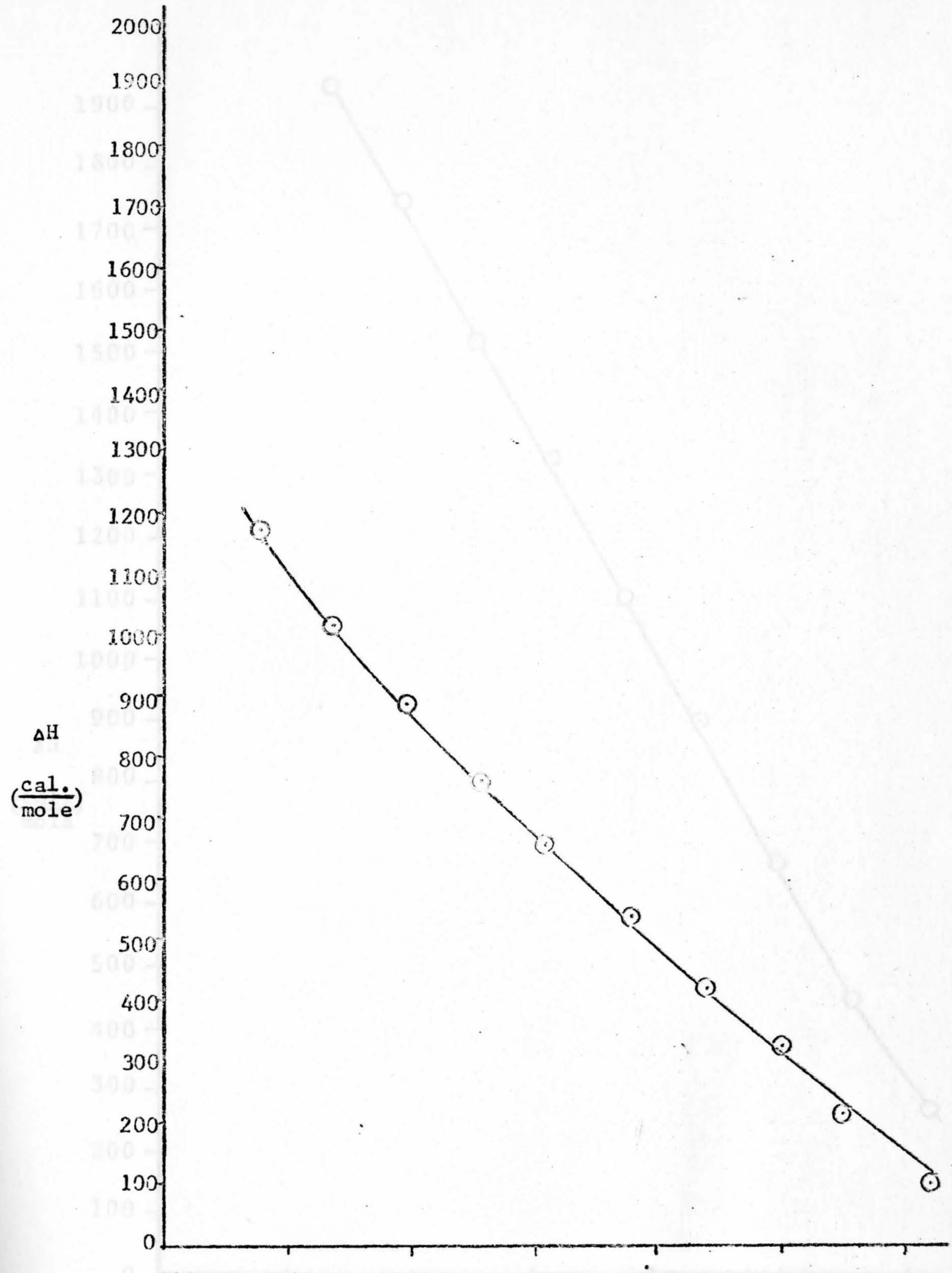

Figure44. Experimental ΔH versus Temperature Curve obtained for pure tin atomic number Sn.

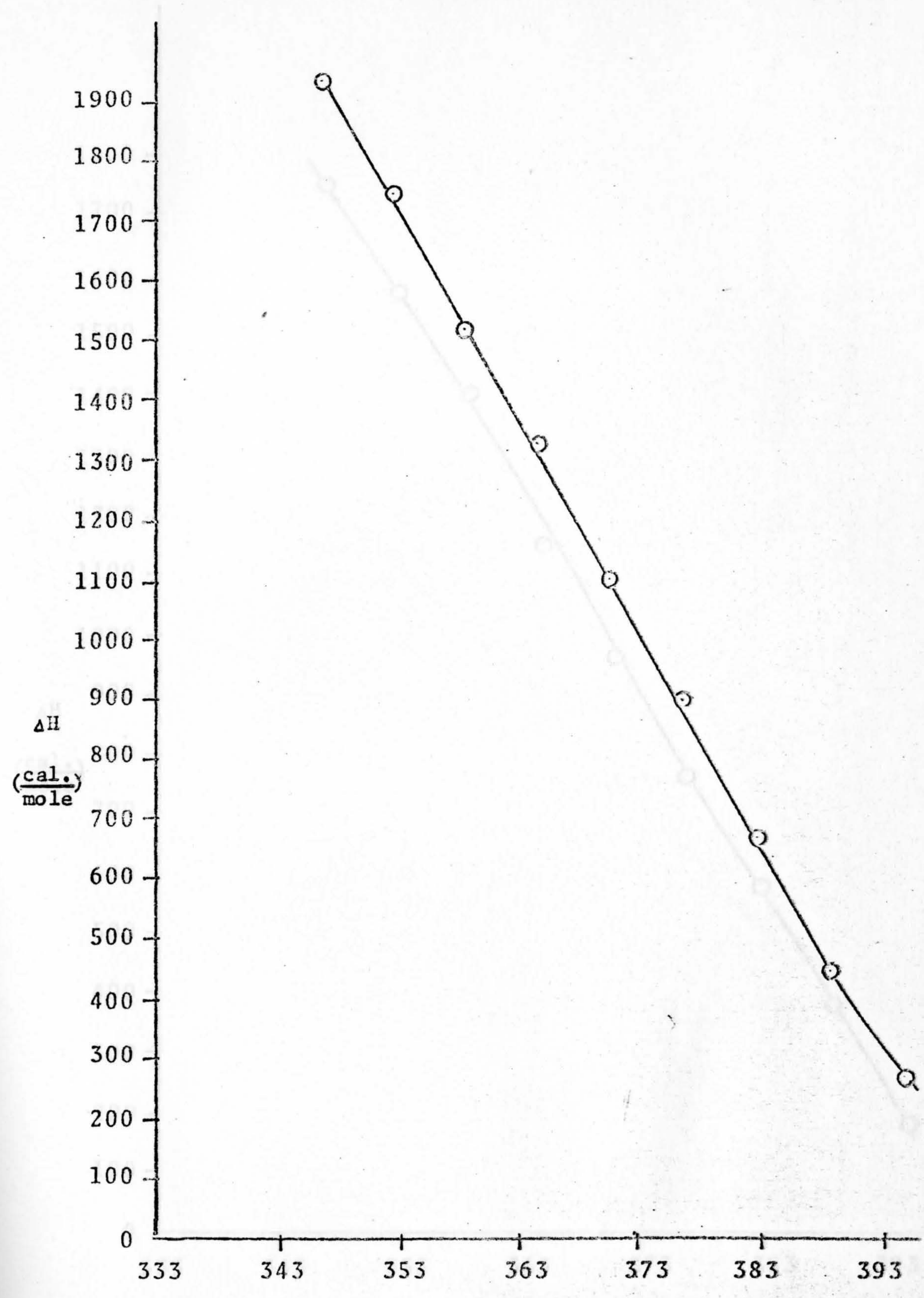

Figure45. Experimental ΔH versus Temperature Curve obtained for .3 atomic percent In.

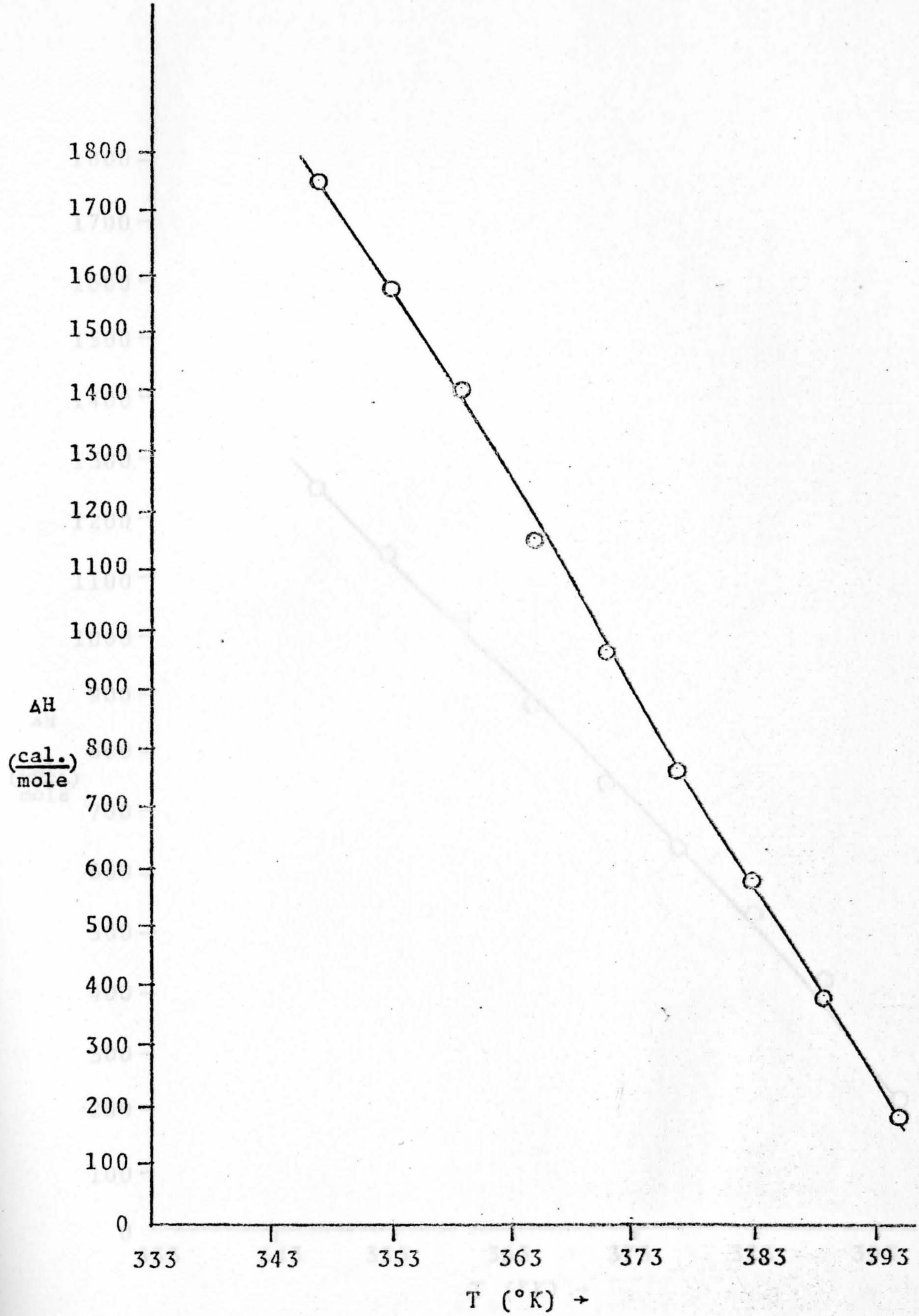

Figure46. Experimental ΔH versus Temperature Curve obtained for .3 atomic percent Sb.

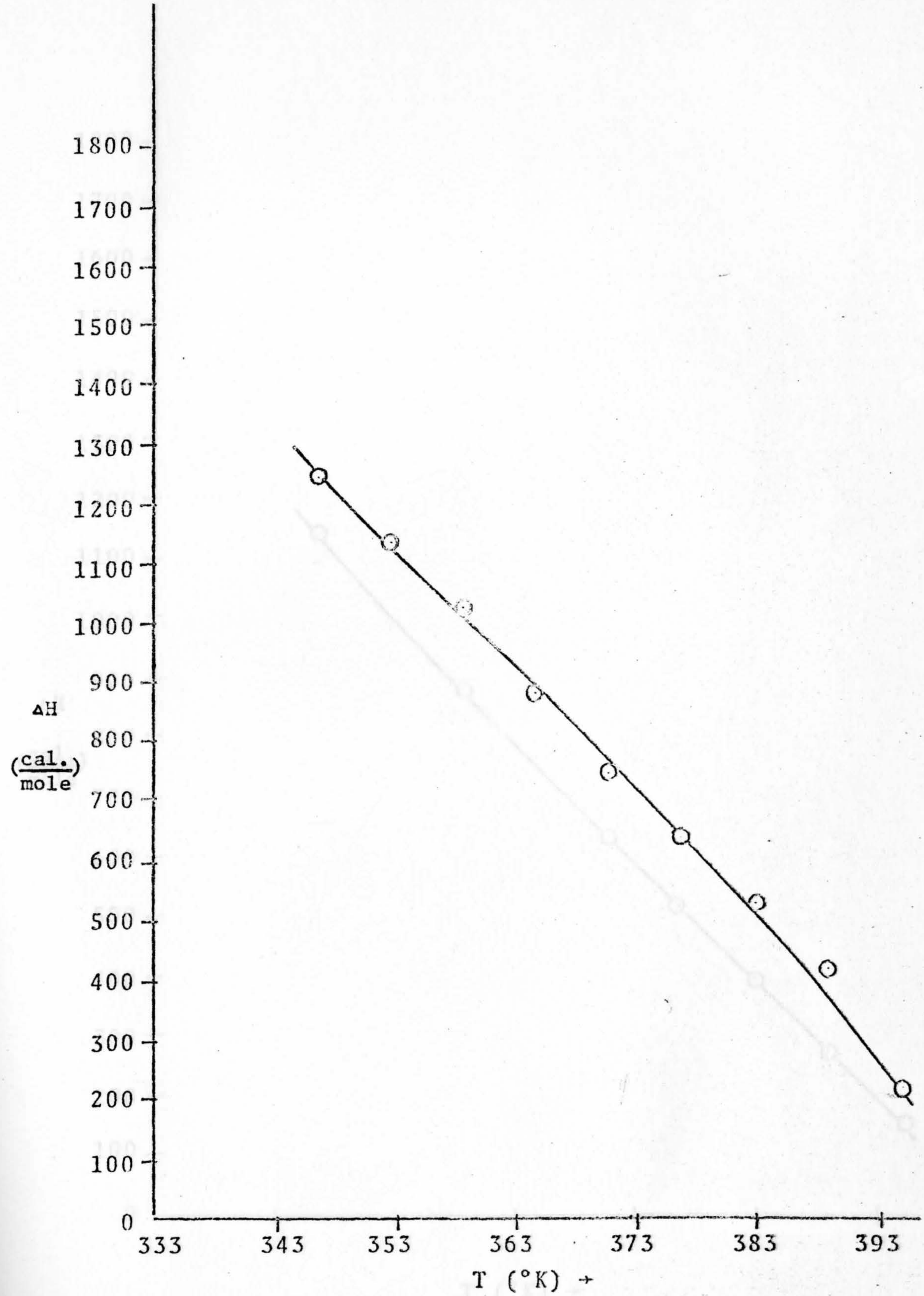

Figure47. Experimental ΔH versus Temperature Curve obtained for .3 atomic percent Cd.

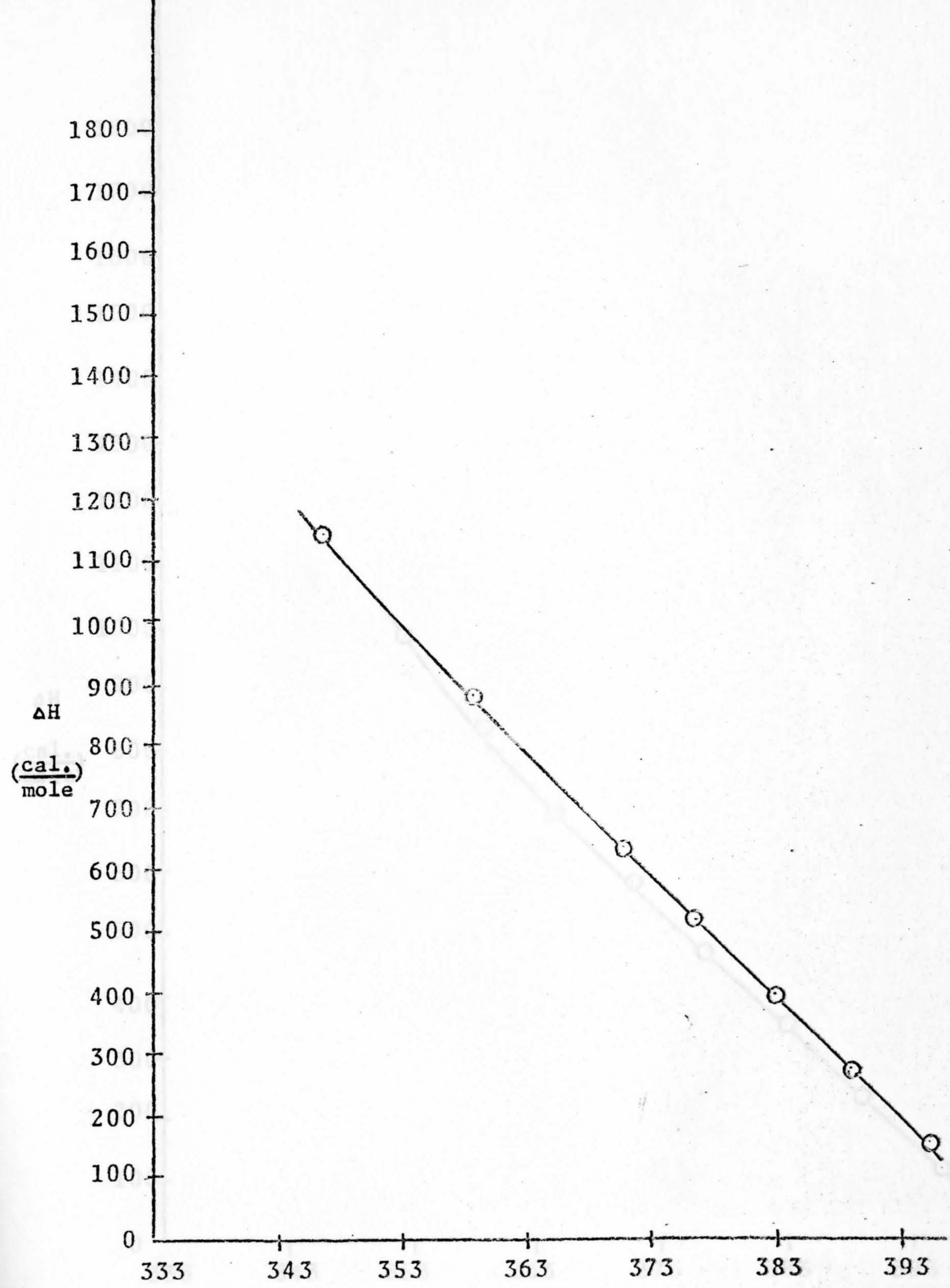

Figure 48. Experimental ΔH versus Temperature Curve obtained for .3 atomic percent Te.

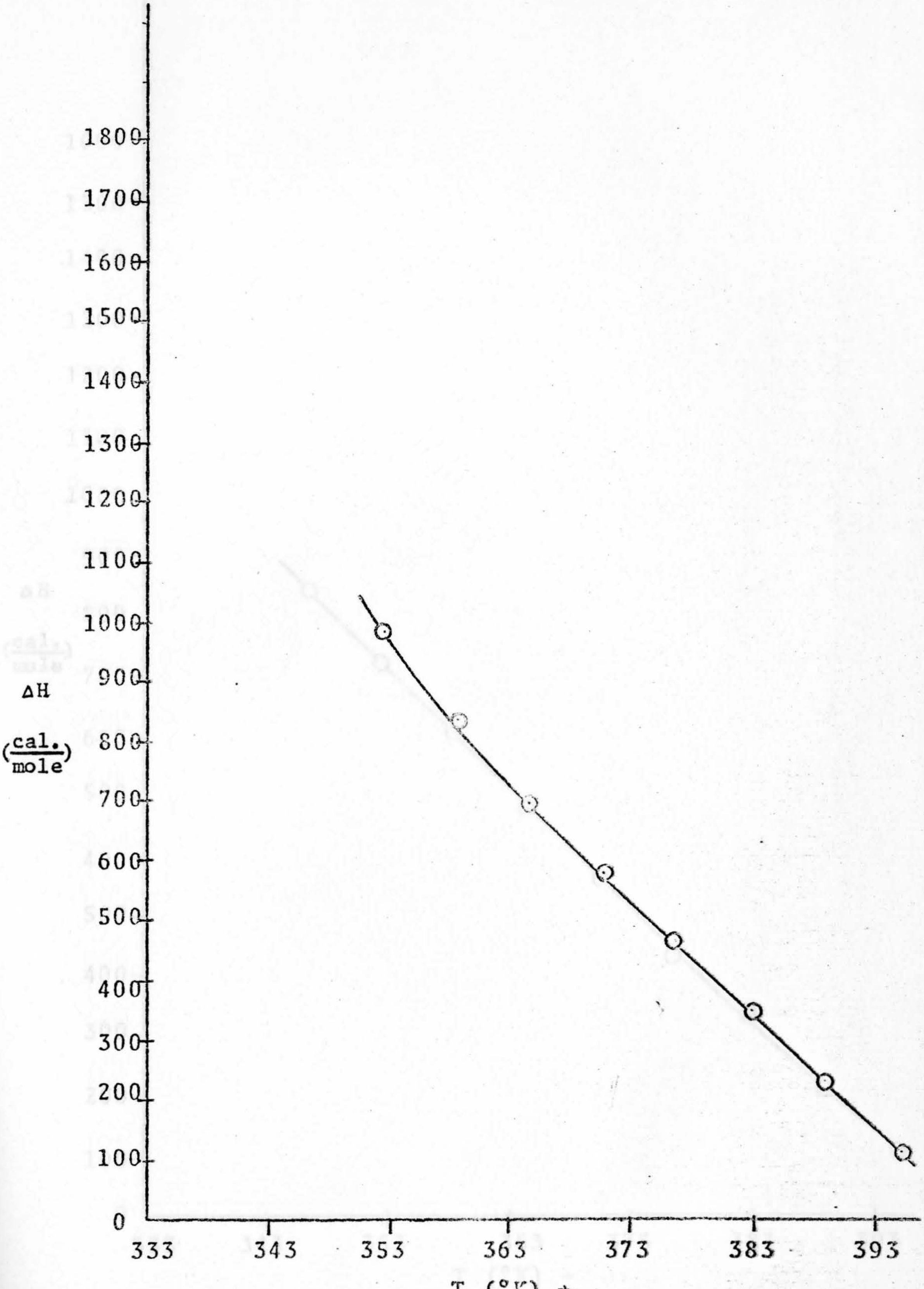

Figure49. Experimental ΔH versus Temperature Curve obtained for .3 atomic percent Zr.

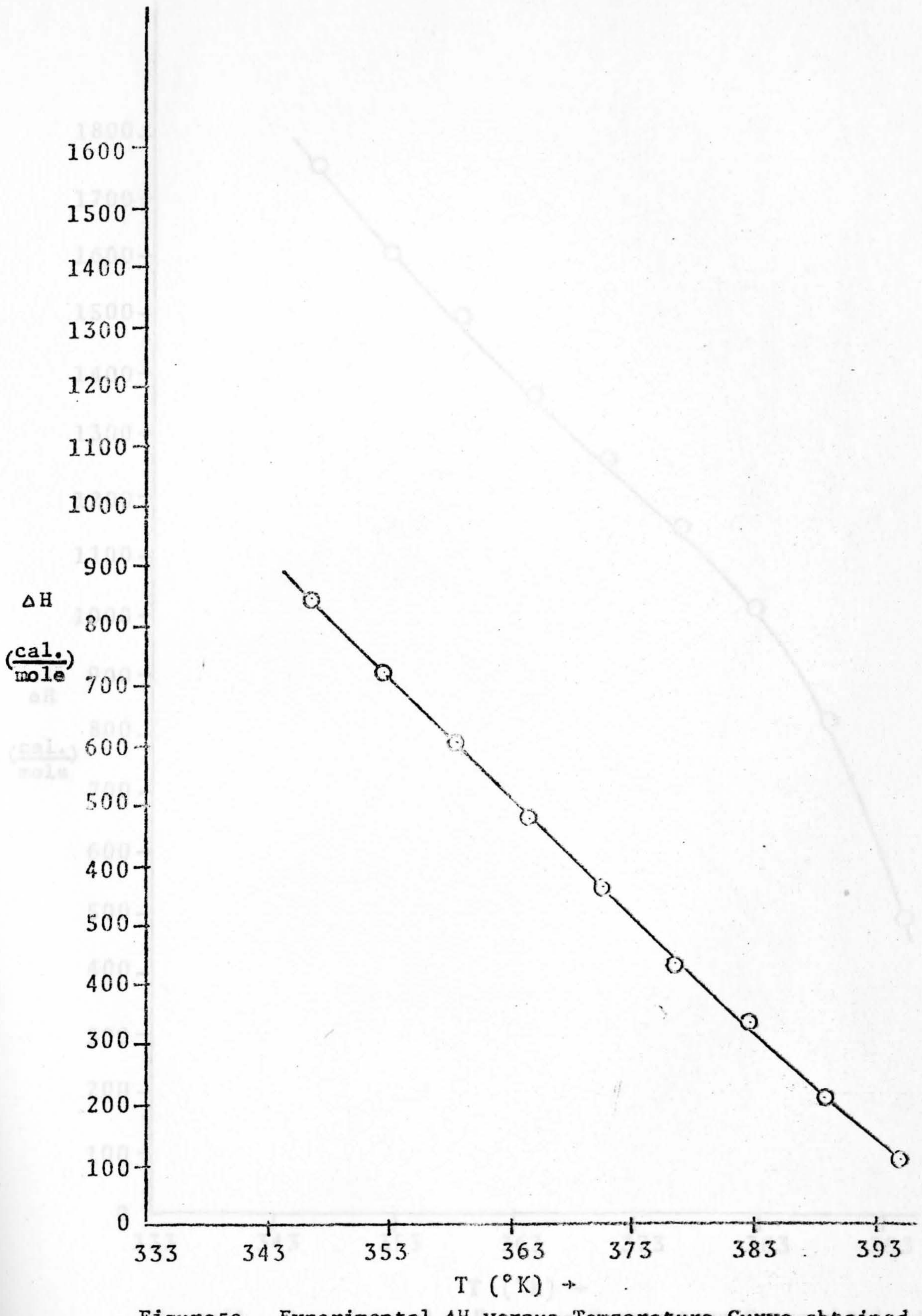

Figure 50. Experimental ΔH versus Temperature Curve obtained for the .3 atomic percent Ag.

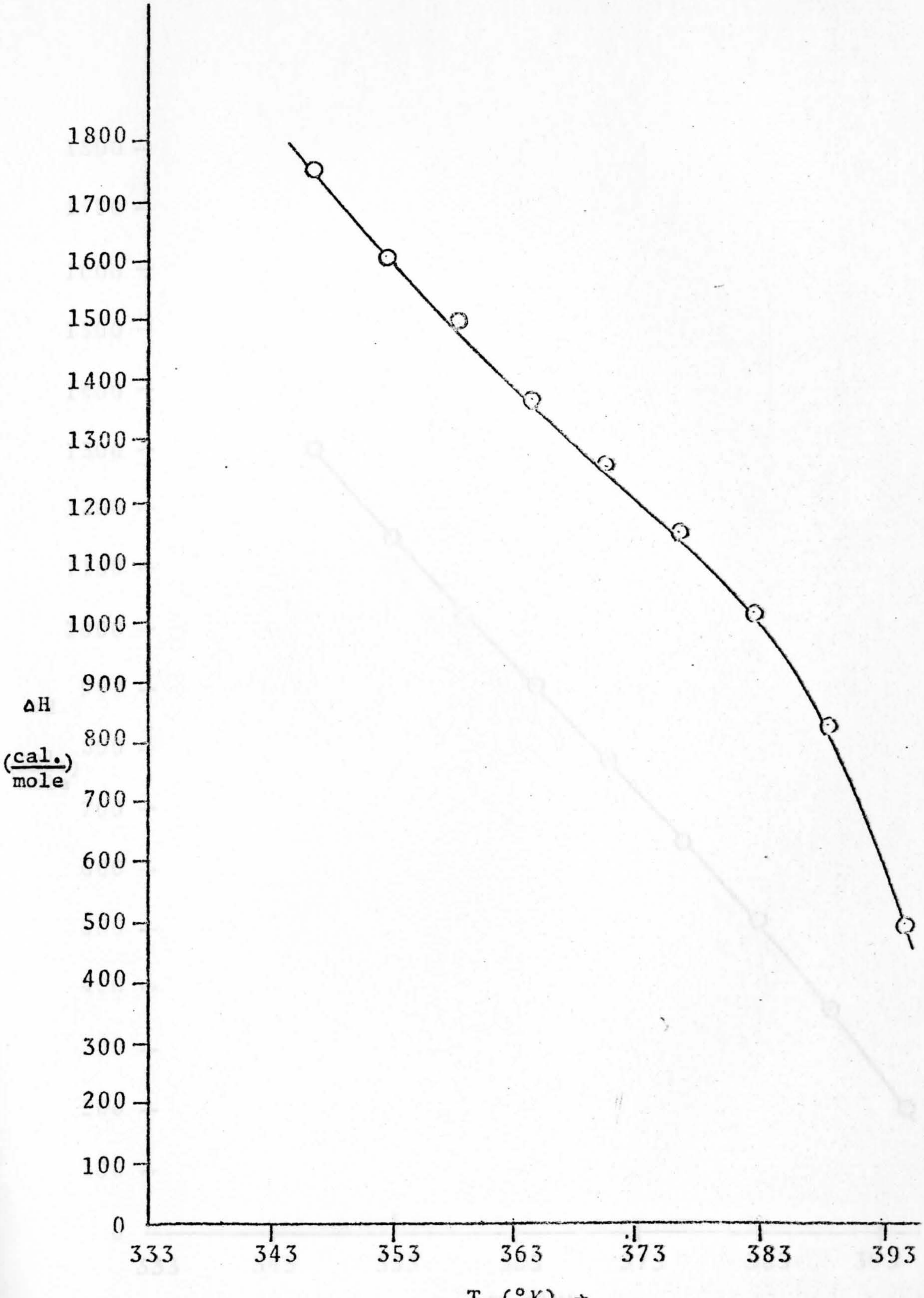

Figure 51. Experimental ΔH versus Temperature Curve obtained for .1 atomic percent Te.

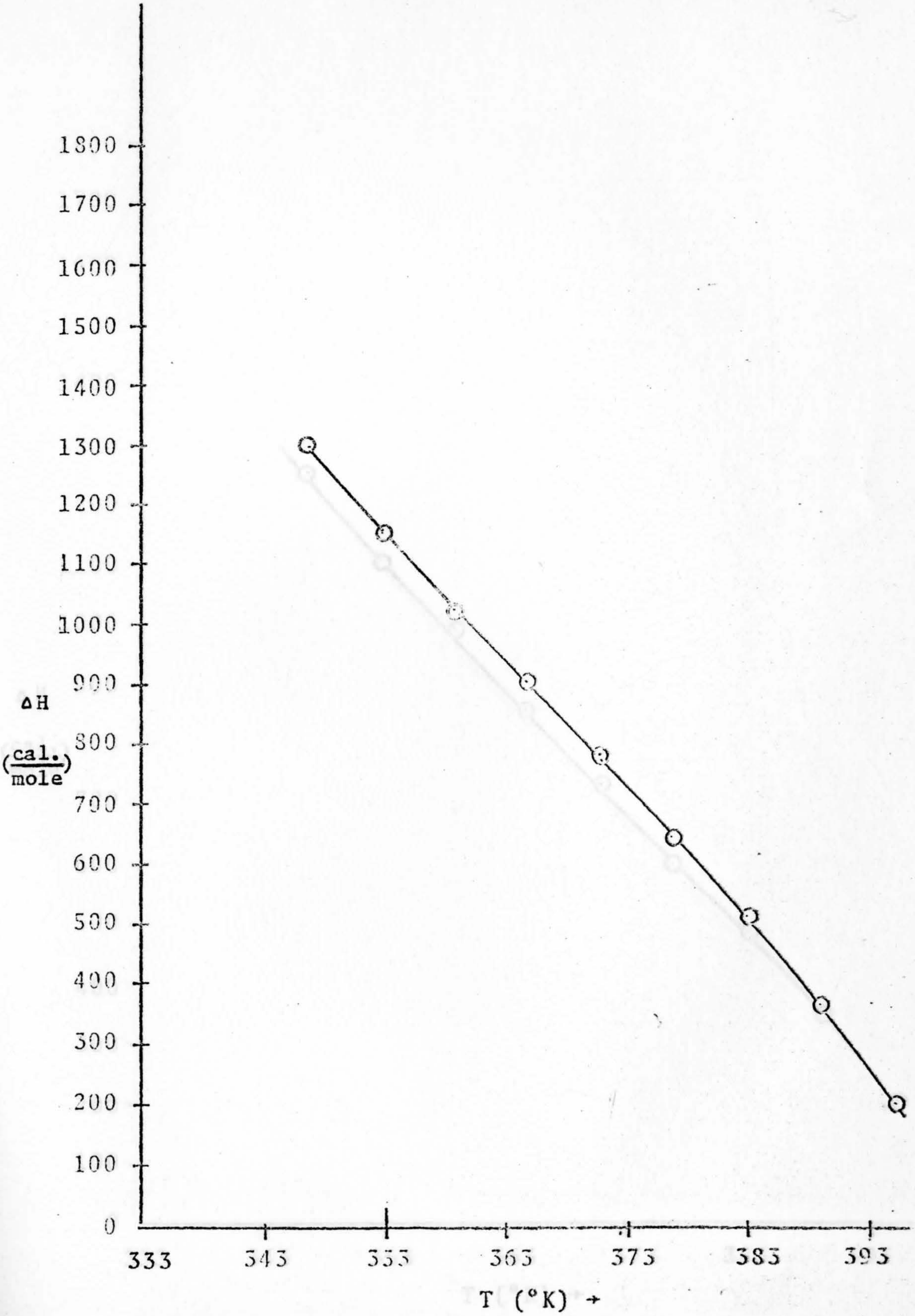

Figure52. Experimental ΔH versus Temperature Curve obtained for the .1 atomic percent Ag.

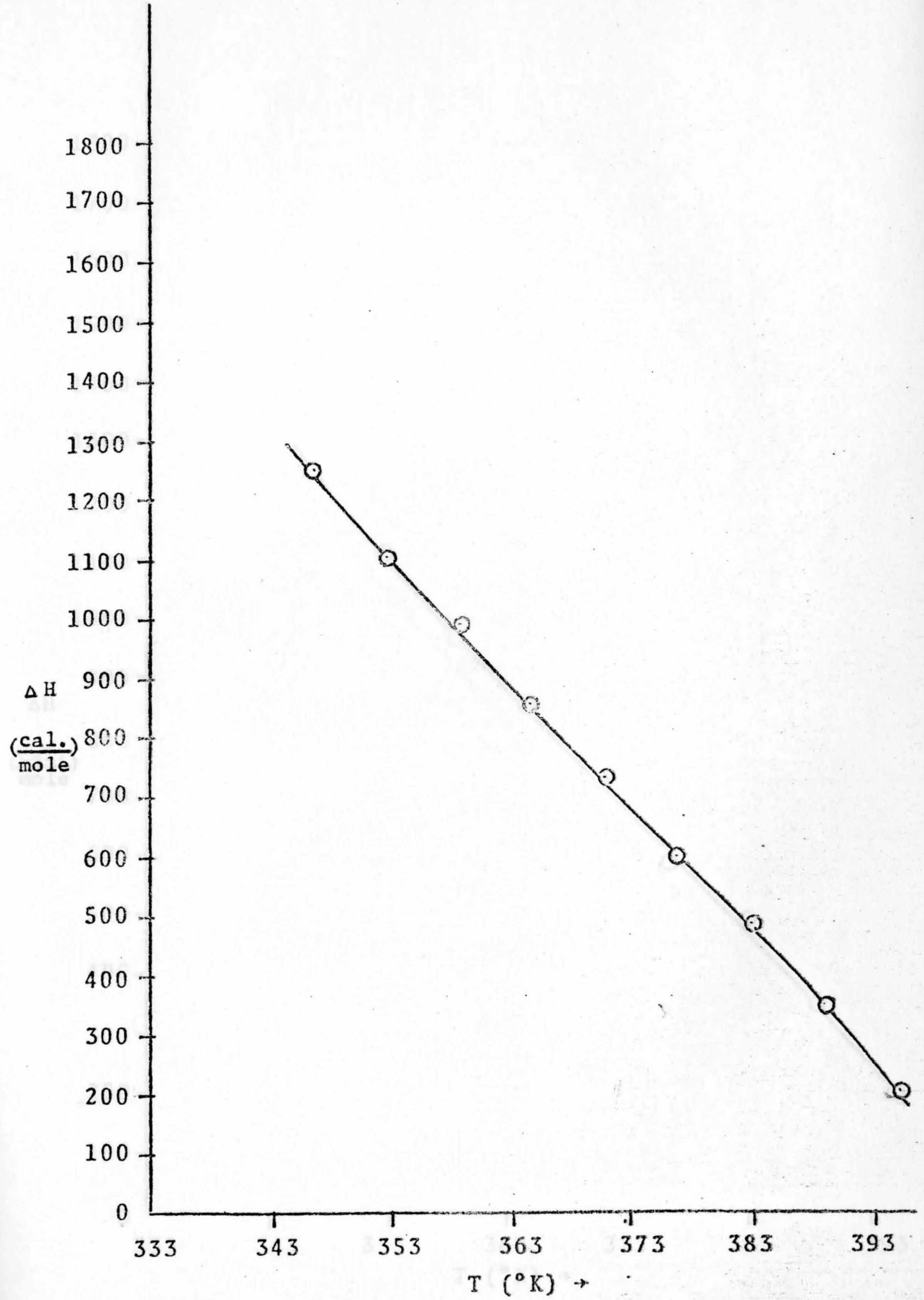

Figure 53. Experimental ΔH versus Temperature Curve obtained for .1 atomic percent Zr.

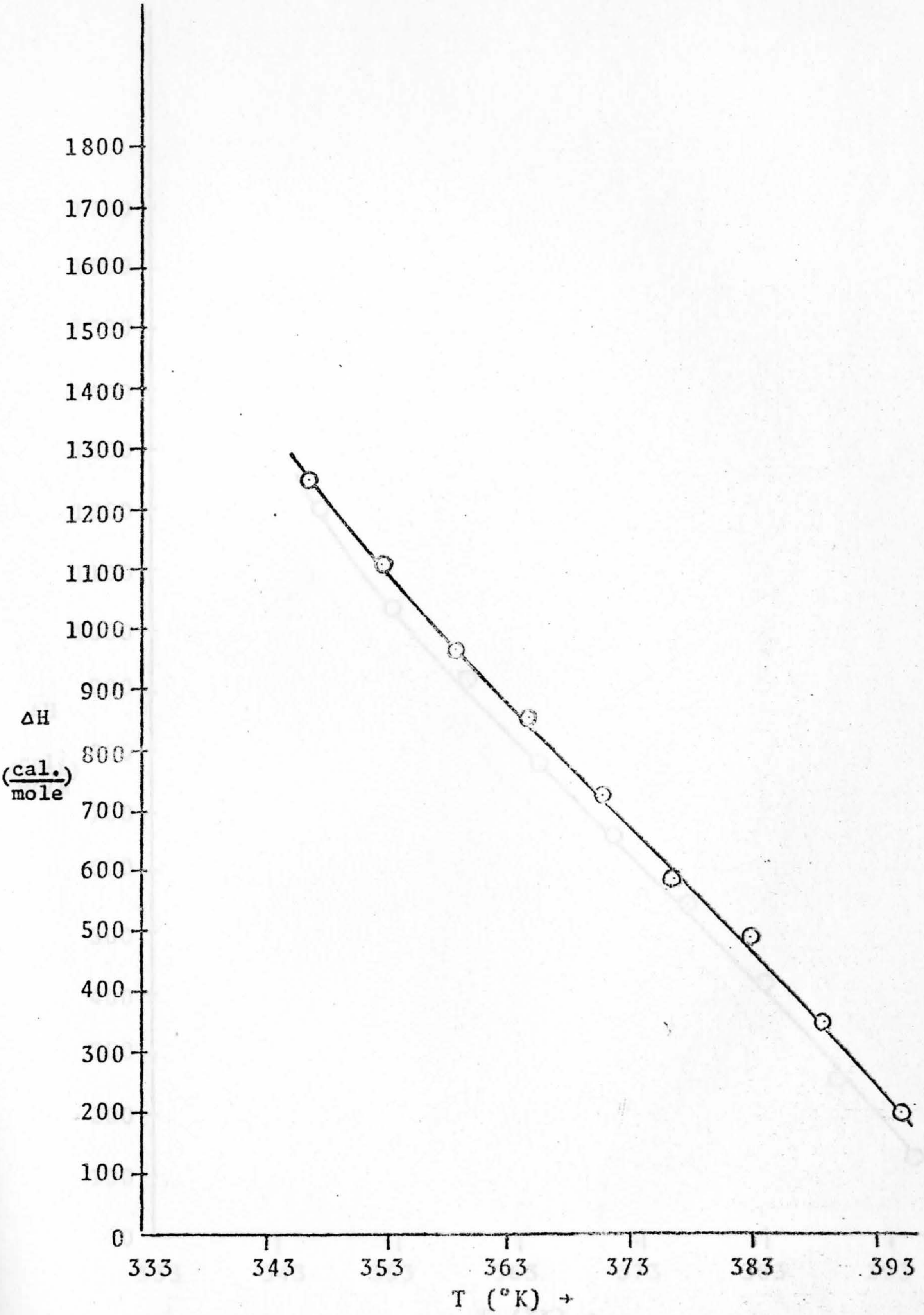

Figure 69. Experimental ΔH versus Temperature Curve obtained for .1 atomic percent Cd.

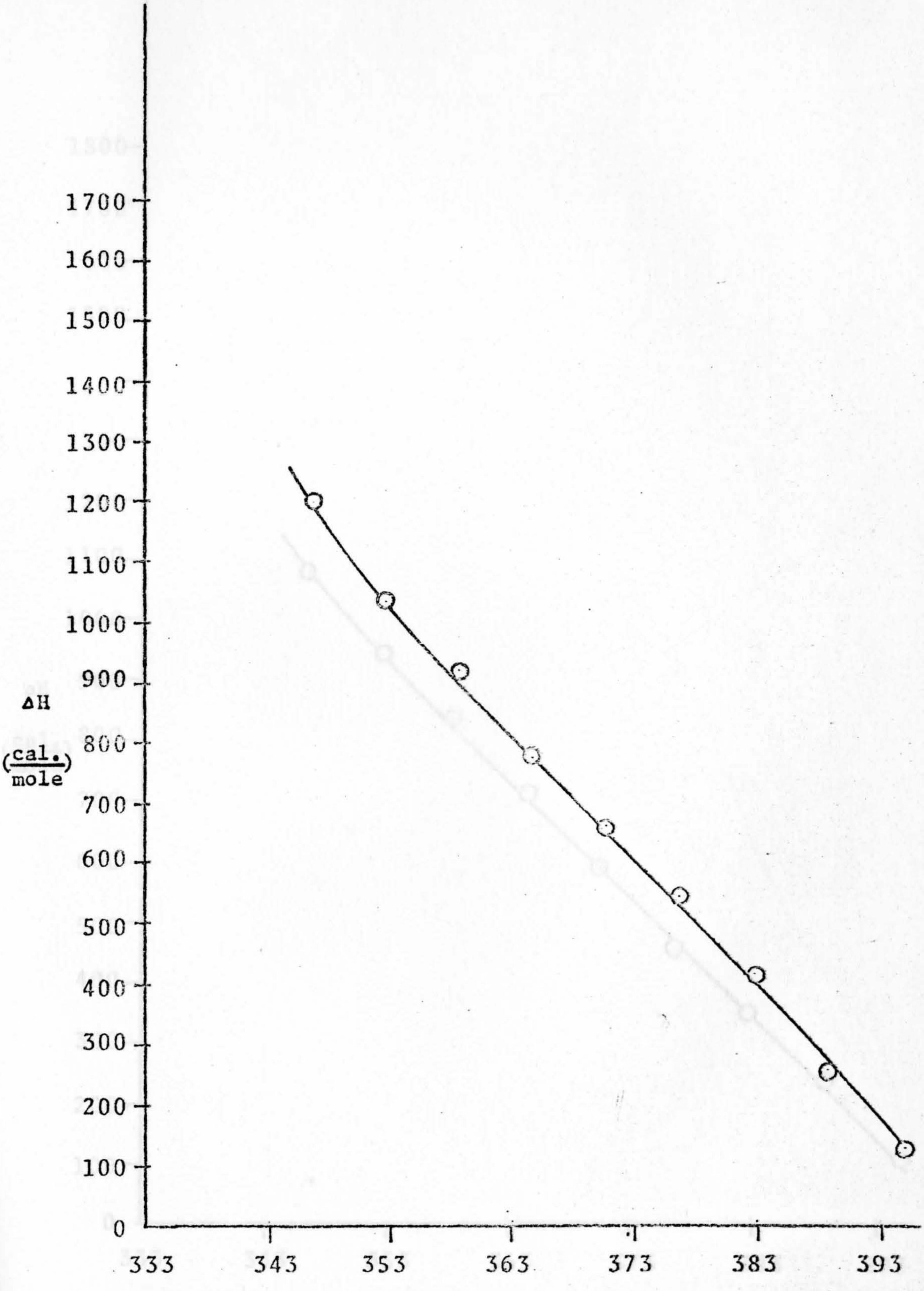

Figure70. Experimental ΔH versus Temperature Curve obtained for .1 atomic percent In.

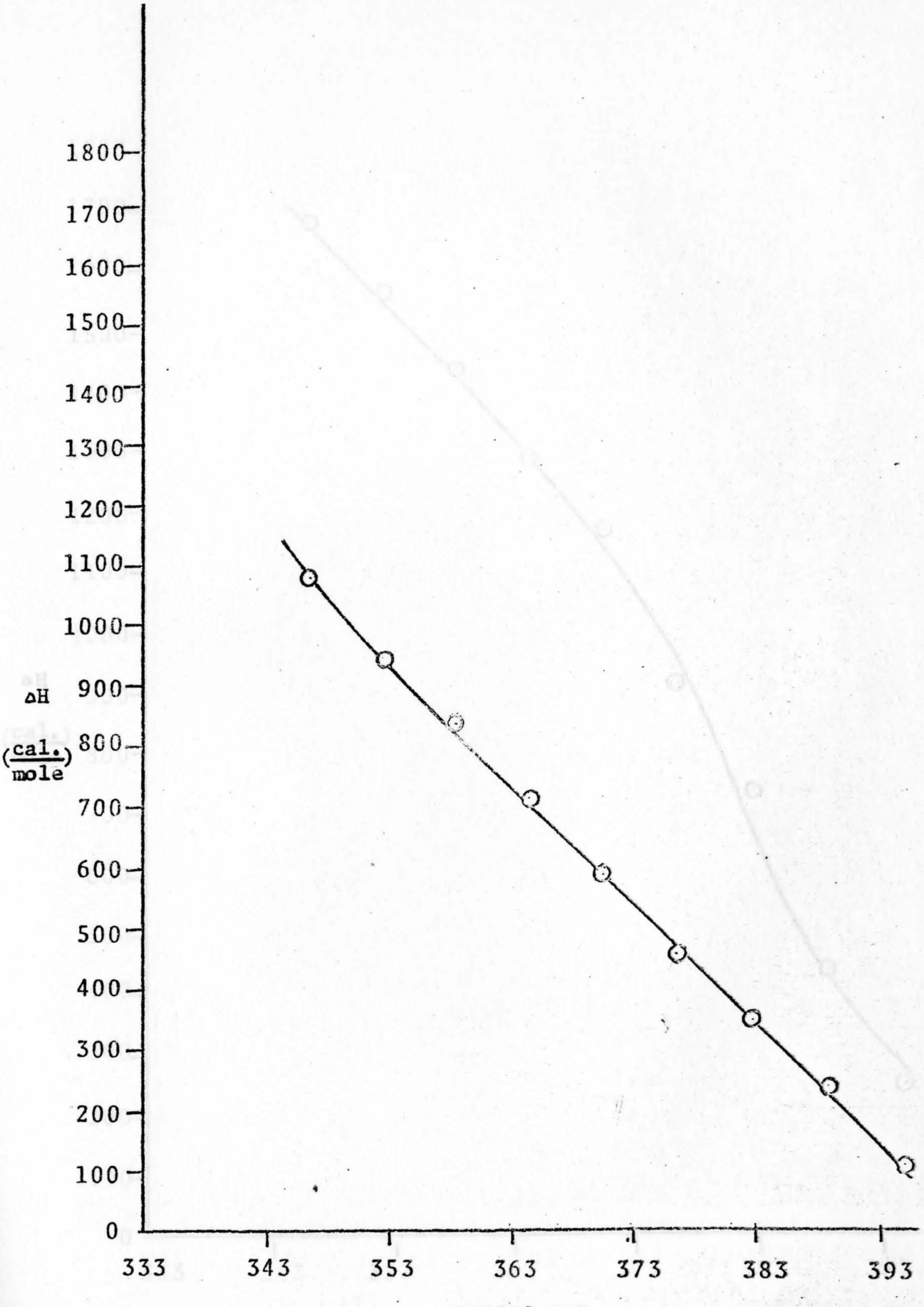

Figure 54. Experimental ΔH versus Temperature Curve obtained for .1 atomic percent Sb.

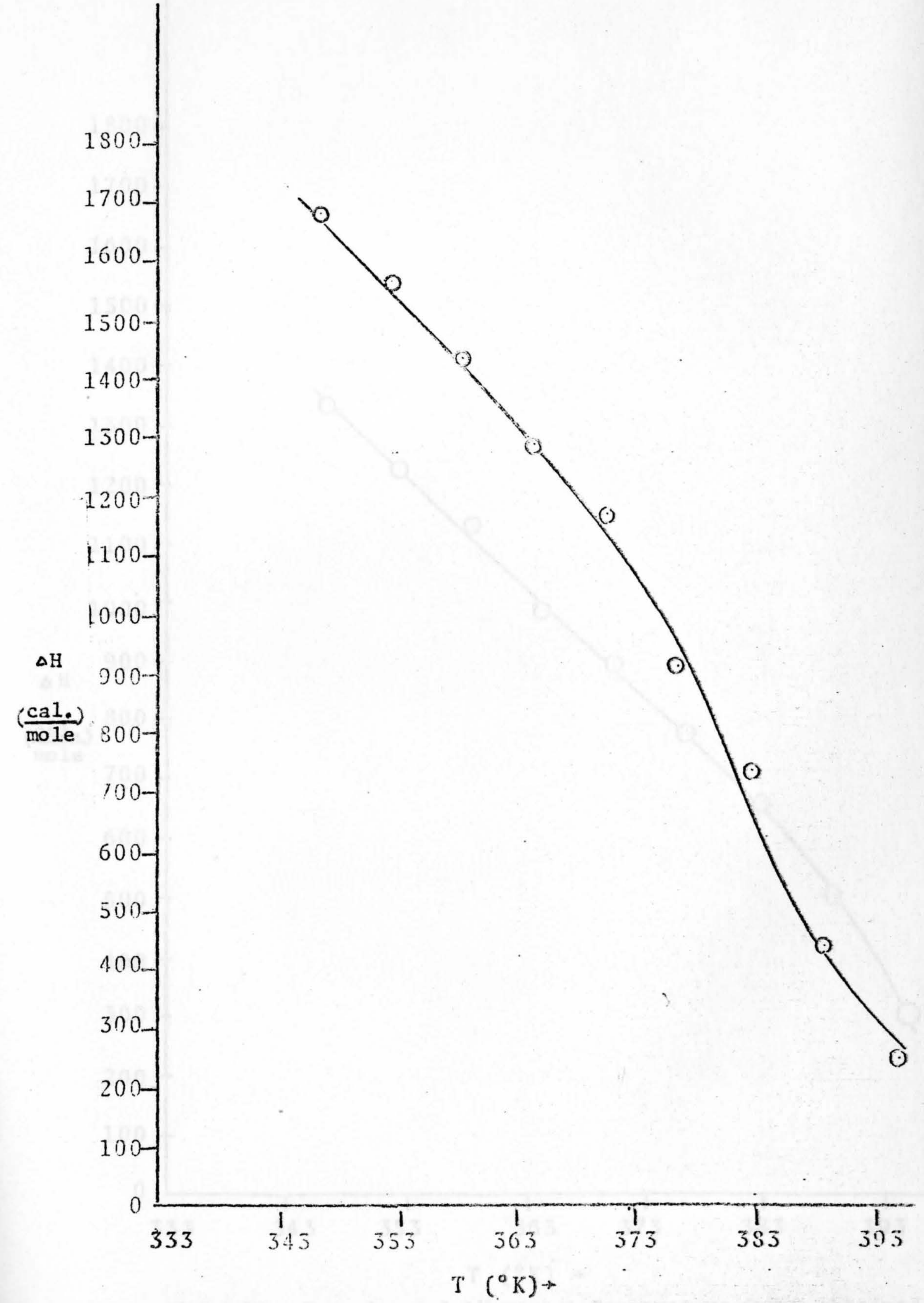

Figure 55. Experimental ΔH versus Temperature Curve obtained for the .05 atomic percent Ag.

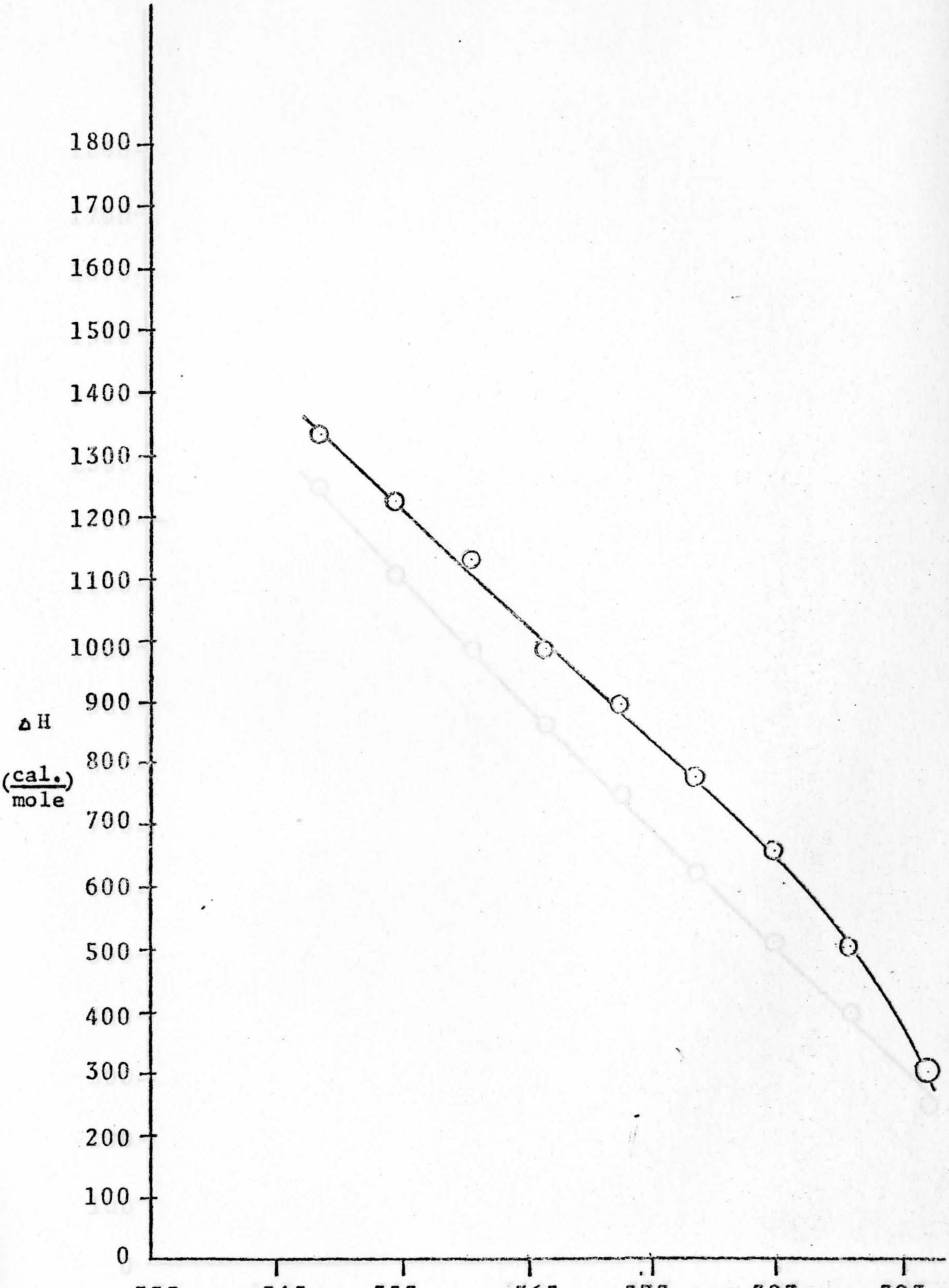

Figure 56. Experimental ΔH versus Temperature Curve obtained for .05 atomic percent Te.

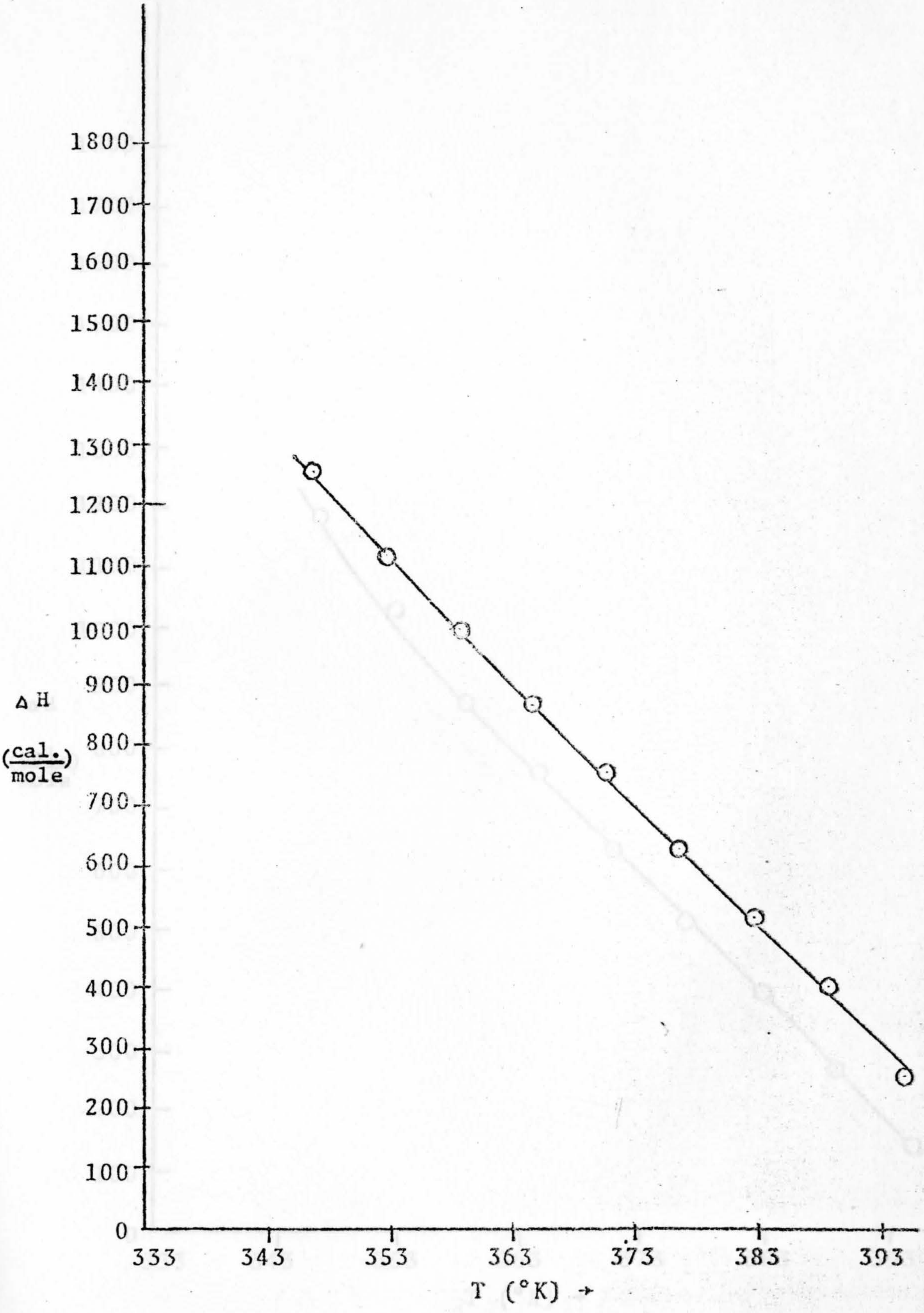

Figure 57. Experimental ΔH versus Temperature Curve obtained for .05 atomic percent Cd.

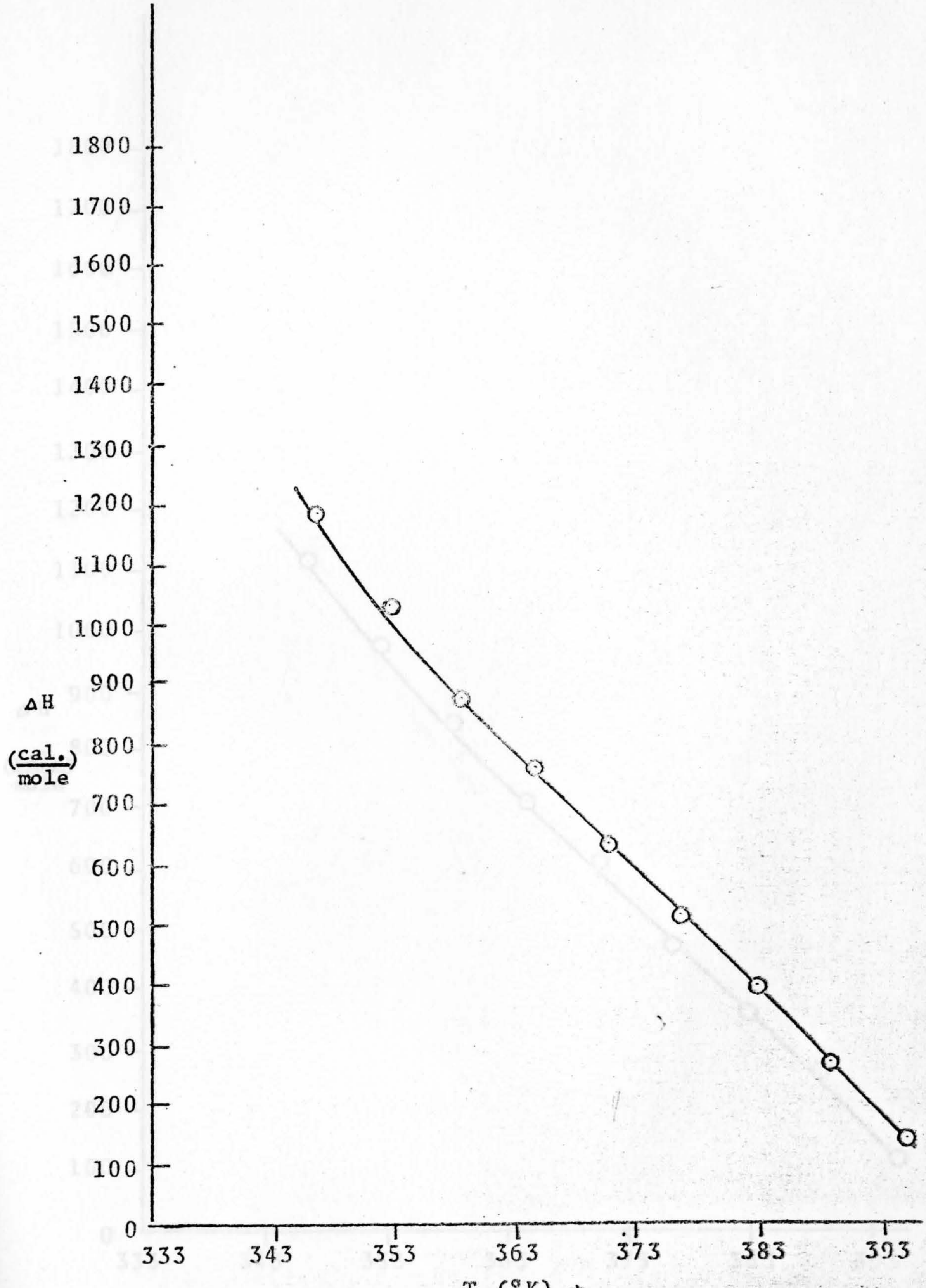

Figure 58. Experimental ΔH versus Temperature Curve obtained for .05 atomic percent In.

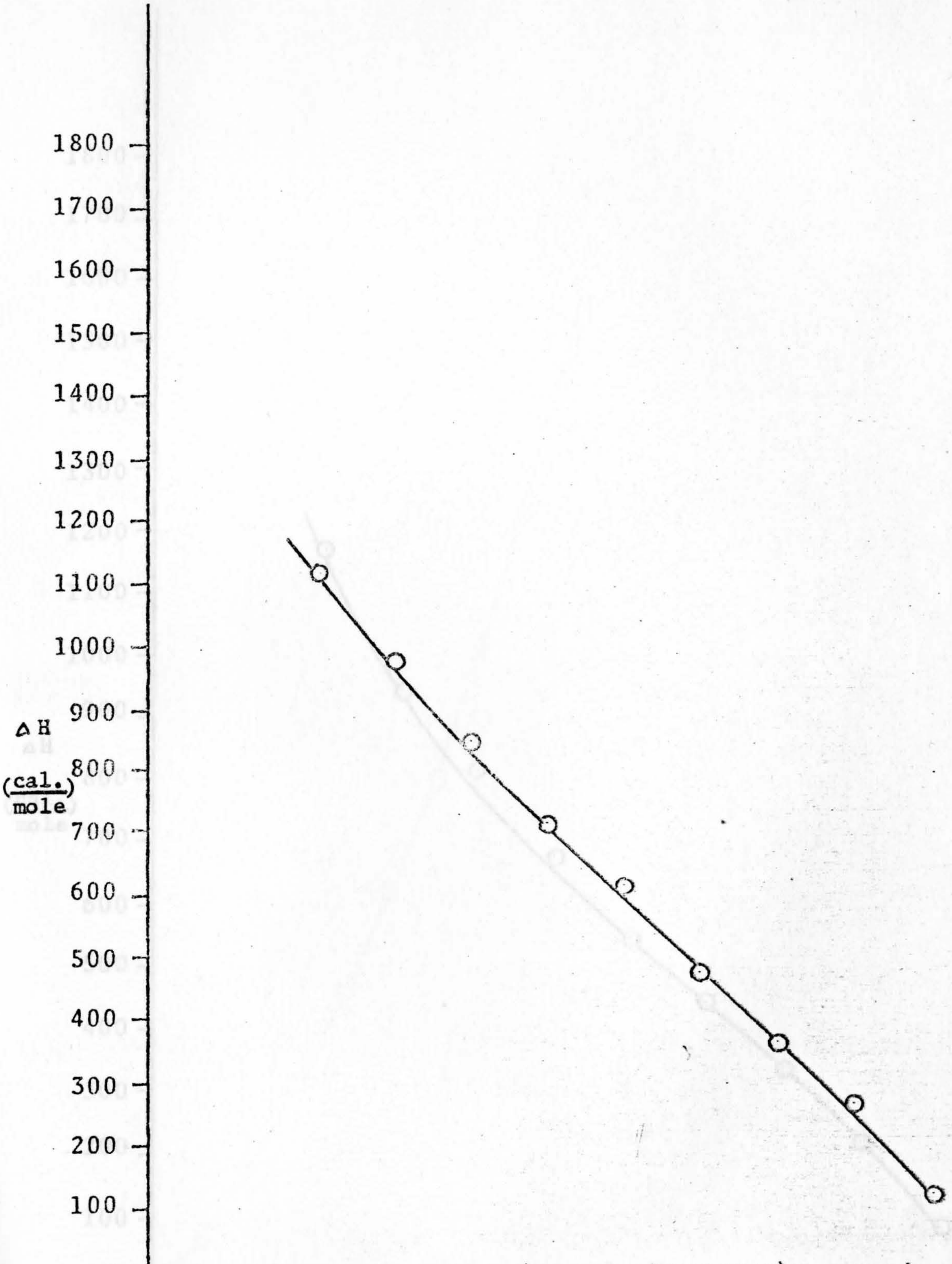

Figure 59. Experimental ΔH versus Temperature Curve obtained for .05 atomic percent Sb.

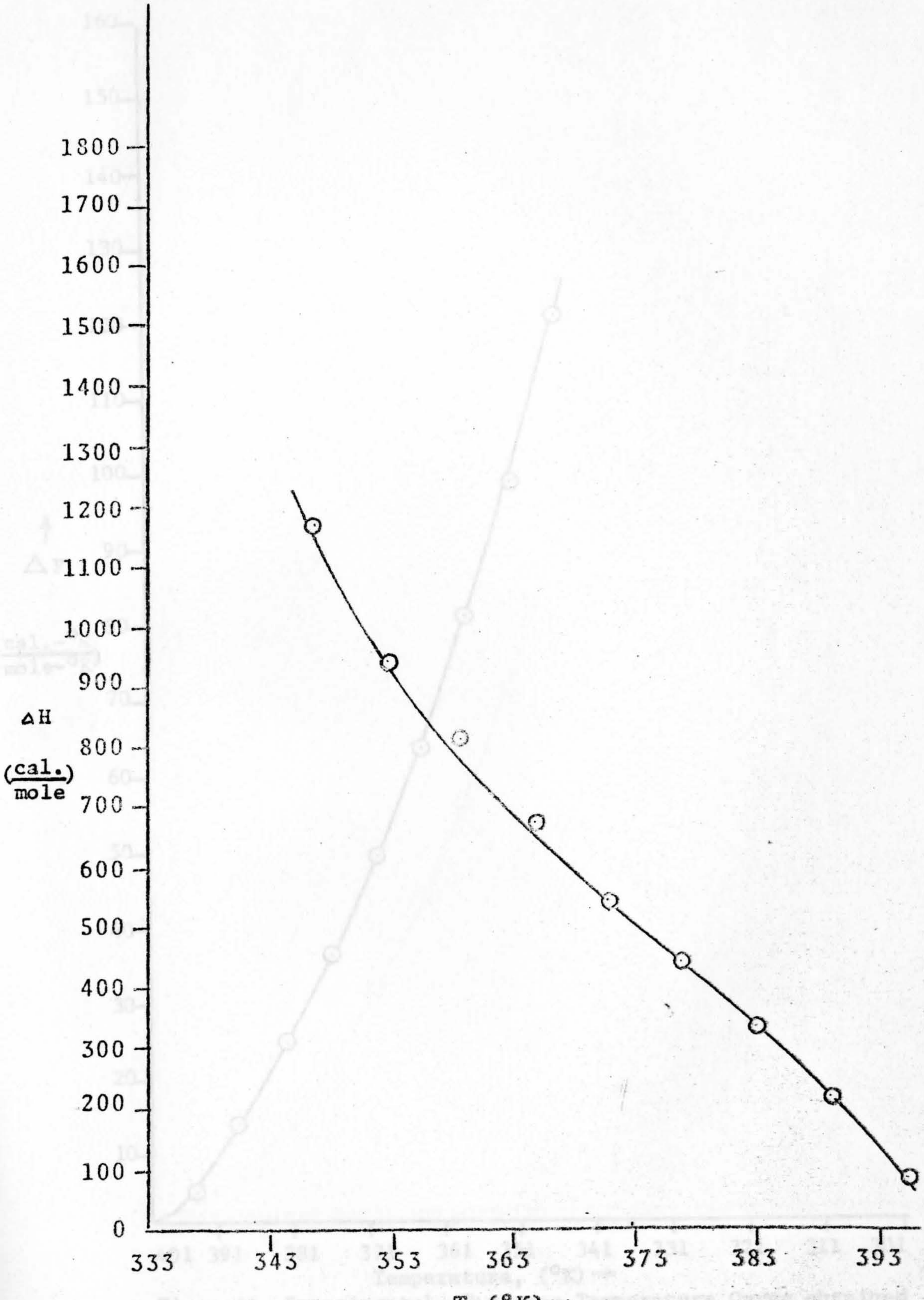

Figure 60. Experimental ΔH versus Temperature Curve obtained for .05 atomic percent Zr.

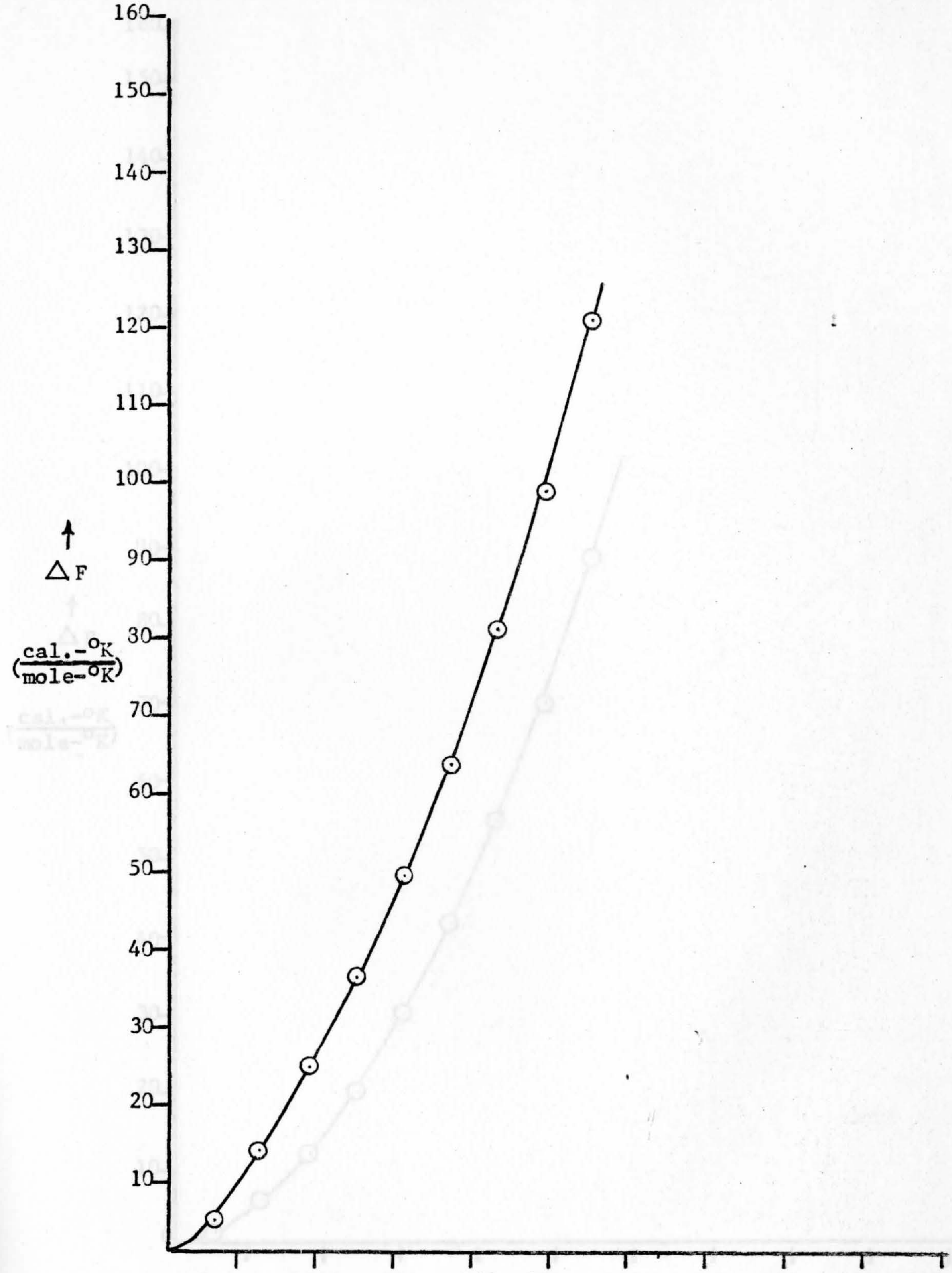

Figure 61. Experimental ΔF versus Temperature Curve obtained for .1 atomic percent Te.

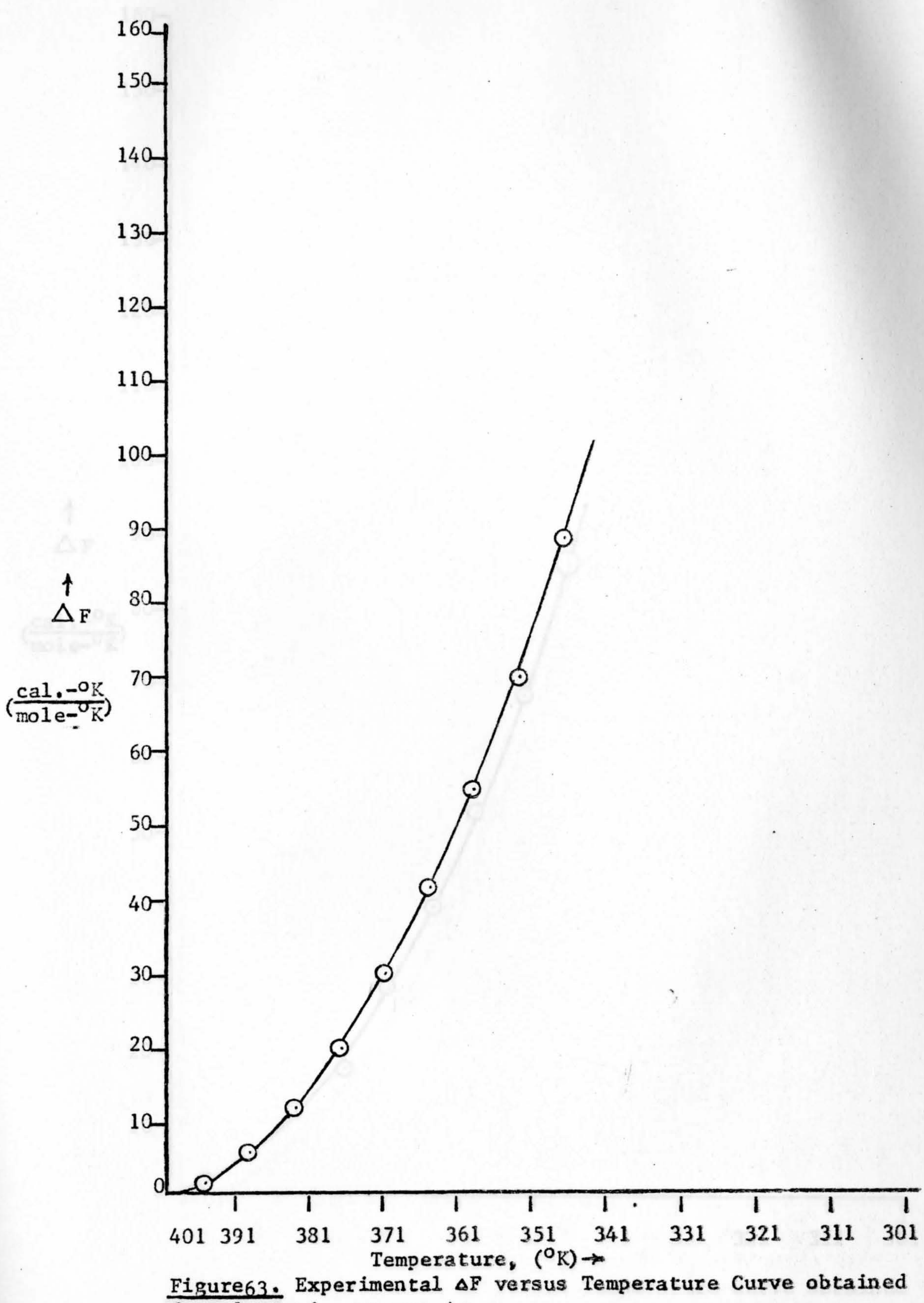

Figure 63. Experimental ΔF versus Temperature Curve obtained for .1 atomic percent Ag.

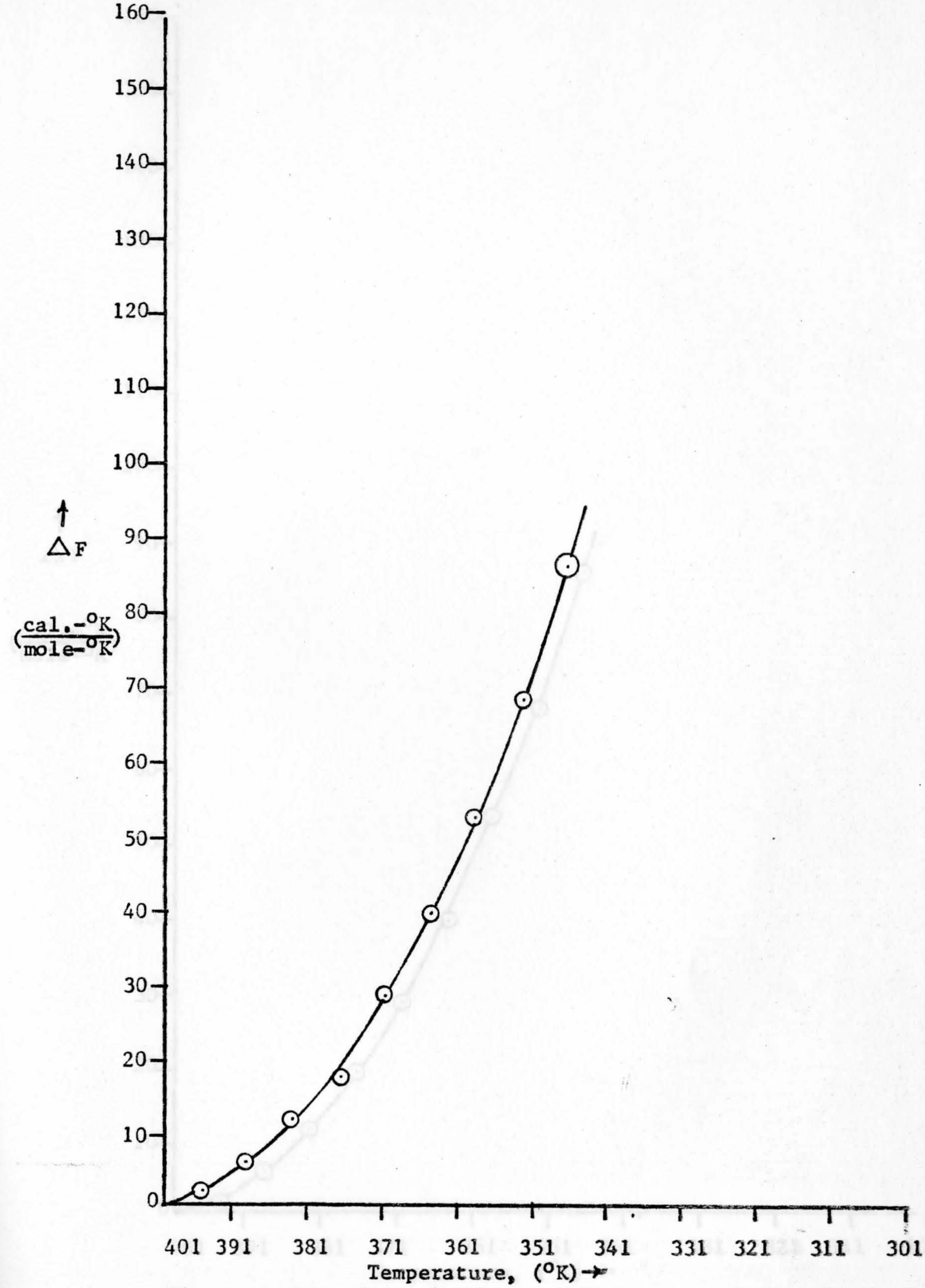

Figure 64. Experimental ΔF versus Temperature Curve obtained for .1 atomic percent Cd.

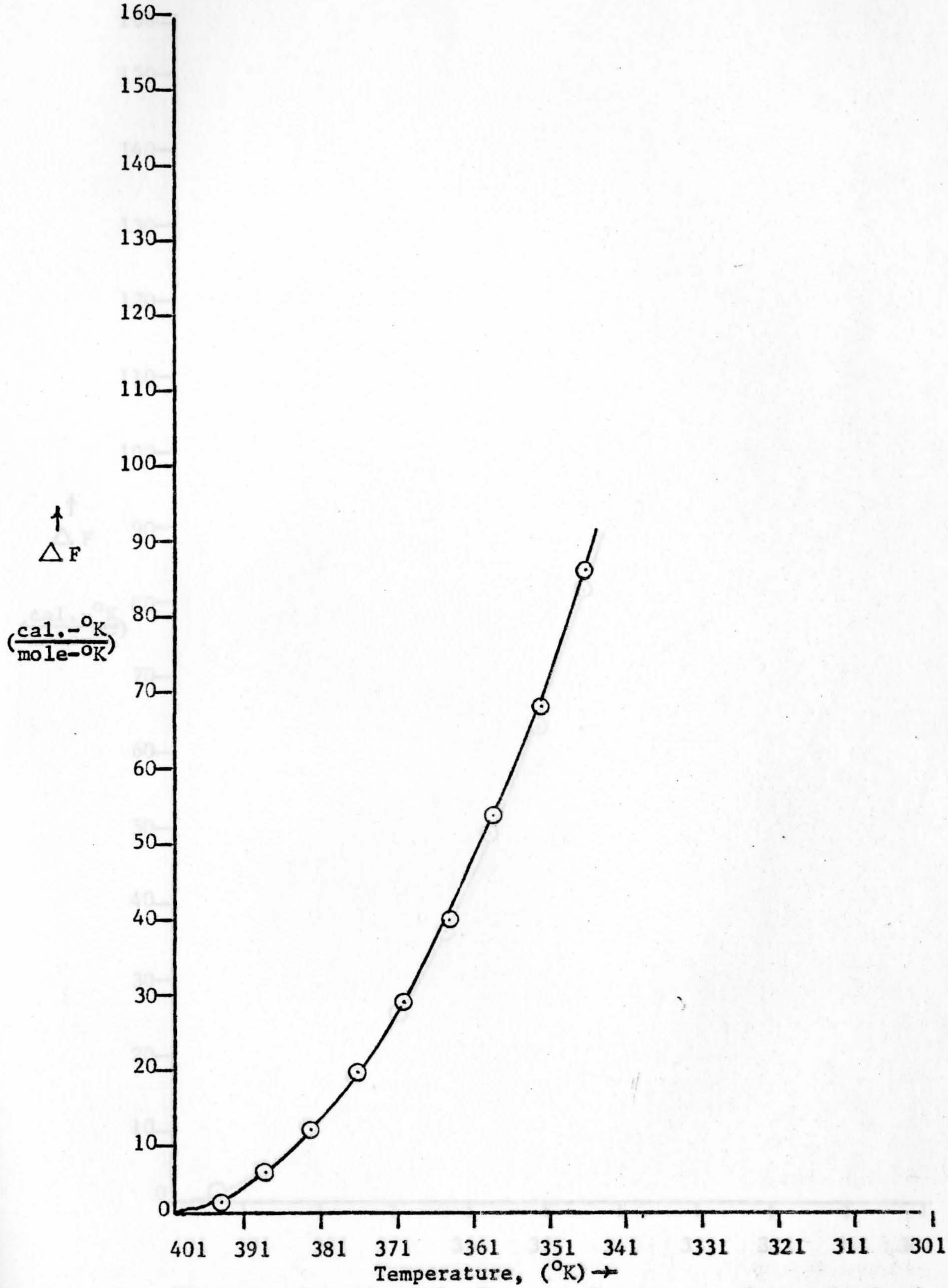

Figure 66. Experimental ΔF versus Temperature Curve obtained for .1 atomic percent Zr.

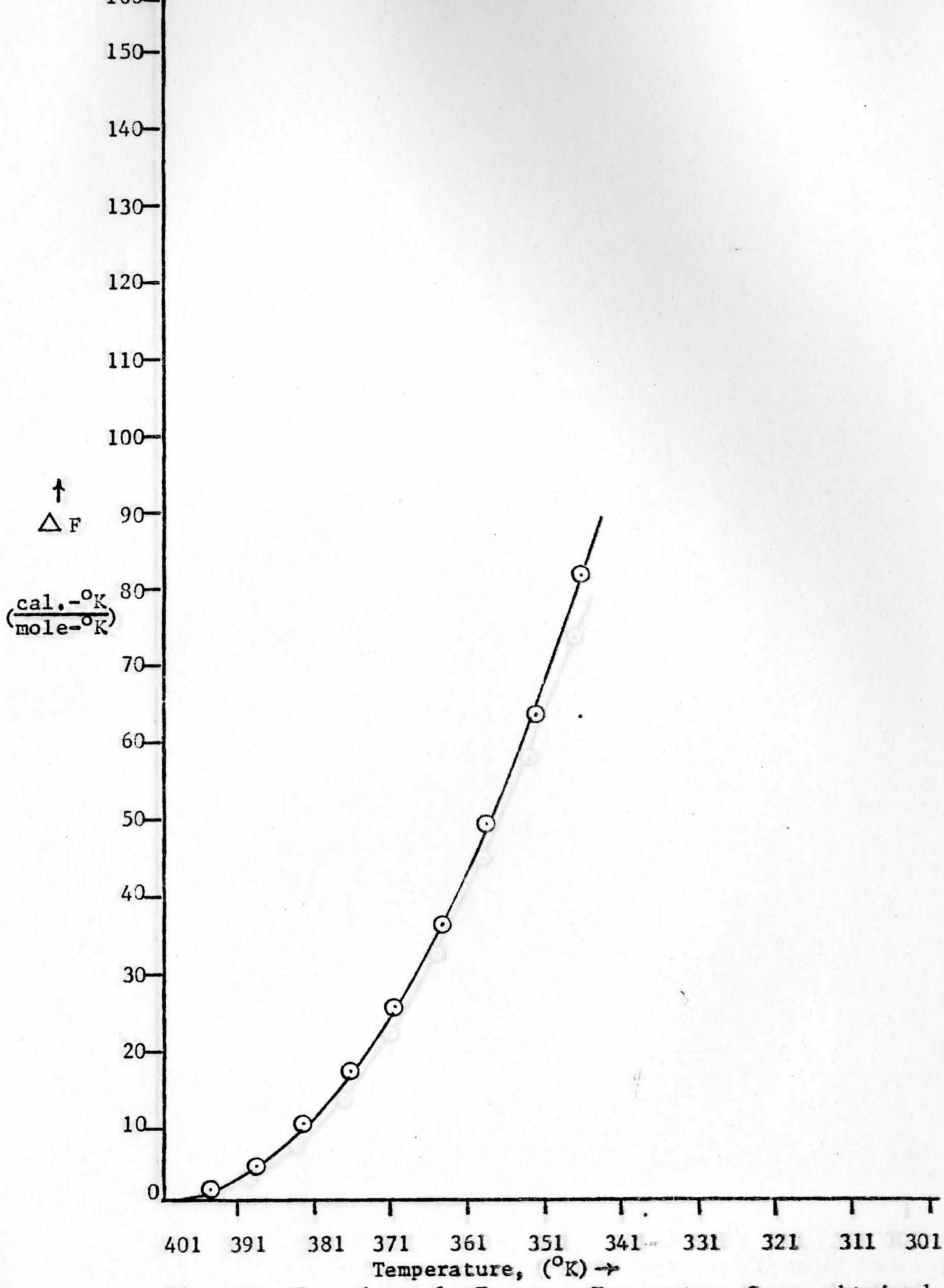

Figure67. Experimental ΔF versus Temperature Curve obtained for .1 atomic percent In.

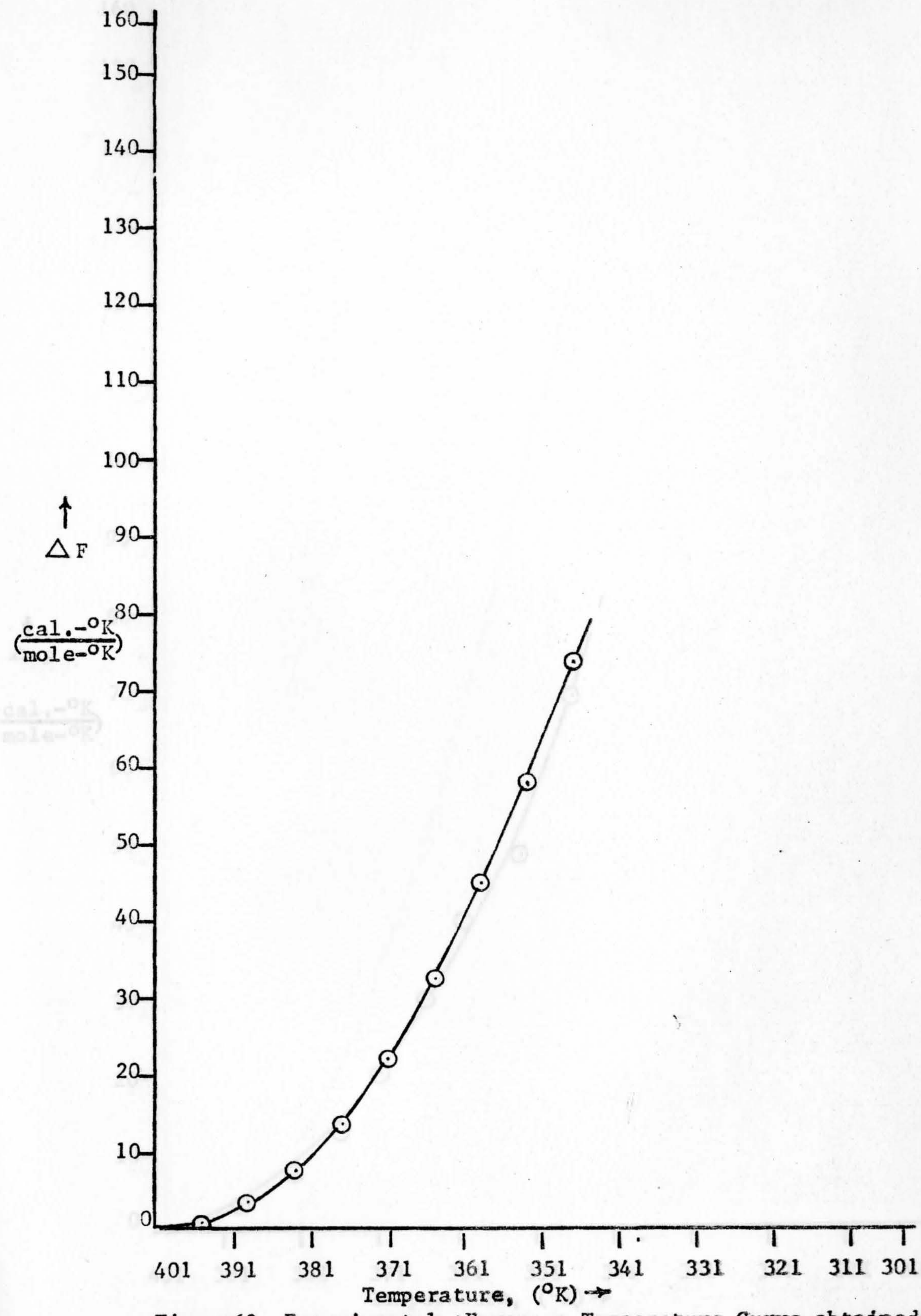

Figure68. Experimental ΔF versus Temperature Curve obtained for .1 atomic percent Sb.

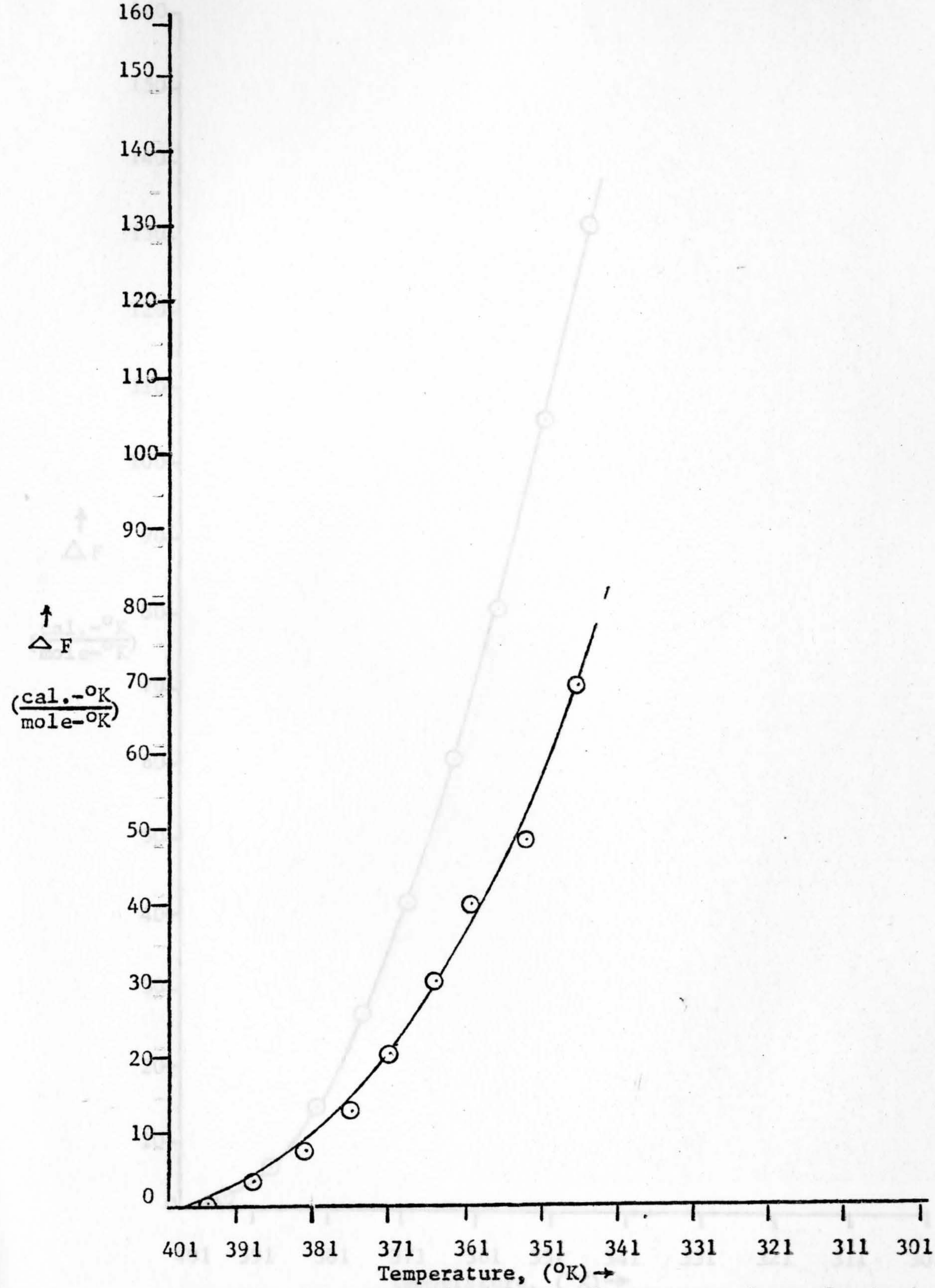

Figure71. Experimental ΔF versus Temperature Curve obtained for Pure Sn.

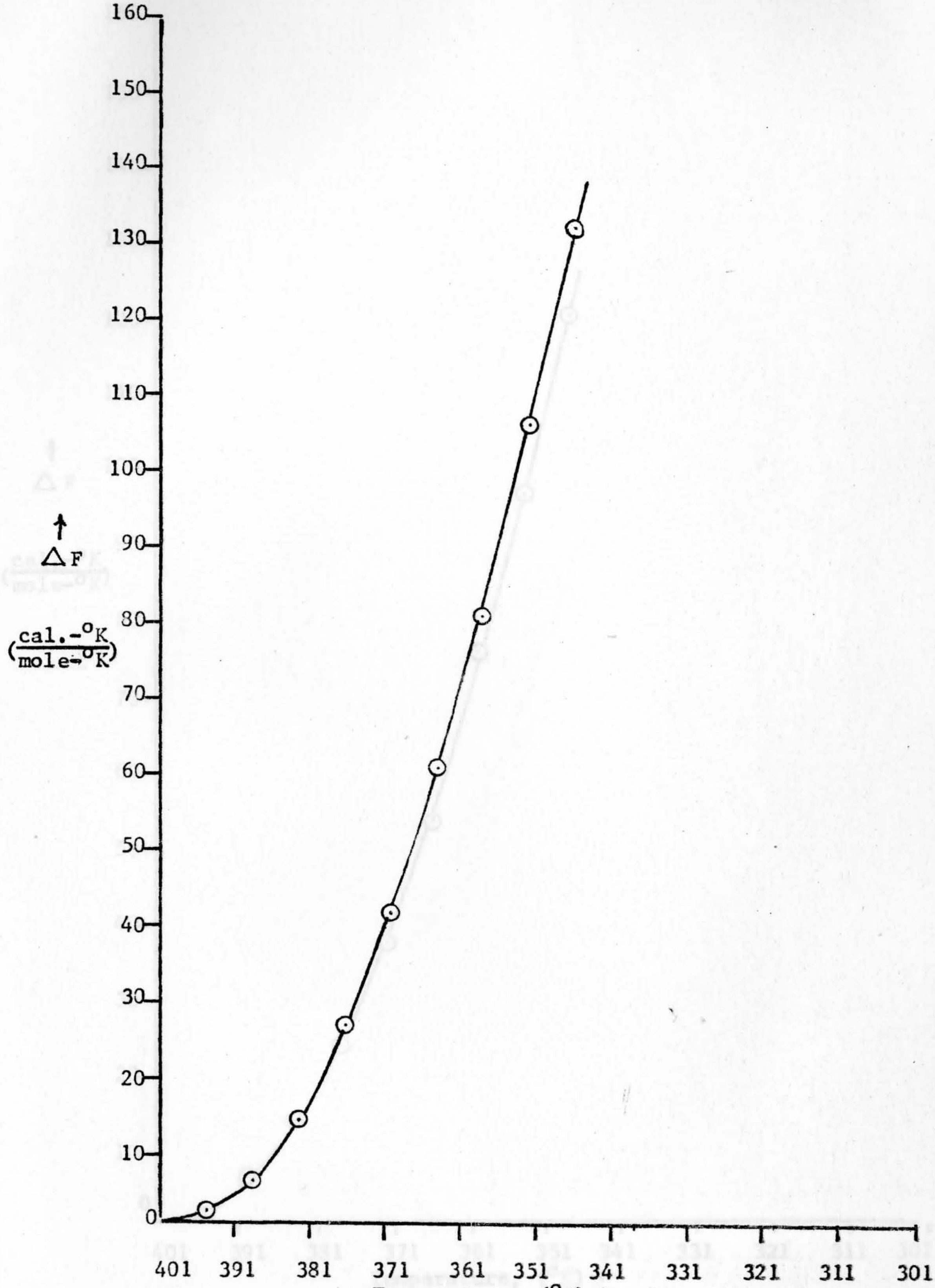

Figure 72. Experimental ΔF versus Temperature Curve obtained for .3 atomic percent In.

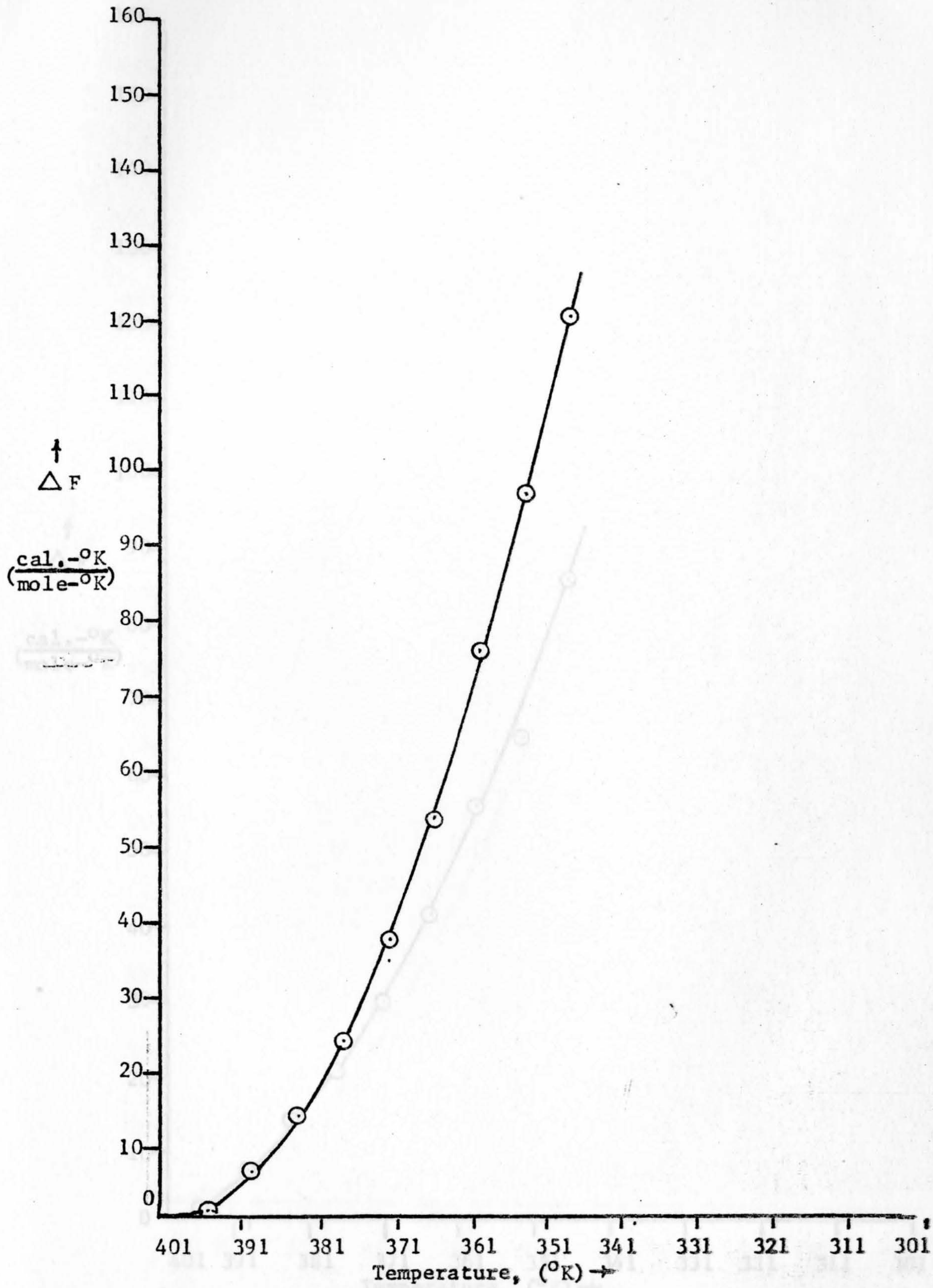

Figure 73. Experimental ΔF versus Temperature Curve obtained for .3 atomic percent Sb.

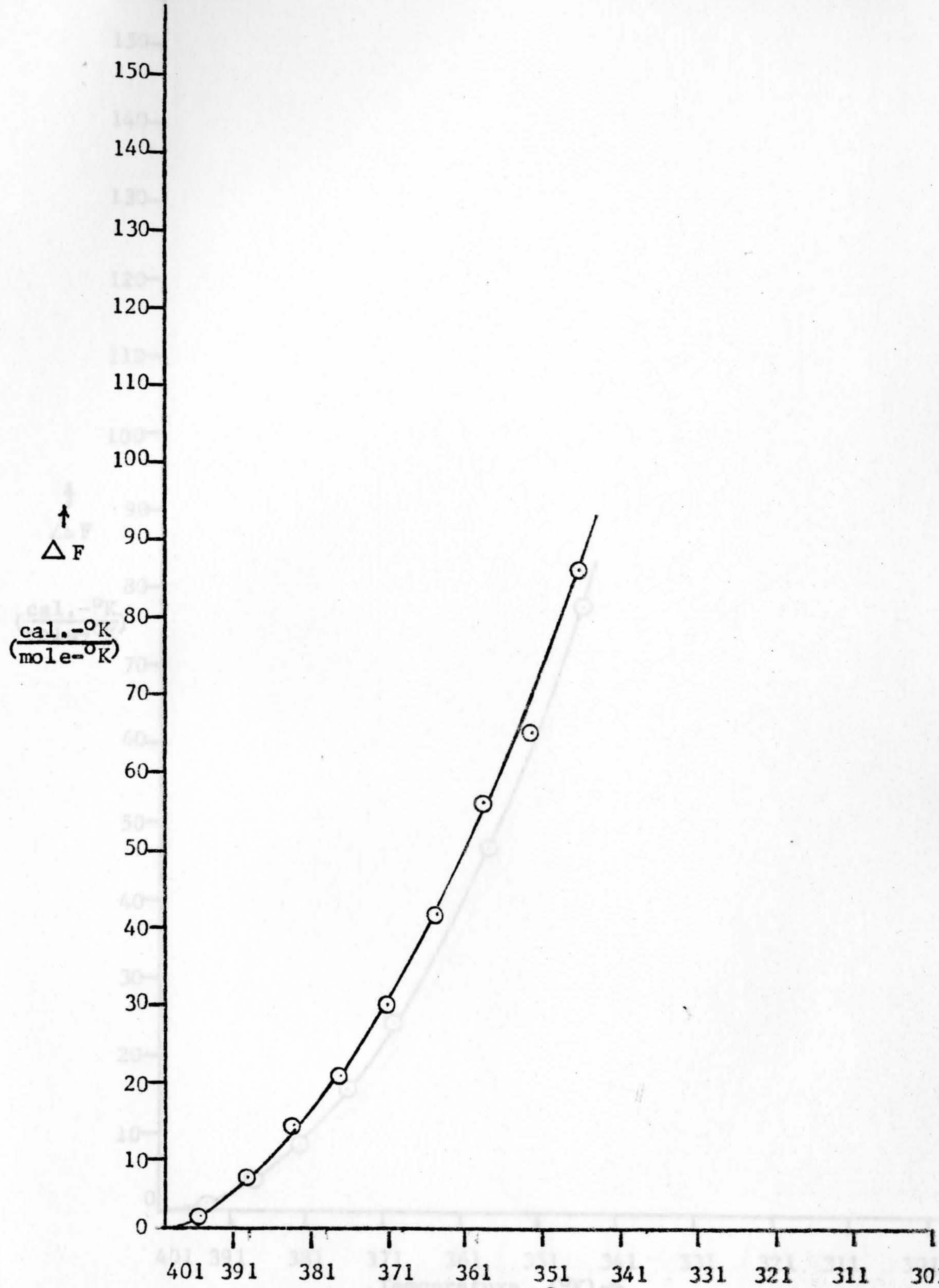

Figure 74. Experimental ΔF versus Temperature Curve obtained for .3 atomic percent Cd.

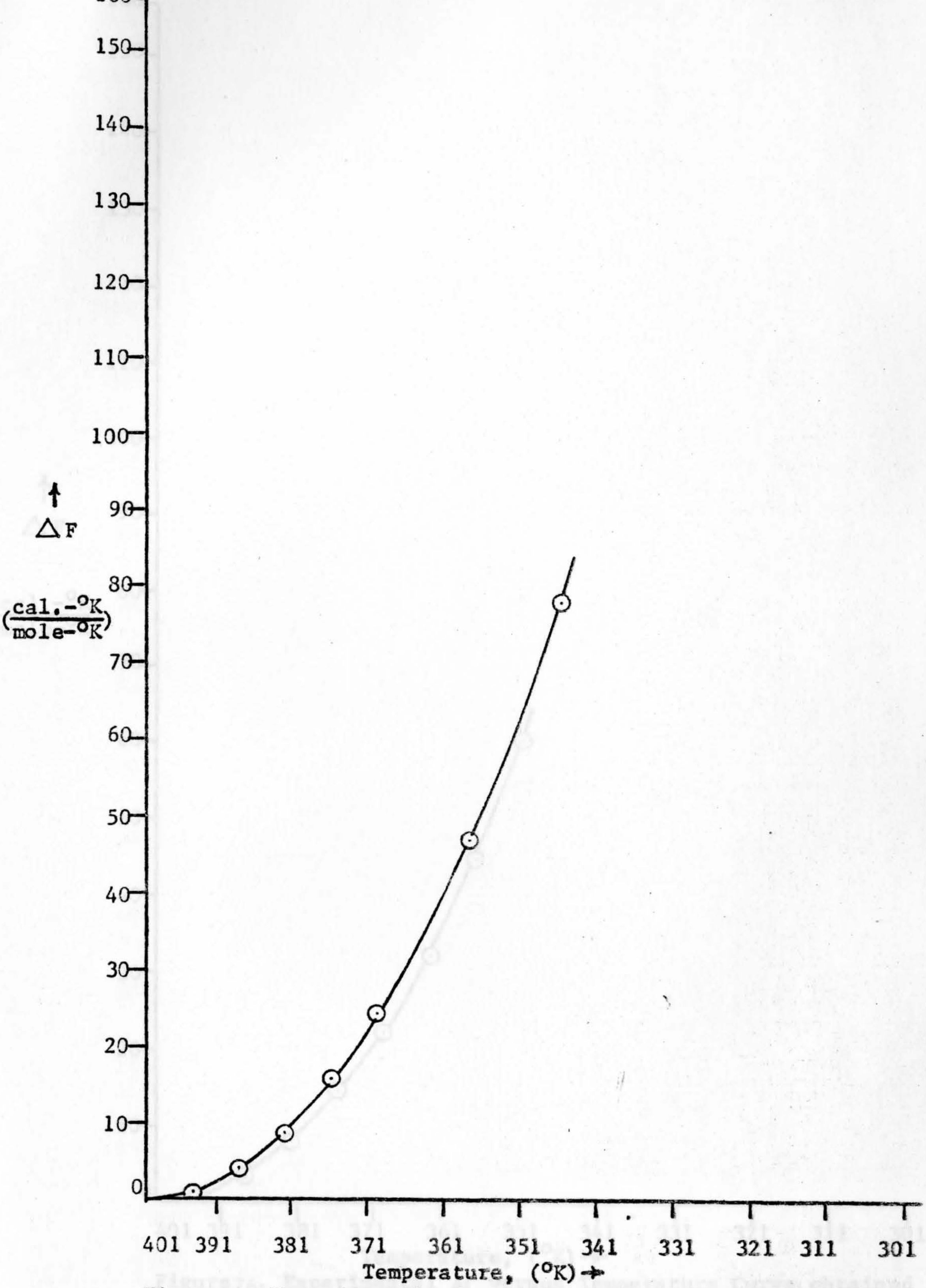

Figure75. Experimental ΔF versus Temperature Curve obtained for .3 atomic percent Te.

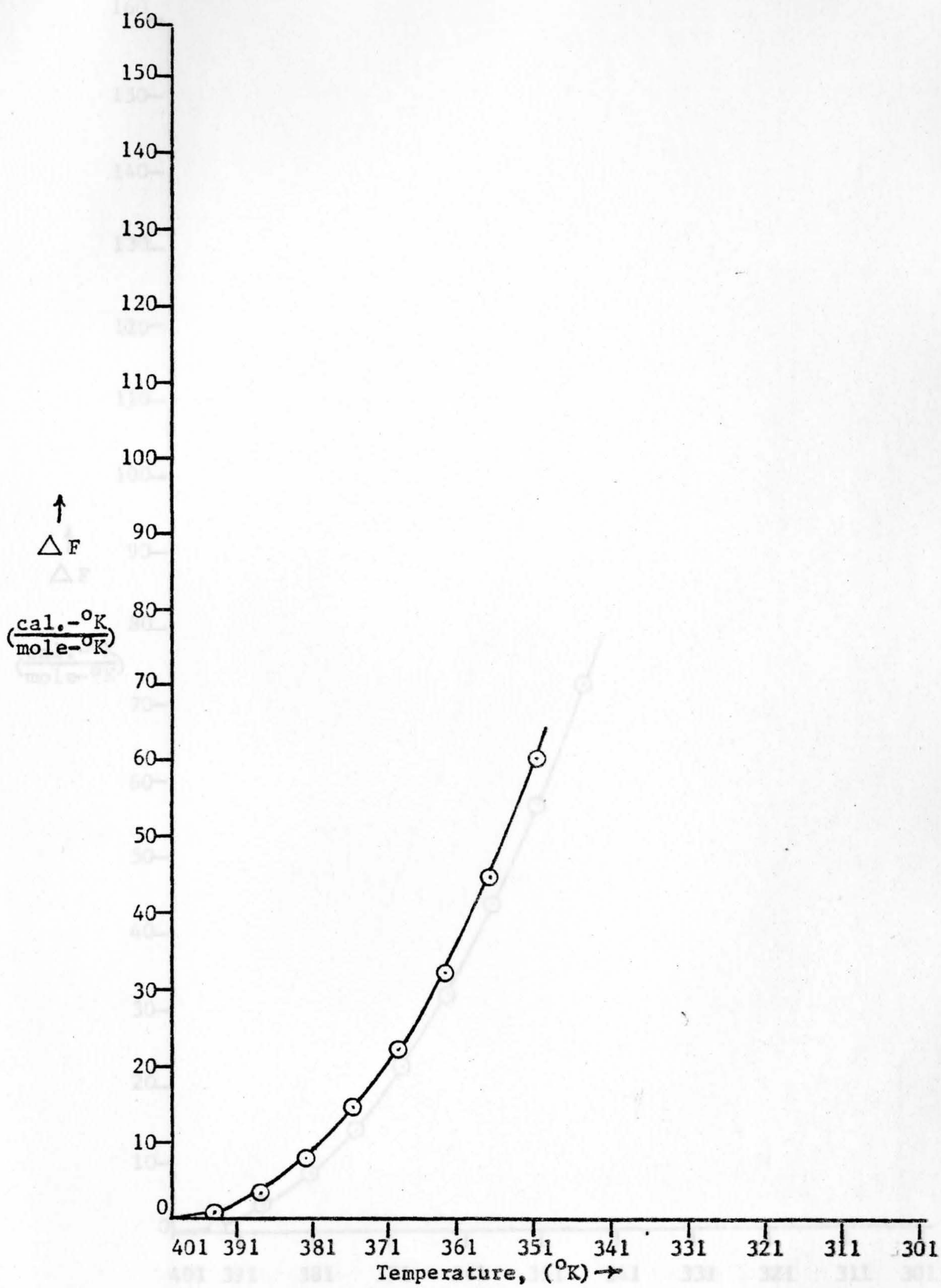

Figure 76. Experimental ΔF versus Temperature Curve obtained for .3 atomic percent Zr.

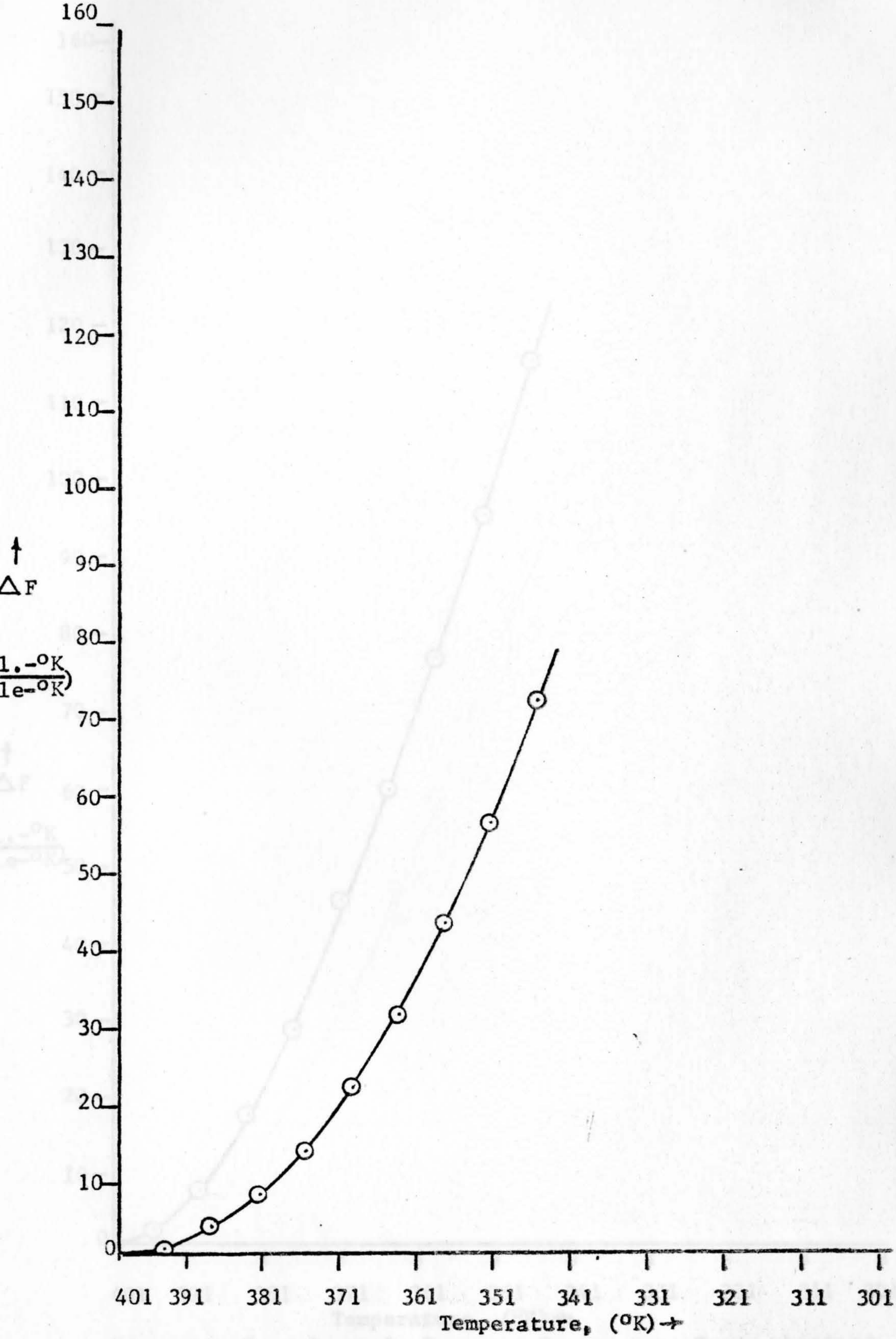

Figure 77. Experimental ΔF versus Temperature Curve obtained for .3 atomic percent Ag.

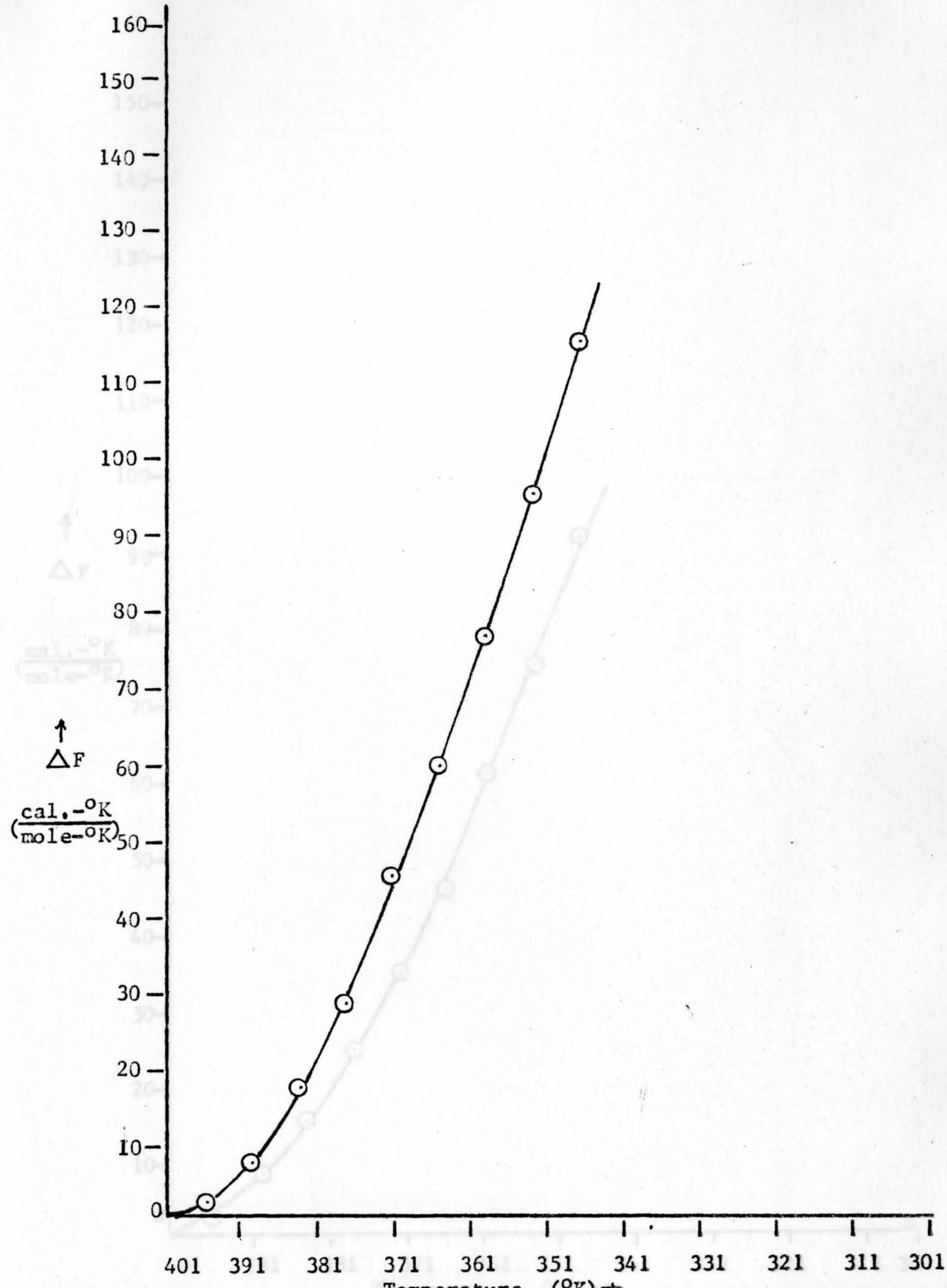

Figure78. Experimental ΔF versus Temperature Curve obtained for .05 atomic percent Ag.

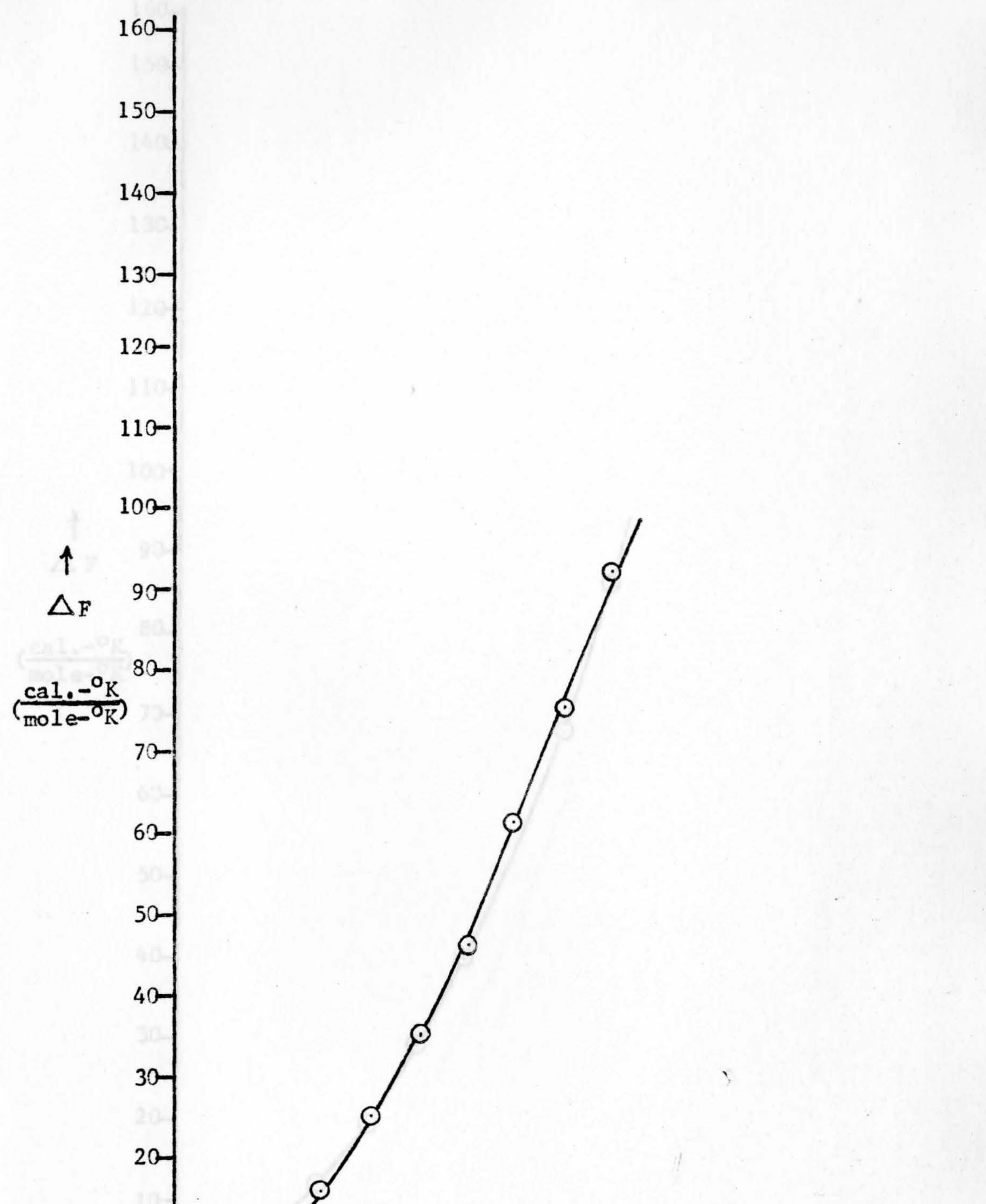

Figure79. Experimental ΔF versus Temperature Curve obtained for .05 atomic percent Te.

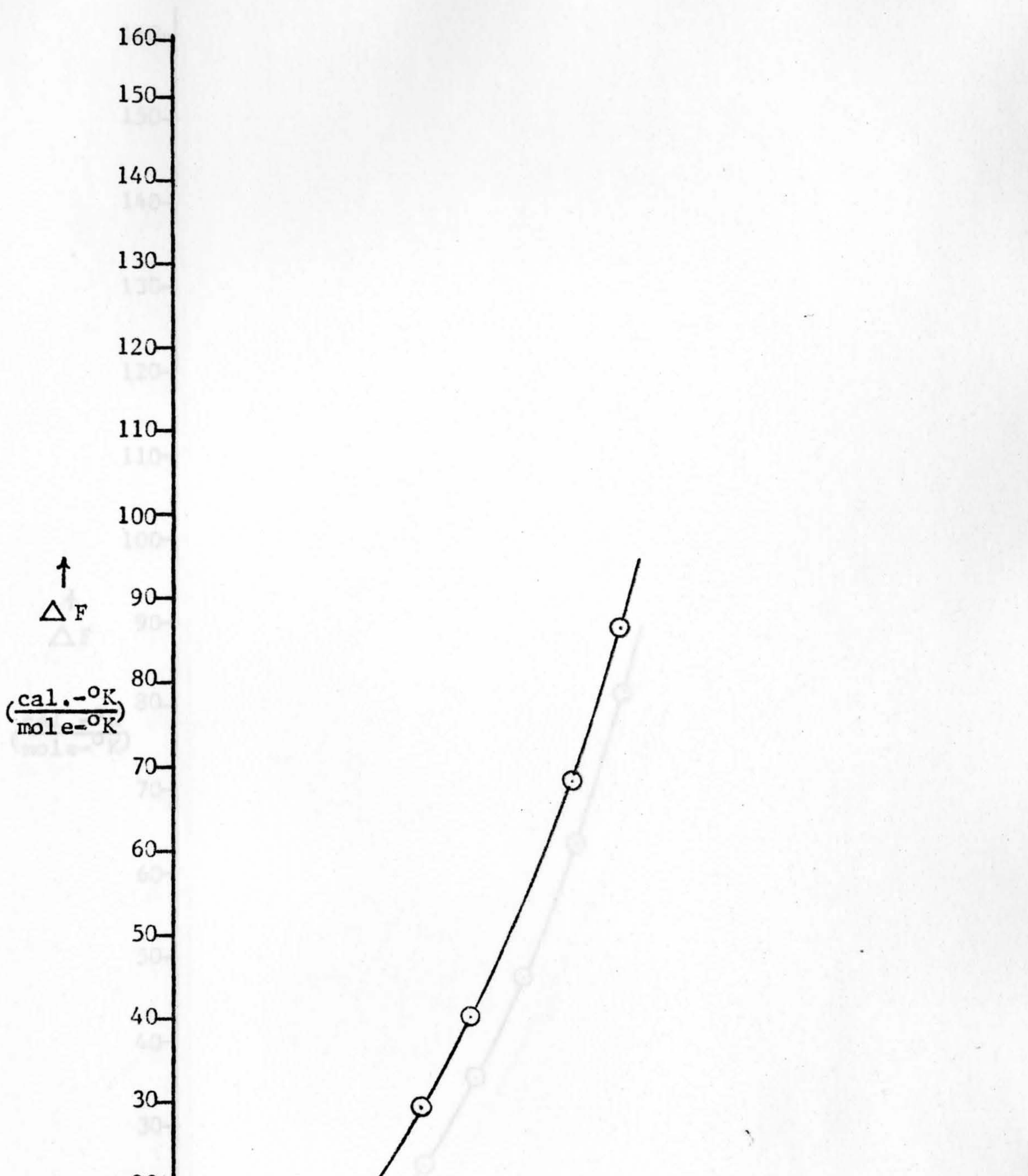

Figure80. Experimental ΔF versus Temperature Curve obtained for .05 atomic percent Cd.

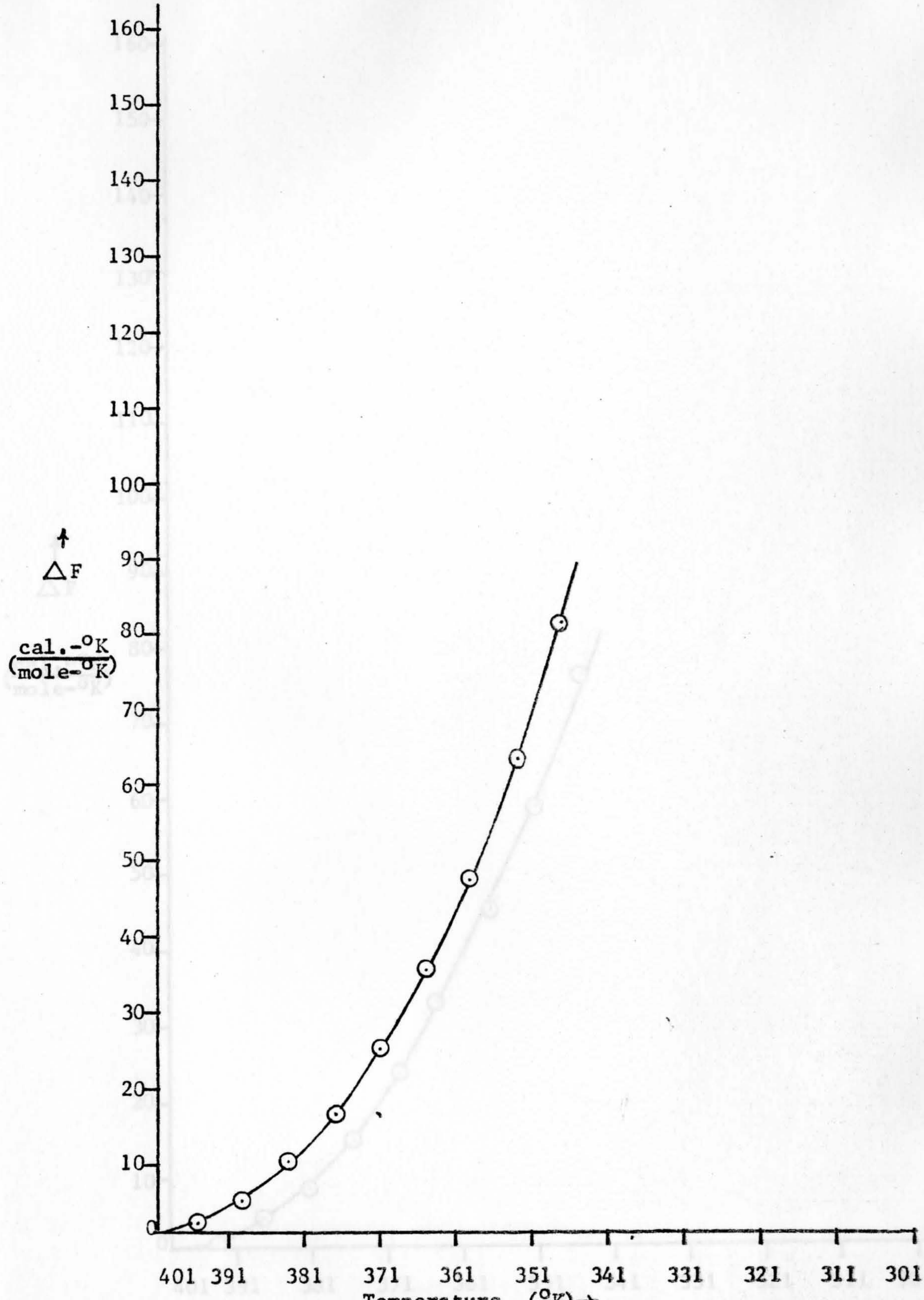

Figure81. Experimental ΔF versus Temperature Curve obtained for .05 atomic percent In.

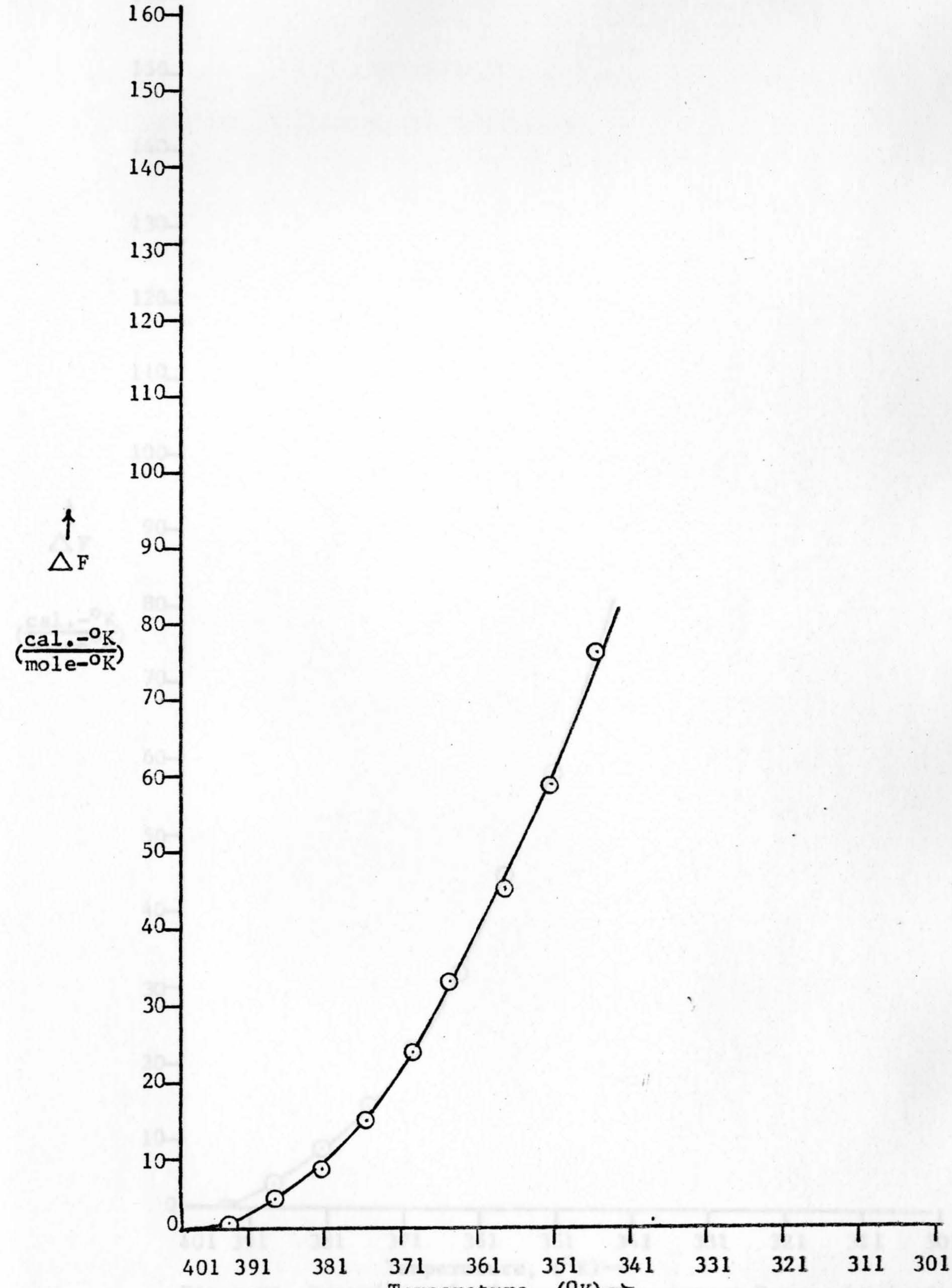

Figure82. Experimental ΔF versus Temperature Curve obtained for .05 atomic percent Sb.

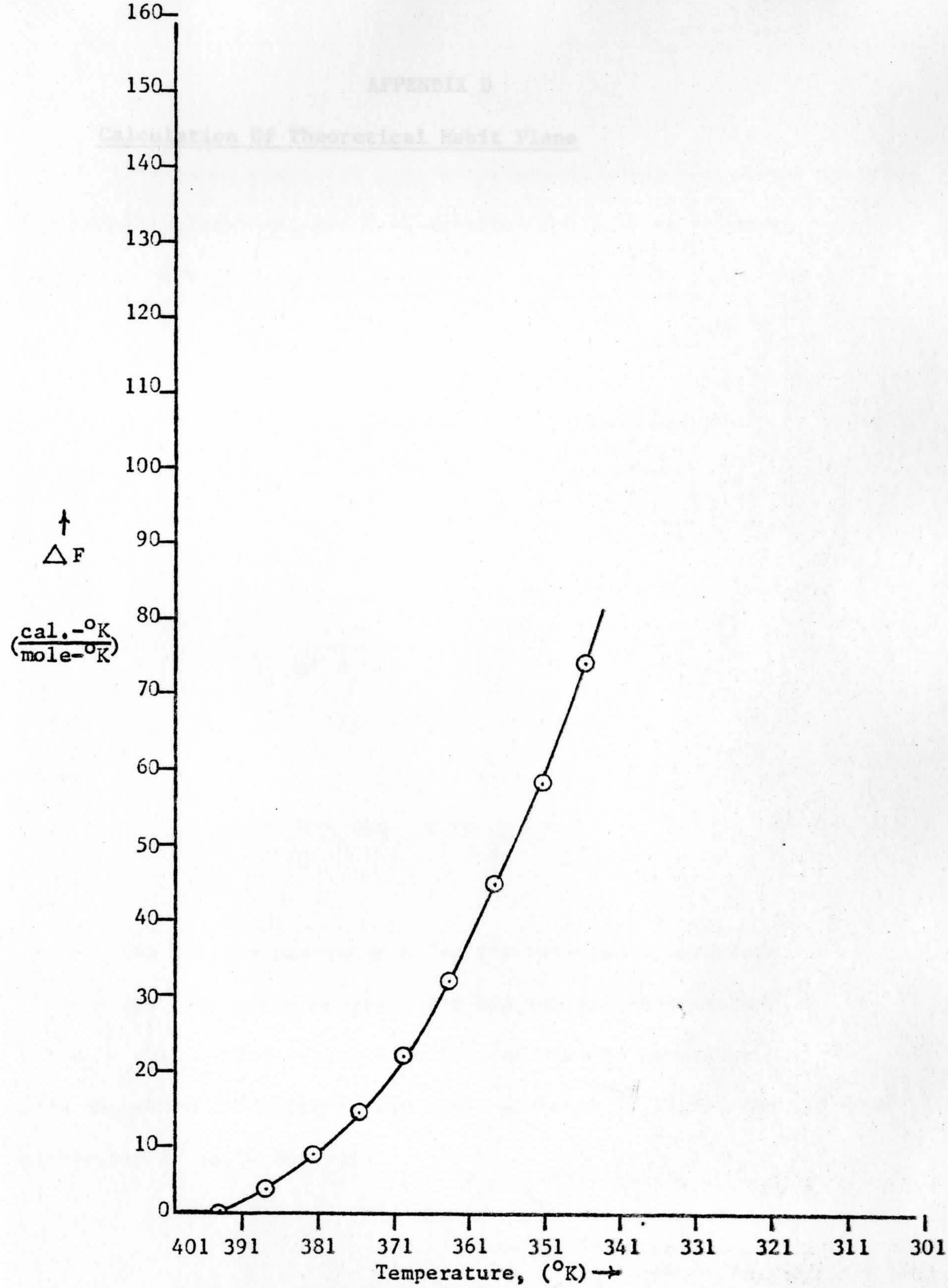

Figure 83. Experimental ΔF versus Temperature Curve obtained for .05 atomic percent Zr.

APPENDIX D

Calculation Of Theoretical Habit Plane

The habit plane for this transformation was calculated by using the Wechler, Lieberman, and Reed equation which is as follows:

$$h = \frac{1}{2n_1}\left[\sqrt{\frac{2n_1^2n_2^2-n_1^2-n_2^2}{n_2^2-1}} - \sqrt{\frac{n_1^2+n_2^2-2}{n_2^2-1}}\right]$$

$$k = \frac{1}{2n_1}\left[\sqrt{\frac{2n_1^2n_2^2-n_1^2-n_2^2}{n_2^2-1}} - \sqrt{\frac{n_1^2+n_2^2-2}{n_2^2-1}}\right]$$

$$l = \frac{1}{n_1}\sqrt{\frac{1-n_1^2}{n_2^2-1}}$$

where

$$n_1 = \frac{a}{a_0} \quad \text{and} \quad n_2 = \frac{c}{a_0}$$

and

a = the lattice parameter a for the tetragonal structure

c = the lattice parameter c for the tetragonal structure

a_0 = the lattice parameter a for the diamond structure

From the above calculations the habit plane is $(\bar{1},11,6)$, and the Bain distortion is 16.34 degrees.

The habit plane for this transformation was calculated by using the Wechler, Lieberman, and Reed equation which is as follows:

$$h = \frac{1}{2n_1}\left[\sqrt{\frac{2n_1^2n_2^2-n_1^2-n_2^2}{n_2^2-1}} - \sqrt{\frac{n_1^2+n_2^2-2}{n_2^2-1}}\right]$$

$$k = \frac{1}{2n_1}\left[\sqrt{\frac{2n_1^2n_2^2-n_1^2-n_2^2}{n_2^2-1}} - \sqrt{\frac{n_1^2+n_2^2-2}{n_2^2-1}}\right]$$

$$l = \frac{1}{n_1}\sqrt{\frac{1-n_1^2}{n_2^2-1}}$$

where

$$n_1 = \frac{a}{a_0} \quad \text{and} \quad n_2 = \frac{c}{a_0}$$

and

a = the lattice parameter a for the tetragonal structure

c = the lattice parameter c for the tetragonal structure

a_0 = the lattice parameter a for the diamond structure

From the above calculations the habit plane is (1,11,6), and the Bain distortion is 16.34 degrees.

BIBLIOGRAPHY

Andon, R.J.L., Counsell, J.F., and Martin, J.F., "Thermodynamic Properties of Organic Oxygen Compounds.", Transactions of the Faraday Society, v. 59, (1963), p.p. 1555-1558.

Anthony, T.R., and Turnbrell, D., "On the Theory of Interstitial Solutions of the Moble Metals in Lead,Tin,Thallium,Indium, and Cadmium." Applied Physics Letters, v. 8, no. 5, (March 1, 1966) p.p. 120-121.

Becker, J.H., "On the Quality of Gray Tin Crystals and Their Rate of Growth." Journal of Applied Physics, v. 29, no. 7, (July, 1958), p.p. 1110-1121.

Burgers, W.G., and Groen, L.J., "Mechanism and Kinetics of the Allotropic Transformation of Tin." Disc. Faraday Soc., v. 23, no. 183, p.p. 183-195.

Bykhovskii, A.L., Larikov, L.M., and Fal'chenko, V.M., "Growth Mechanism of -Modification Centers in High Purity Tin." Soviet Physics-Crystallography, v. 12, no. 3, (Nov.-Dec., 1967), p.p. 460-462.

Cagle, F.WM. Jr., and Eyring, Henry, "An Application of the Absolute Rate Theory to Phase Changes in Solids." Journal of Physical Chemistry, v. 57, (1953), p.p. 942-946.

Christian, J.W., The Theory of Transformations in Metals and Alloys. Oxford:Pergamon Press, 1965.

Edwald, A.W., and Tufte, O.N., "Gray Tin Single Crystals." Journal of Applied Physics, v. 29, no. 7, (July 1958), p.p. 1007-1009.

Hultgren, Ralph R., et.al., Selected Values of Thermodynamic Properties of Metals and Alloys., American Society for Metals, Metals Park, Ohio, 1973.

Jaros, M., "Covalent Effects in -Sn." Solid State Communications, v. 7, (1969) p.p. 521-523.

Jaros, M., "On the Theory of Covalent Bonding in Solids.", Physics, v. 50, no. 3, (Dec. 7, 1970), p.p. 356-364.

Klug, Harold P., and Alexander, Leroy E., X-Ray Diffraction Procedures, John Wiley and Sons, Inc., New York, 1962.

BIBLIOGRAPHY CONT.

Kramer, W., and Nolting, J., "Anomale Spezifische Warmen und Fehlord nung der Metalle Indium,Zinn,Blei,Zink,Antimon, und Aluminium." Acta Metallurgiew, v. 20, (Dec., 1972), p.p. 1354-1359.

Lohberg, V.K., and Presche, P., "Beitrag zur -Umwandlung des Zinns." Z. Metallkunde, v. 59, no. 1, (Jan., 1968), p.p. 74-81.

Panyushkin, V.N., "Shift of the Mossbauer Line of -Sn During its Phase Transformation Under Pressure." Soviet Physics-Solid State, v. 10, no. 6, (Dec., 1968), p.p. 1515-1516.

Raynor, G.V., and Smith, R.W., "Transition temperature of the Transition between Grey and White Tin.", Proceedings of the Physics Society, v. 70B, p.p. 1135-1143.

Sherrington, D., and Kohn, W., "Speculations about Grey Tin." Reviews of Modern Physics, v. 40, no. 4, (October, 1968), p.p. 767-769.

Wolfson, R.G., Fine, M.E., and Ewald, A.W., "Transformation Studies of Gray Tin Single Crystals." Journal of Applied Physics, v. 31, no. 11, (Nov., 1960), p.p. 1973-1977.